UNIVERSIDAD EAFIT

Applied Sciences and Engineering School
Design Engineering Research Group (GRID)

A Propulsion System Design Methodology Based on Overall Efficiency Optimization for Electrically-Powered Vessels

Graduation manuscript presented as partial requirement to obtain the

Master of Science in Engieneering

AUTHOR:

Ing. Juan David Mira Pineda

ADVISOR:

Ricardo Mejía-Gutiérrez, PhD.

March 2022

Abstract

Boats have historically been an important mean of transportation, both for passengers and cargo, mainly in water-rich countries. Today, the electrification of transportation includes fluvial navigation, but energy efficiency remains a key issue. Energy consumption, in electrically powered vessels, is strongly influenced by several technical systems (e.g. hydrodynamics, battery, propulsion, etc.). While advances in some of those main systems are found in the literature, this research work focuses on the design and optimization of the "propulsion system (PS)" (Motor–Transmission–Propeller). By implementing an electric motor, the interaction of the mechanical components can be analyzed to find the optimal variables that will govern the performance of the vessel and that allow the optimal Motor–Transmission–Propeller combination. This manuscript presents the development of a multivariable optimization methodology to maximize the overall efficiency of a propulsion system and, therefore, the autonomy of an electrically powered river vessel. The methodology starts with the analysis of the physical variables that define the performance of the propulsion unit components, and establish an optimality problem and an exhaustive search model that considers all possible values of the key design parameters. A case study is presented for the design of an electrically powered river boat, for the transport of people, within the framework of the ENERGETICA 2030 project. This methodology enabled the choice of the PS's components, while optimizing the energy consumption.

Keywords: Electric vessel, Optimal matching, Energy efficiency, Electric propulsion system, Powertrain architectures.

Resumen

Las embarcaciones han sido históricamente un medio de transporte muy relevante, tanto de pasajeros como de carga, principalmente en países con gran riqueza hídrica. Hoy en día, la electrificación del transporte incluye estas alternativas, pero el uso eficiente de la energía sigue siendo una cuestión clave. El consumo de energía en las embarcaciones de propulsión eléctrica está muy influenciado por varios ámbitos técnicos (por ejemplo, hidrodinámica, batería, propulsión, etc.). Asi como en la literatura se encuentran avances en algunos de los principales sistemas, este trabajo de investigacón se centra en el diseño y la optimización del "sistema de propulsión" (motor-transmisión-hélice). Al implementar un motor eléctrico, se puede analizar la interacción de los componentes mecánicos para encontrar las variables óptimas que regirán el rendimiento de la embarcación y que permiten establecer la combinación óptima de motor-transmisión-hélice. Este manuscrito presenta el desarrollo de una metodología de optimización multivariable para maximizar la eficiencia global del sistema de propulsión, y por tanto la autonomía, en el diseño de embarcaciones eléctricas. Se propone una aproximación desde las variables físicas que definen el rendimiento de los componentes de la unidad de propulsión, a través de una formulación del problema de optimalidad y un modelo de búsqueda exhaustiva que considera todos los valores posibles de los parámetros clave de diseño. Se presenta un caso de estudio para el diseño de una embarcación fluvial de propulsión eléctrica, para el transporte de personas dentro del marco del proyecto ENÉRGETICA 2030. A partir de los resultados de este trabajo de investigación, se diseña y presenta el sistema de propulsión de este buque en sus fases de diseño conceptual y de detalle, así como la información técnica para su fabricación.

Palabras Clave: Embarcación eléctrica, Adaptación óptima, Eficiencia energética, Sistema de propulsión eléctrica, Arquitecturas de tren motriz.

Personal publications

Several scientific articles were generated and published during the development process of this research project:

Scientific Indexed Journals :

- Mira, J. D., Mendoza, F., Betancur, E., Manrique, T., and Mejía-Gutiérrez, R. (2021). **"A Propulsion System Design Methodology Based on Overall Efficiency Optimization for Electrically-Powered Vessels."** *IEEE Transactions on Transportation Electrification*, DOI: 10.1109/TTE.2021.3104763. ISSN: 2332-7782. Indexed in WoS (Q1) & Scopus (Q1).

Conferences:

- Mira, J. D., Valderrama, S., Londono, M. J., Giraldo-Perez, E., Betancur, E., Osorio-Gomez, G., Mejía-Gutiérrez, R. (2020). **"Preliminary design tools applied to a solar powered vessel design: A South American river analysis."** *2020 15th International Conference on Ecological Vehicles and Renewable Energies, EVER 2020, 2020-January.* DOI:10.1109/EVER48776.2020.9242537. ISBN: 978-1-7281-5641-5.
- Mira, J. D., Gómez-Oviedo, S., Betancur, E., Mejía-Gutiérrez, R. (2020). **"Preliminary Sizing of a Propulsion Unit for an Electrically-Powered Vessel Using a Screw Propellers Performance Comparison Tool."** In: Figueroa-García J.C., Garay-Rairán F.S., Hernández-Pérez G.J., Díaz-Gutierrez Y. (eds) Applied Computer Sciences in Engineering. WEA 2020. Communications in Computer and Information Science, vol 1274. Springer, Cham. https://doi.org/10.1007/978-3-030-61834-6_40

Project context

Author would like to thank Universidad EAFIT and the alliance "ENERGETICA 2030", which is a Research Program, with code 58667 from the "*Colombia Científica*" initiative, funded by The World Bank through the call "778-2017 Scientific Ecosystems". The research program is managed by the Colombian Ministry of Science, Technology and Innovation (Minciencias) with contract No. FP44842-210-2018

Acknowledgements

First of all, I would like to thank my advisor Ricardo Mejía-Gutiérrez, who has not only been my teacher, director and boss in the project, but also the best example to follow. Thank you for each of those counseling spaces that were always productive and left a lesson in me, thank you for making me a researcher and thank you for opening the doors to EAFIT University, a place where I always wanted to be and to be part of. I thank this institution for providing financial support and resources during the development of this project.

I thank my colleagues in the GRID design engineering research group, other professors and all the people who supported me during the development of this project, especially Esteban Betancur, Erick Gómez, Santiago Bernal, Santiago Echavarría and Erick Giraldo for his constant accompaniment and encouragement in the development of this research work.

Mom, everyone should undertake a great project at least once in life, this has been and will be mine. Thank you for believing in me, for your patience and for accepting my years of study, I have always tried to give you the best.

Contents

List of Figures

List of Tables

List of Symbols

$\eta_{overall}$	Propulsion system overall efficiency (-)
ω	Motor angular speed (rev/min)
$\omega^{(l)}$	Lower limit of motor angular speed (rev/min)
$\omega^{(u)}$	Upper limit of motor angular speed (rev/min)
$\psi_{pll-set}$	Commercially available propellers set (-)
ρ	Water density (slugs/ft^3)
$\sigma_{\bar{x}}$	Mean squared error (x$_i$ units)
τ	Motor torque (Nm)
ζ_i	Component parameters (-)
A_d	Developed area (ft^2)
A_p	Projected area (ft^2)
BAR	Blade Area Ratio (-)
C_i	Regression coefficient(-)
C_n	Nominal capacity of battery (kWh)
D	Propeller diameter (ft)
I_n	Nominal current of battery (A)
J	Advance Coefficient (-)
K_Q	Torque Coefficient (-)
K_T	Thrust Coefficient (-)
n	Propeller RPM (rev/s)
P/D	Pitch ratio (-)
P_B	Brake power (kW)
P_D	Power delivered by propulsors when propelling ship (kW)
P_{EL}	Electric power (kW)
P_E	Effective thrust power (kW
P_T	Thrust power developed by propulsor (kW)
Q	Propeller torque (ft-lb)
R_T	Total resistance (kN)
S_R	Slip ratio (-)
T	Propeller thrust (lb)
t	Thrust deduction factor (-)
T_E	Effective Thrust (kN)
t_r	Transmission ratios (-)
V_A	Propeller advance speed (ft/s)
V_n	Nominal voltage of battery (V)
V_S	Ship speed (ft/s)

w	Wake fraction factor (-)
Z	Number of blades (-)
$t_{r(i)}$	Gear Ratio Stage for electrification [-]
$t_{r(outboard)}$	Original Outboard Gear Ratio Stage (-)
BAR	Blade-Area Ratio (-)
DAR	Disc-Area Ratio (-)
η_D	Quasi-propulsive efficiency (-)
η_H	Hull efficiency (-)
η_M	Motor efficiency (-)
η_O	Open water efficiency (-)
η_R	Relative rotative efficiency (-)
η_T	Transmission efficiency (-)

Chapter 1

Introduction

1.1 Background

EAFIT University, through the Design Engineering Research Group (GRID)[1] since 2009 has developed and implemented sustainable transport solutions, from electric wheelchairs, through bicycles and motorcycles, to 100 % electric vehicles. These experiences led EAFIT University and the local utility company (EPM) to develop the first Colombian Solar Vehicle, called "*Primavera*", which competed in the "World Solar Challenge (WSC)[2]" 2013 and 2015 and won the National Engineering Award from the SCI (Colombian Society of Engineers) in 2014 and the Antioquia Engineering Award from the SAI (Antioquia's Society of Engineers and Architects) in the same year. Based on these and other experiences in issues related to renewable energy and sustainable mobility, EAFIT University, in alliance with other institutions and companies in the electricity sector, articulated, formulated and presented an ambitious research program, to be financed by the World Bank through the call from Colciencias 778-2017, called "Scientific Ecosystem" created by the Ministry of Education and the Ministry of Trade, Industry and Tourism, through Colciencias and Icetex. The research topic was around Renewable Energies and the alliance was created as "*ENERGÉTICA 2030: Strategy for the transformation of the Colombian energy sector in the horizon of 2030*". The alliance comprises a set of 10 research projects and one "Institutional Strengthening" project in which the different partners interact. The ENERGÉTICA 2030 program was awarded with the first place in the call and in mid-2018, work began on the project, where a multidisciplinary work team was set up with professors, consultants and undergraduate and graduate students from the different institutions. Within the 10 projects, Universidad EAFIT is leading 4 of them in the topics: 1) Sustainable Mobility, 2) Sustainable Construction, 3) Distributed Generation and 4) Energy Markets. The duration of the program is 4

[1] `www.eafit.edu.co/grid`

[2] The top solar vehicles competition, held every 2 years in Australia (`www.worldsolarchallenge.org`)

years. Currently the work is focused on the development and materialization of the different prototypes (known as "Living Labs") in which the different results of design, innovation and different developments resulting from the research processes are consolidated.

In particular, the *sustainable mobility* project seeks to develop a multi modal transport solution based on three elements to be developed: i) an electrically-powered vessel, ii) hybrid motorcycles and iii) a photovoltaic charging stations. In the development of the electrically-powered vessel, an analysis of the context of river mobility in the country was carried out, identifying an interesting possibility in sustainable passenger transport. One of the motivations of the project is then to develop solutions to the navigable potential of Colombia, being the 6^{th} country in the world with the greatest amount of kms of navigable waterways in the world ranking only after China, Russia, Brazil, Brazil, Vietnam and the United States (Central Intelligence Agency (CIA), 2020), which will represent future commercial opportunities. It is also worth mentioning that this alternative of river transport is part of the national interests, reflected in the 2020's call 879 of the National Unit for Energy-Mining Planning, UPME[3], which seeks strategies to develop solutions for electric mobility to promote rail and river modes for the transport of cargo and passengers in order to strengthen the productive chain of the country (Minciencias, 2020). This means that the business potential of these solutions will grow considerably in the country in the medium and long term

1.2 Research justification

Air pollution has two possible causes, natural causes and anthropogenic causes. According to Edenhofer (2015), natural causes are responsible for 5% of the gases emitted as air pollutants and focus on emissions generated by animals and vegetation, waste from volcanic eruptions, dust and forest fires. For their part, anthropogenic causes generate the greatest contribution to air and atmospheric pollution. With a total of 95% of contribution, the anthropogenic causes can be grouped in those generated by the decomposition of waste in sanitary fillings, extensive agriculture and cattle raising and the burning of fossil fuels, processes that have as main product the generation of methane gas and CO_2 and hydrocarbons respectively (Edenhofer, 2015).

According to the Intergovernmental Panel on Climate Change (IPCC) in between 1750 and 2011, 2040 ± 310 Gt of CO_2 equivalent have been emitted to the atmosphere due to anthropogenic causes, of which 75% are due to the burning of fossil fuels (IPCC, 2014) . Considering the above and taking into account the need for mobility of people and cargo, which represents 19% of total energy consumption in the world by 2013, the study shows that the transport sector is responsible for 14% of emissions due to the burning of fossil fuels, and is the one that contributes 10% of total anthropogenic causes

[3]Acronym in Spanish for "*Unidad de Planeacion Minero Energética*". (`www.upme.gov.co`)

with a total of 211 $GtCO_2$ equivalent and the remaining 86% is distributed among power generation with 47%, the industrial sector with 30% and other sources contribute 9%.

Due to the this, humanity is moving decisively towards an electrification of transport, being a priority sector when considering its impact on climate change , its high consumption of fossil fuels, its accelerated growth and the urgent need to reduce Greenhouse Gas (GHG) emissions and pollutants that affect the health of the population and deteriorate air quality (Minambiente, 2019).

In Colombia, according to the National Planning Department (DNP), the costs associated with poor air quality in the country amounted to 12 billion of pesos in 2018 and were related to 8,000 deaths. Additionally, according to numbers from the Colombian Institute of Hydrology, Meteorology and Environmental Studies (IDEAM)[4], 12% (28 million TCO_2) of the pollutant emissions in Colombia come from the transportation sector, which consumes 40% of the country's total energy, concentrating 96% of that energy in the consumption of fossil fuels (Minas-Energia, 2021; UPME, 2020; Minambiente, 2019) (see Figures 1.1 and 1.2). In addition to this situation, the activity concentrates 54% of the total energy losses due to energy efficiency because only 24% of the energy used is converted into useful energy, with an approximate cost of US$3.000M. Following the signing of the Paris agreement on climate change, a commitment was made to reduce pollutant emissions by 51% by 2030, and compliance with the national target will depend on what happens in the transport sector. The diagnosis reveals that the implementation of energy efficiency measures and technological change is essential. The current solutions, therefore, involve technological developments focused on new propulsion systems, mainly electric, and the incorporation of new energy sources such as natural gas or hydrogen that enable migration towards sustainable, low-carbon transport.

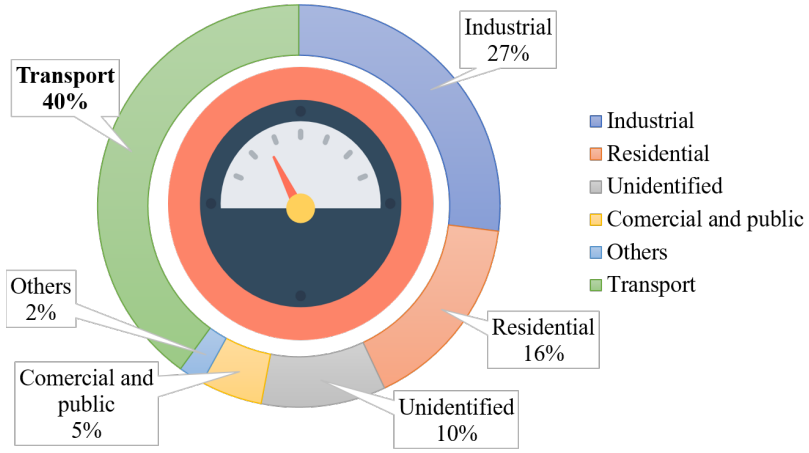

Figure 1.1: *Energy consumption for transportation sector (Minambiente, 2019; UPME, 2017, 2020)*

[4] Acronym in Spanish for "*Instituto de Hidrología, Meteorología y Estudios Ambientales*". (`www.ideam.gov.co`)

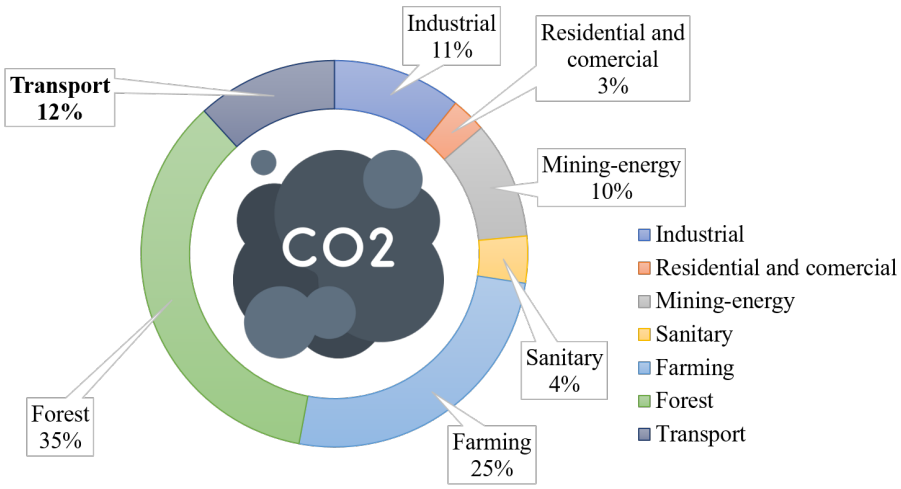

Figure 1.2: *Emissions rate of transportation sector (Minambiente, 2019; UPME, 2017, 2020)*

The emissions of gases contributed by the transport sector are mainly due to the fact that the equipment used for loading and transportation (vehicles, boats, trains, airplanes, etc.) incorporate mobility based on the use of ICEs. The distribution of energy consumption by sub-sectors that typically use combustion engines is shown in the Figure 1.3.

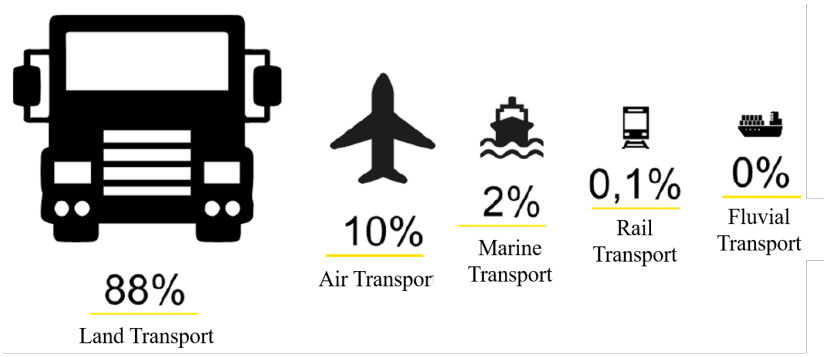

Figure 1.3: *Energy consumption in the sub-sectors that use ICE (Minambiente, 2019; UPME, 2020)*

Due to this and other factors such as fluctuating prices and the scarcity of oil, along with the development of new technologies, other types of energy and mobility sources have become more important, including electric mobility. In places such as Latin America and the Caribbean, which have the highest density of navigable rivers in the world, river electric mobility has emerged as an alternative for the transportation of people and cargo, being a sustainable transportation solution that contributes to the reduction of polluting emissions. The Figure 1.4 summarizes schematically what has been presented up to this point, starting from air pollution and its causes to the formulation of mobility alternatives based on the development of vehicles for river transportation implemented in areas of greater water wealth.

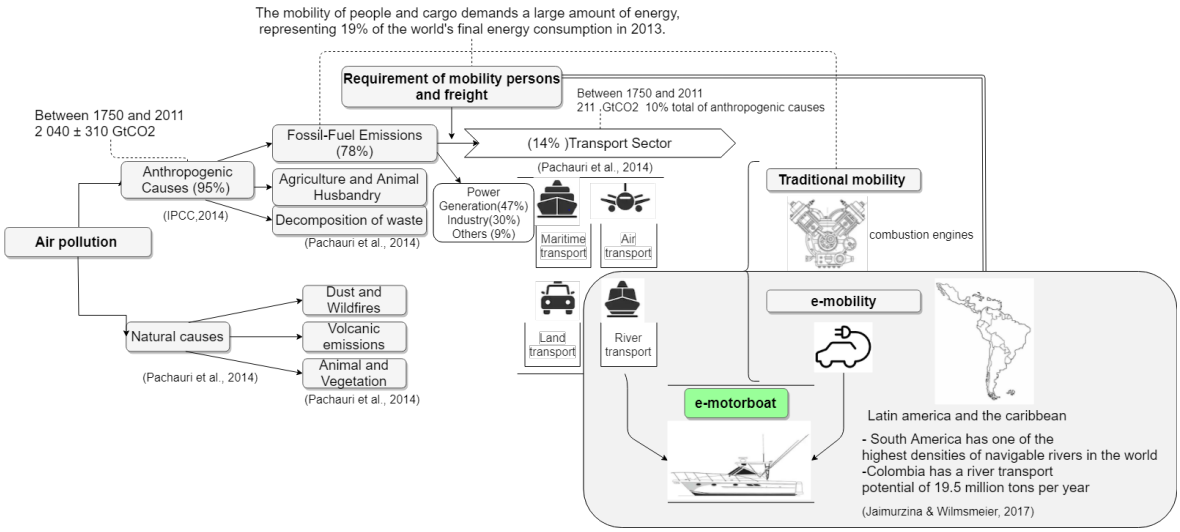

Figure 1.4: *Background scheme (Pachauri et al., 2014; Jaimurzina and Wilmsmeier, 2017)*

This diagnosis reveals that the implementation of energy efficiency measures and technological change is urgent. That is why Colombia has proactively proposed different strategies that are aligned with the global trend of migrating towards electric mobility, not only around land and air transportation, but also river transportation. The Table 1.1 presents a list of the different policies developed by the Colombian government to accelerate the incorporation of zero and low emissions means of transportation and that include river mobility as a focus within the action plans.

For example, the "National Strategy for Electric Mobility" (2019) contemplates that by the year 2022 action plans must be implemented by the Ministry of Transportation to include river mobility within the mobility plans, these actions are focused on the development of infrastructure and new transportation networks through rivers, which is also ratified in the "Inter-modal Transportation Master Plan" (2015) where with an investment of 6.95 Billion COP projected between 2015 and 2035, the intervention of 8 different rivers is planned, totaling 5,065km of waterways for their integration with the basic transportation network. Finally, other studies recognize the advantages of using river mobility such as the reduction of existing freight rates for cargo and how this type of mobility induces and generates new types of cargo and facilitates multi-modality in addition to reducing emissions due to higher volume transported.

The fact that sustainable river mobility alternatives are taking center stage in public policies is largely due to Colombia's water wealth and the high growth and technological development of electric boats in recent years. If we focus on Colombia's water wealth we find that, as a country, Colombia has 5 main basins (see Figure 1.5): Atrato, Magdalena, Orinoco, Amazonas and Pacífico, which total add up to 24,725 km of waterways, of which 18,225 km are suitable for navigation (ARCADIS Nederland BV and JESYCA S.A.S, 2015). Main rivers such as the Magdalena have a total of 6,381,243

Table 1.1: *Summary of Policies and studies to promote sustainable mobility in Colombia*

Public Policies and Studies	Year	Organizations and Institutions	Main Approach
Energy transition: a legacy for Colombia's present and future.	2021	Ministerio de Minas y Energía Banco Interamericano de Desarrollo	- Actions developed with respect to technological changes and the incorporation of new energy sources that allow us to migrate towards sustainable and low-carbon transportation.
National Energy Plan 2020-2050	2020	Ministerio de Minas y Energía Unidad de Planeación Minero Energética UPME	- Long-term energy scenarios - Analysis of technological and economic aspects associated with energy transformation
Electric Mobility. Advances in Latin America and the Caribbean, , 4ta Edition	2020	ONU-Programa de las Naciones Unidas para el Medio Ambiente (PNUMA)	- State of electric mobility in Latin America and the Caribbean. - Decarbonisation plans, mobility strategies and regulatory elements that enhance and accelerate the transition to more sustainable models, both in the energy and transportation sectors.
National Electric Mobility Strategy	2019	Ministerio de Ambiente y Desarrollo Sostenible Ministerio de Minas y Energía Ministerio de Transporte Unidad de Planeación Minero Energética UPME	- Accelerating the implementation of electric mobility - Reduce emissions from the transportation sector - Efficient and rational use of energy - Improve quality of life
Roadmap for the Transition to Zero and Low-Emission Vehicles	2017	Unidad de Planeación Minero Energética UPME	- International context of fuel consumption distribution and emissions generated by transportation modes. - Projection of future measures for the incorporation of other energy sources and technologies in the transport sector under the need of norms, regulations, laws and decrees.
Energy Demand Situation in Colombia	2017	World Bank Group Departamento Nacional de Planeación DNP Korea Green Growth Partnership Enersinc	- Energy demand, with emphasis on the analysis of energy intensity, new and more efficient technologies, analysis of related policies, the challenges to achieve greater energy efficiency and a projection of penetration scenarios for these technologies from the demand side.
Intermodal Transportation Master Plan (PMTI)	2015	Ministerio de Transporte Agencia Nacional de Infraestructura ANI Instituto Nacional de Vías INVÍAS Departamento Nacional de Planeación DNP Cámara Colombiana de la Infraestructura Fedesarrollo Financiera de Desarrollo Nacional	- Intermodal infrastructure projects - Methodology for projecting the infrastructure and transportation sector according to Colombia's evolving needs.

inhabitants on its banks, which is equivalent to 13% of the national population, and in municipalities such as Magangué, located in the Momposina depression which is an area of interference of the ENERGÉTICA 2030 project, a total of 39,172 passengers are mobilized on average per month. By the year 2035, it is projected that a total of 4.5 million passengers will be mobilized by waterways and most of them will travel along the Magdalena River. In terms of river freight, Colombia has the potential to transport 19.5 million tons per year (Aponte and Fragozo, 2017). Figure 1.5 show the potential of river mobility in the country, which, combined with the use of electric energy and its massification as a source of energy for the transportation sector, make the development of electric vessels a projects of great projection in the short and medium term.

Regarding the technological growth developed around the electric boats we find that during history,

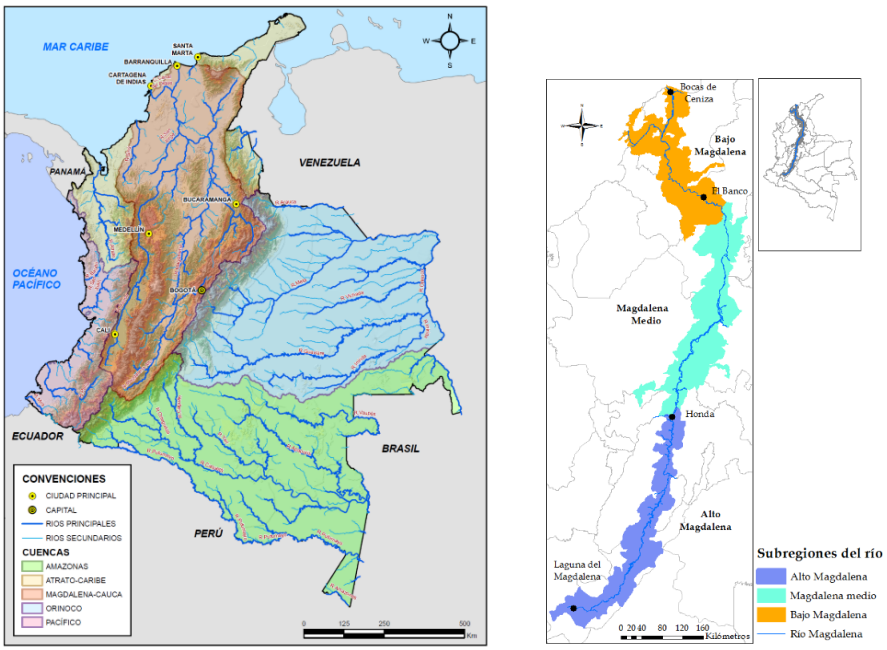

(a) Main basins (b) Magdalena river sub-regions

Figure 1.5: *River potential in Colombia (ARCADIS Nederland BV and JESYCA S.A.S, 2015)*

the first report of an electric boat appeared in the mid-nineteenth century. Similarly as with the first electric land vehicles, there was a great potential for diffusion of this type of propulsion, thanks mainly to the relatively simple construction of the DC electric motors, their high efficiency and their ease of controlling their rotation and spin direction. Unfortunately, this did not happen, because from the very beginning the main problem was too little capacity of batteries in relation to expectations. In a short time, after 1908, motor vehicles were dominated by the combustion engine. This was largely due to Henry Ford, who introduced the ICE in his cars. At the same time, the combustion system on the vessels became widespread, not only stationary, but also outboard combustion motors for small vessels were produced (Łapko, 2019a). However, over the years this has changed and electric engines have gained prominence. Some studies, such as the one presented by Nykvist and Nilsson (2015) and The Economist (2017), revealed the increased prospect of the use of all types of commercially competitive electric vehicles, due to the decreasing cost of batteries and their increased storage capacity and energy delivery. The literature review evidenced that costs are falling and that lithium-ion batteries are dominating the market. According to Nykvist and Nilsson (2015) the cost has been decreasing by 14% annually between 2007 and 2014 achieving a current cost of 410 USD per kWh, and an increase in battery capacity from 100 Wh/kg to 400 Wh/kg by 2022. The electrification of boats is no stranger to these advances and the electric propulsion systems are increasingly used on vessels. These are mainly

recreational vessels motorboats and yachts, in which electric motors can be a main or auxiliary system. To these reasons we can also add not only the reduction of pollutants emitted into the atmosphere but also the reduction of noise and vibration levels that could pose serious difficulties to people working on such vessels (Łapko, 2019b). Figure 1.6 shows how battery pack costs have plummeted, thanks to improved chemistries and increased production volumes.

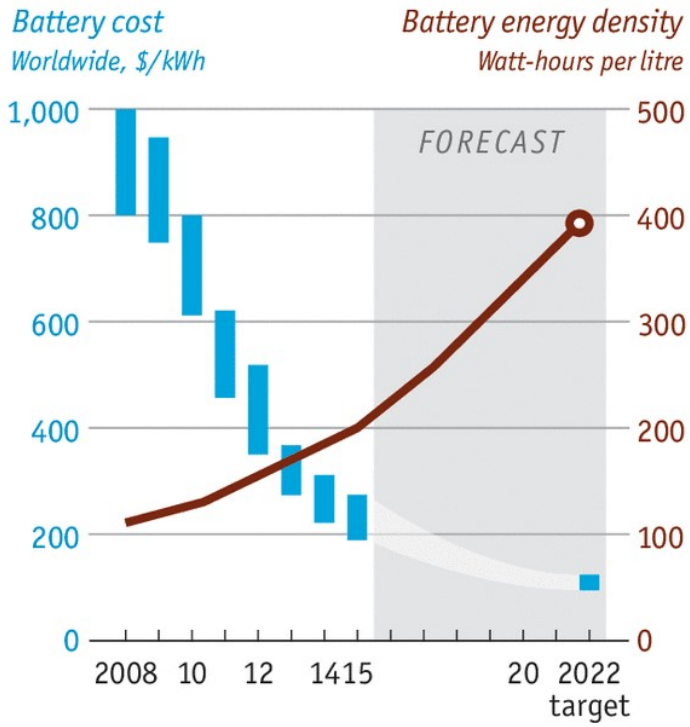

Figure 1.6: *Evolution over time of battery cost and energy density (The Economist, 2017)*

The main technological factors that have favored the development of electric boats can be summarized in the following seven aspects (Pestana, 2015; Łapko, 2019b; Yang et al., 2016):

- Development of power electronics DC/AC.
- Increased autonomy-development batteries (lithium 200-400 Wh/kg).
- Versatility and simplicity of electric motors.
- Introduction of electrical podded propulsion (Hybrid systems)[5].
- High levels of manoeuvrability.
- Oil price movements.
- A reduced amount of pollutants emitted to the atmosphere.

[5]The Podded-Azipod is a 360 steerable unit where the electric motor is installed directly on the propeller shaft in an underwater unit (Hansen and Wendt, 2015)

- A low level of noise generated and no vibrations.

All of the above shows that we are in an economically and technically feasible moment for the use of electrically propelled vessels on an increasing scale. The growth figures of the electric boat fleet over the last 10 years are evidence of this. Figure 1.7 shows that the number of electric boats has a growing trend, three times faster than the world fleet with an exponential increase since 1995 .

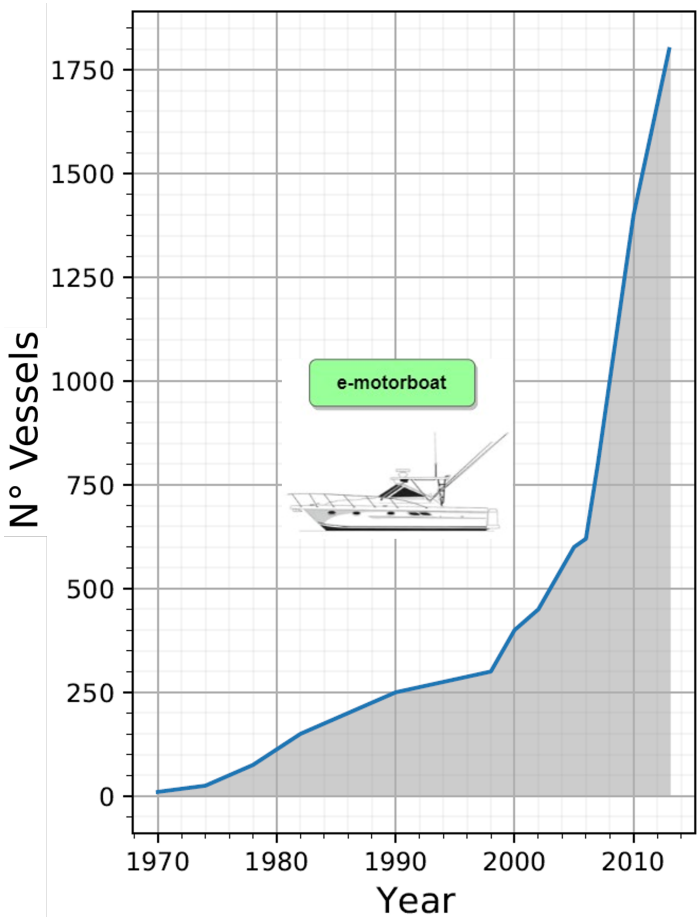

Figure 1.7: *Development of electric propulsion fleet. Elaborated from : (Pestana, 2015)*

This is how the development of electric boats, under an environment of public policies that are decisive and decided towards the use of different types of mobility, is projected as one of the alternatives that make up the sustainable solutions in the present and near future, allowing the reduction of polluting emissions of this type of vehicles. However, electric boats has still challenges to overcome, even harder than in Electric Vehicles. On boats, achieving an adequate performance to meet the requested demands will depend on the efficient use of the energy available in the batteries. This issue becomes a key aspect in the design process of boat's subsystems, especially the propulsion system, which is the focus of this project.

1.3 Research Problem definition

There are different challenges when developing sustainable mobility solutions, specifically Electric Vehicles (EVs) of any kind. One of them is to achieve their democratization, which consists of opening the opportunity for users to access this type of solutions in an affordable way, since they are usually of a high cost mainly due to the technologies they employ. Part of the democratization also consists in identifying which mobility solution meets the specific needs of each type of user. This enables to generate different vehicle solutions that incorporate technologically sound and cost-effective solutions versus the features for which they were designed. This is fundamental while the substitution of transport technologies is achieved by natural replacement. Another important challenge to be considered is the charging infrastructure necessary for the operation, which guarantees easy access to the required energy and with a long-term projection. There is also the challenge of overcoming the myths unfounded by experiences in early stages of development and that still exist in the users. Finally, and most important for the engineers who develop this type of vehicles, **the maximum utilization and efficient use of the energy available in the power supply (batteries) and that is consumed by the sub-systems that allow the develop the functions for which it is designed**. Most of this consumed energy is invested in overcoming i) the inertia to the motion and ii) the resistance exerted by the external forces acting on the vehicle. In the case of boats, the reaction exerted by the water must be overcome, while the boat is moving at a defined speed (Giraldo-Pérez et al., 2020). When designing a vessel, cruising speed and the demand for cargo and/or passenger transport capacity are taken as a starting point to dimension and define the shape of the hull, which must allow to act safely and stably in the different static and dynamic situations. It must also exercise the least possible opposition to movement.

Once the geometry of the boat is known, it is subjected to hydrodynamic studies to estimate the thrust necessary for its displacement. Thrust and velocity define the power that must be delivered by the **PS** to the vessel in order to meet its operating requirements and achieve the desired speed in the routes and context in which it will perform. The design process then focuses on three subsystems that will determine the final performance of an electric boat:

- The first subsystem is the **"Energy Source"**, which is constituted by a battery or a set of these, which will provide the necessary electrical power to put in operation the propulsion unit. For this component it is necessary to work on optimizing the energy density of the battery pack ($Energy/MassUnit$) in order to achieve the lowest weight of it and thus reduce the amount of mass to be displaced. The battery pack has a strong influence on the final weight of the boat.

- The second subsystem is the **"Boat Hull Geometry"**, this geometry must fulfill among many other factors, be able to accommodate all the components that will go inside it and as mentioned

above, its hydrodynamic design must allow the boat to exercise the least resistance to displacement. It is at this point where the design of this geometry is decisive for energy consumption and a factor where the designer can make a greater intervention.

- Finally, the third subsystem is **"The Propulsion Drive"** or PS, in charge of converting the electrical energy supplied by the batteries into effective thrust (see Figure 1.8). The **PS** consisting of **Motor–Transmission–Propeller** is in charge of supplying these thrust requirements to achieve the movement of the vessel.

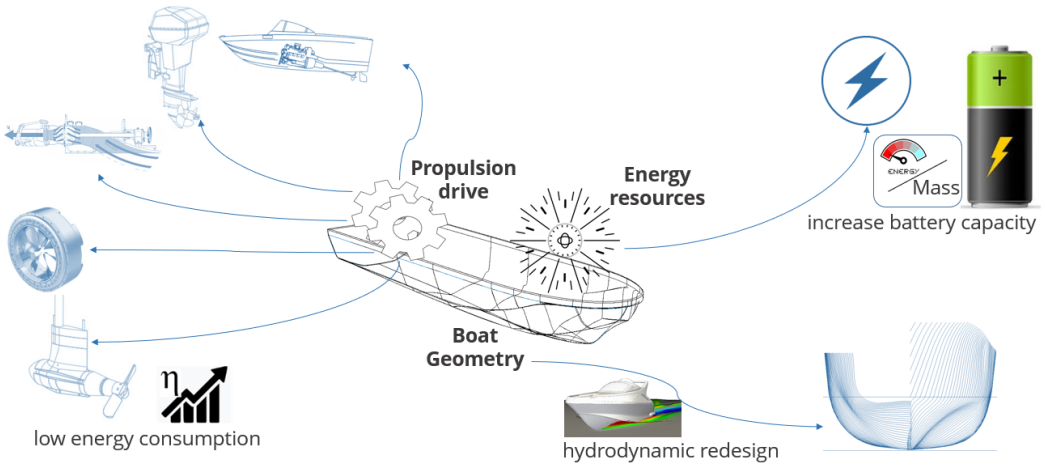

Figure 1.8: *Features and performance factors of a electrically-power vessel*

Most existing vessels make use of propulsion units incorporating ICEs, using a fossil fuel energy source that has 100 times more energy density (kWh/kg) than, for example, a battery that powers the propulsion unit of an electric boat. This issue corroborates that energy efficiency is a mandatory and determining factor for the design of an electric boat (Galindo, 2010). The efficiency of the energetic transformation processes, carried out inside the propulsion system, is decisive for estimating the power to be installed and the losses generated here are translate into: i) decrease of autonomy and ii) need for an increase in the installed capacity (batteries, solar panels or a combination of these). This issue means that those losses must be covered, in order to achieve the desired performance. The increase in installed capacity means that there is a loss of available space inside the vessel, an increase in weight and cost overruns due to the need to purchase more electrical power delivery elements. This cascade of effects could lead to a technically unfeasible outcome or require a significant reduction in certain benefits. These conditions make the optimal use and the efficient transformation of energy at each point of the kinematic chain of the electric boat, to be considered as the main **PS** design process milestone. The Figure 1.9 schematically illustrates those considerations, as well as the propulsion flow of energy, where it is evident that energy losses can reach a value of up to 30% when it comes to

electric boats.

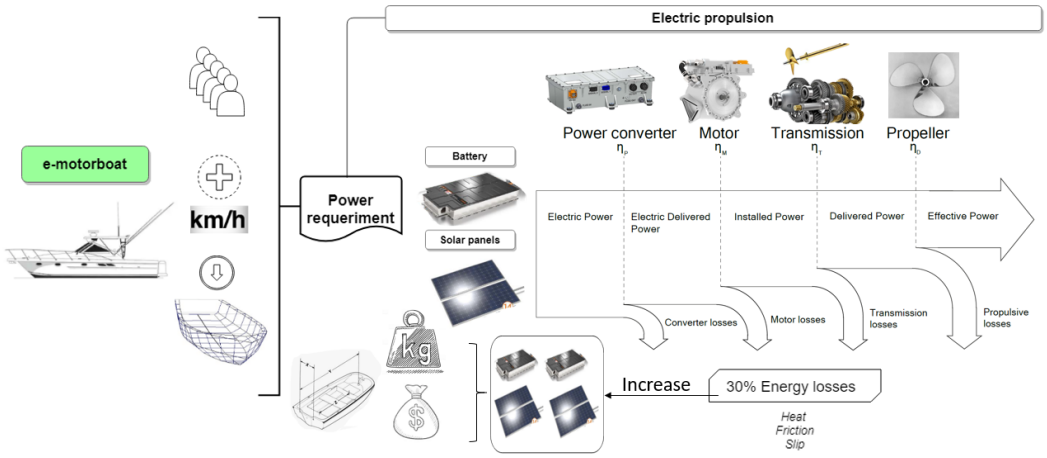

Figure 1.9: *Electrically-Power Vessel global considerations*

Now, if the same exercise was performed on boats that use ICE (whose losses reach 60% (Roberts et al., 2014)), it could be concluded that, in the best case, only 27% of the energy originally supplied in a combustion boat, is converted into effective thrust. This is why, in order to achieve the desired performance in traditional boats, the combustion systems are highly oversized and have high fuel intakes. This contrasts with the fact that fossil fuels and this type of non-renewable energy sources have a high energy density per unit mass, which can be translated into greater autonomy without the need for refueling (see Figure 1.10). Thus, the calculations lead us to identify that there is a 43% difference in efficiency in favor of electric propulsion systems vs combustion propulsion systems, and where, despite the low energy density in the batteries, there is a lot of potential for improvement due to the higher efficiencies in electrically powered systems.

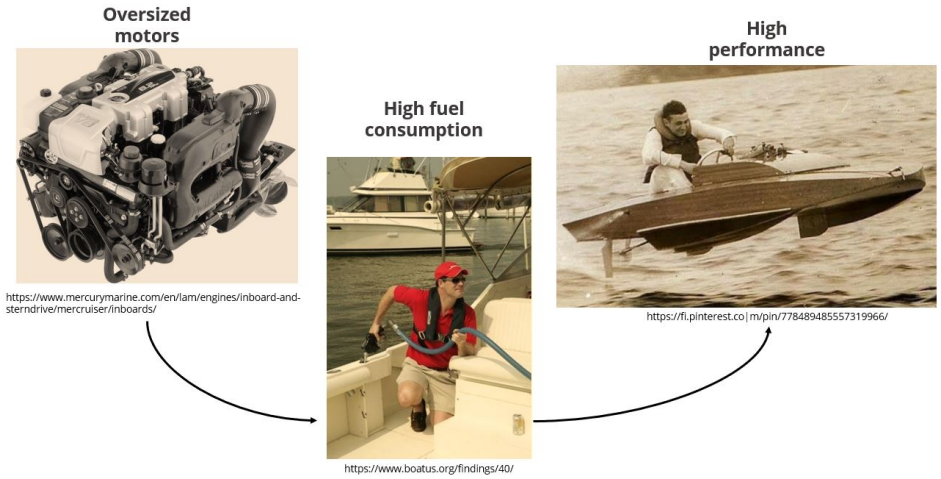

Figure 1.10: *Effects of the combustion propulsion chain*

Achieving performance characteristics of an electrically powered vessel, comparable to an ICE vessel, implies to optimize the operating conditions of the **Propulsion System (PS)** as design constraints. This operating conditions optimization is known as **"Matching"** and will determine the operating point of the PS. It consists in adjusting the operating curve of the propulsion machinery and the load experienced by the propulsion machinery. In boats design, the PS components (motor, transmission and propeller) must be adjusted, so that the power available at prime mover, matches the power required by the propeller in stationary conditions (Klein Woud and Stapersma, 2019).

The load experienced by the machinery is usually the load of the vessel's resistance to movement under its maximum draught(draft)[6]. However, in the case of inland waterway navigation, it may happen that the hull resistance and the service speed of the vessel vary significantly during operation. Therefore, in the process of designing the propulsion unit, it should be taken into account that the vessel should optimally respond to variations in the operating conditions. If the actual operating conditions of the ship are different from those assumed in the design procedure, the PS will operate with lower performance, with higher energy consumption, with engine power not fully utilized, or with the engine overloaded by torque or speed (Michalski, 2007). The matching determines the performance of ship sailing, and further influences the ship economy and emissions (Ren et al., 2019).

Some methods have been developed to estimate the amount of power that should be available for the operating conditions (drag and speed) as those proposed by Molland et al. (2017); Ghose (2004); Papanikolaou (2014); Birk (2019); Carlton (2018); Gillmer and Johnson (1982); Eliasson et al. (2014). They constitute the basic naval engineering literature and, since the first use of propellers as propellants in 1850, they have not changed (Ekinci, 2011). These methods are based on the calculation of the so-called "Interaction Parameters"[7] and are the basis of current developments. These interaction parameters seek to consider the efficiencies of the propulsion devices and the efficiency of their interaction with the hull of the vessel. Having at hand the performance information of all possible propulsion devices (propellers) is key to obtain success when applying these methods and that is why the design is usually performed with propeller diagrams developed from experiments with models. These diagrams-results summarize the performance information of each propeller and are tabulated in the literature, but reading errors during the use of these diagrams is inevitable, due to its high complexity. Additionally, these methods have a sequential type structure in which one step is

[6]**Draught** - The depth of the ship below the waterline measured vertically to the lowest part of the hull, propellers, or other reference point. When measured to the lowest projecting portion of the vessel, it is called the extreme draft, when measured at the bow, it is called forward draft, and when measured at the stern, the after draft (Gillmer and Johnson, 1982).

[7]The main interaction parameter is the **Quasi-propulsive (η_D)** coefficient and is defined as the ratio between the effective power and the power delivered to the thruster. This coefficient accounts for how much of the power that is delivered is converted into actual thrust of the vessel.

consecutively followed by another. So, an error in one of the stages can generate an erroneous result in a design context, where decisions of greater impact are made in early design phases, when there is less information and more uncertainties (Marques et al., 2019a; Ren et al., 2019). In fact, these estimation methods consider typical values tabulated in the literature for the efficiencies of each of the PS's components, so there may be differences when an estimate closer to reality is desired. In other methods, such as the one presented by Tupper and Rawson (2001), the concept of spiral design is proposed, where parameters in the design process are numerous and interrelated, complicating the design procedure of the PS (Tupper and Rawson, 2001; Ren et al., 2019).

When performing an analysis of existing methods and evaluating their use in the design of electric boats, it was found that there is a gap in finding references that address the matching of propulsion systems that make use of electric motors. Existing methods do not allow a comparative analysis between variables associated with different architectures and how these alternatives can influence the estimates and final results. Furthermore, energy efficiency is not a concern in the methods; they only provide an over-dimensioning in terms of the associated losses and additional estimated margins, supported by the possibility of fossil fuels to have a high energy density per unit mass. Additionally, there is uncertainty in the estimation stages of the required energy, which can generate a high impact at the moment of developing a PS for an electric vessel. Finally, applying this type of methodologies to the case of an electric boat design, may result in solutions that are not technically feasible or that require a considerable reduction of performance parameters or design demands.

Hence, it becomes evident that there is a close correlation in the design process of each of the components that make up the PS; correlation that if it is correctly established, it will lead to an efficient use of energy and where there is a closed loop between the different decisive performance variables. Each variable influences the design parameters of the next one and, therefore, its erroneous definition can have implications on the whole system performance. To improve energy efficiency, PSs design can be approached either (i) individually (usually by selecting a suitable propeller or engine operating point) or (ii) by optimizing the whole system simultaneously (understanding the ship and propulsion as an integrated system). This simultaneous approach, applied to the electrification of PS, has been identified as a research opportunity. The use of nowadays computational capabilities enable to obtain more accurate results in a faster way, by minimizing the margin of error. The scope of this research is limited to the use of information from: i) Permanent Magnet Synchronous Motor (PMSM) type motors, ii) transmission systems that make use of gearboxes and/or toothed belts, and iii) screw propeller type drives.

1.4 Research question

The previous sections address the gaps and challenges found in PSs design, oriented to the main barriers and aspects that influence energy consumption, which is a main concern in electrically powered vessels design for fluvial mobility. This becomes the main interest of this research and, therefore, the following research question has been set:

How to reduce the impact of losses to improve energy consumption in the design of propulsion systems for electrically-powered vessels?

1.5 Objectives

1.5.1 General objective

To develop a method for an optimal Motor–Transmission–Propeller matching through efficiency analysis in order to reduce energy consumption to foster the development of electrically-powered vessels.

1.5.2 Specific objectives

- To identify the methods that are currently used for the design of propulsion systems through an analysis of the state of the art to evaluate its applicability in an electrically powered river boat case of study.
- To characterize the different propulsion architectures through an efficiency chain that allows to identify the energy conversion points, their associated losses and physical variables that govern the performance of each component (Motor–Transmission–Propeller).
- To Develop a efficiency-based method by establishing orderly stages to simulate the architectures (Motor–Transmission–Propeller) and determine which one offers the best performance.
- Validate the developed method through a test cycle based on simulations of a river boat case study with electric propulsion in order to determine the efficiency gain with respect to the use of traditional methods.

1.6 Research Scope

An exploratory research approach is proposed where, according the literature , it was evident that there are shortcomings and limitations in what is currently developed in the state of the art, as well as the scarcity of PSs design methods for electric boats. Consequently, this project proposed a method with an efficiency based approach, that considers the impact of energy losses.

This PS design methodology is based on a multivariable optimization process to maximize the overall efficiency of the system that propels electric boats. An exhaustive search optimization algorithm with a holistic approach is developed (Rudolf et al., 2021; Miranda et al., 2016), used to provide a solution by exploring all possible values for the design variables, having a fixed hull design, a set of electric motors, a set of available propellers and different cruise speeds established under the interest of developing boats operating in the area of interference of the ENERGETICA 2030 project.

The availability of components is defined taking into account commercial and design constraints. The methodology here proposed seeks to run through all possible combinations by systematically varying the transmission ratio (key variable), the motor angular speed and the propeller, the set of candidates for this last element is defined from commercially available propellers. A tool for the design of PSs, is provided for boats' electrification, in which propulsion units (originally with ICEs) may be adapted, establishing the best operating point under the optimal values for design variables, when there are several options for choosing the components Motor–Transmission–Propeller. This is achieved through a polynomial regression of the information provided by the motor manufacturer (efficiency map), establishing the possible reduction ratio ranges, and mathematically modeling the design parameters that influence the performance of standard series of propellers, under the pitch, diameter and area constraints, developed by the commercially available propeller blades. The results are presented for each cruising speed as coordinates of RPMs-Reduction Ratio-Overall Efficiency values of the optimum combination. Also the power demand and vessel's range, under the desired operating conditions, are presented. Additionally, the model allows the visualization of 2D and 3D graphs of the global efficiency behavior during the different iterations. This allow designers to visualize the location of the optimal operating point on the map, for all possible operating scenarios and defining zones and desired ranges for design variables.

A final validation is developed by means of a test cycle, based on simulations, allowing a comparative analysis of the results, obtained with respect to a "Baseline" that, for this study, is the direct electrification [8] of a commercial outboard propulsion. This project is then concentrated in the motor–transmission–propeller triad, based on a given outboard propulsion unit (YAMAHA F100BETX). Additionally, as part of this manuscript, and applying some of the results obtained from this research, the design and manufacture of a fully functional prototype of an electric outboard propulsion unit is carried out in parallel. This prototype constitutes a verifiable instance of experimental execution that allows a better understanding of the phenomenon and the approach and formulation of improvement possibilities.

[8] **Direct electrification** is understood as the possibility for the designer to electrify or "retrofit" a propulsion unit originally designed to work with a combustion engine without modifying any constructive parameters and making use of the standard components and accessories used prior to electrification.

1.7 Research Approach

The methodology used is Research in Design Context (RiDC) (Horváth et al., 2007). This methodology allows to understand the relationship between the phenomenon, the research variables and the design requirements, framed within the context of the development of an electro-solar boat. The systematic process of application of this methodology seeks to explore, describe, understand and explain the phenomena that answer the research question.

The methodological cycle is developed in six stages that are executed in order: **(i) exploration, (ii) induction, (iii) deduction, (iv) verification, (v) validation and (vi) consolidation.**

The **exploratory** stage focuses on the study and analysis of the background within the field of research, identifying the gaps and delimiting the problem, in order to define the possible solution methods. In this stage the commonly used methods were identified for the design of PSs, based on an analysis of the state of the art, and were evaluated to see if they can be applied to the development of electric propulsion systems. Based on the aggregation of knowledge resulting from the exploratory stage, the **induction** phase starts, where the hypothesis of a model based on efficiencies is generated in order to later define the objectives and scope of the method in the **deduction** stage. Once the method is developed, a test cycle based on simulations was generated and which is contained in the **verification stage**, to then **validate** it with a comparative analysis with respect to a baseline that constitutes a direct electrification of a propulsion unit, to finally move on to the **consolidation** and generalization of the method.

Figure 1.11 presents the general structure that has been described as the methodological framework for this research.

1.8 Thesis organization

This research is structured in 7 chapters as follows.

This **Chapter 1**, described the research problem approaching it from the point of view of the technological development required to design and manufacture electric boats and how the optimization in the use of available energy is key to the design of this type of mobility solutions that contribute to reduce air pollution in countries with high water resources. The general and specific objectives as well as the methodology proposed for the research are also presented there.

Chapter 2, corresponds to the review and analysis of the state of the art, there is presented a theoretical framework that exposes basic concepts related to the design of propulsion systems for boats, in addition to an analysis of advantages and disadvantages of each of the possible types of architectures to be used in a boat. An analytical summary of the works developed around the methods for the design of propulsion systems and Motor–Transmission–Propeller matching is also presented, supported by

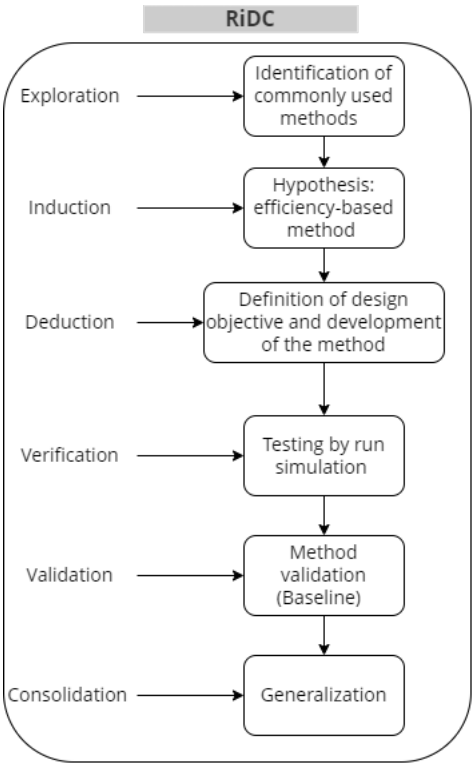

Figure 1.11: *Research Methodology adapted from Research in Design Context (Horváth et al., 2007)*

tables and graphs as a result.

Chapter 3 presents the development of the proposed methodology under the framework of the proposed objectives. It begins with the mathematical formulation to maximize the global efficiency of the propulsion systems with an approximation from the physical variables that define the performance of the different components, the previous product of a chain analysis of efficiencies. Subsequently, both the methodology and the proposed algorithm are presented describing in detail the three main steps of the methodology and how a part of the algorithm is executed in each of the steps.

Subsequently, **Chapter 4**, presents a case study applied to the electrification of a boat for the transport of people operating in the rivers of Colombia, generating an optimal choice analysis on a set of n=24 possible Motor–Transmission–Propeller combinations using the presented method. Here it is also presented, in Section 4.2, the final design of the functional prototype of the electric outboard unit to be implemented in the ENERGÉTICA 2030 project designed with the parameters that optimize the overall efficiency of the combination using the Wolong EG80 engine and the Yamaha F100BETX commercial outboard engine and that were suggested by the proposed method.

Chapter 5 presents the design results obtained from the application of the method for two speeds of interest, which are 47 km/h and 55 km/h in this case. These speeds are the average speeds reached by similar combustion boats operating in the area of interference of the ENERGÉTICA 2030 project

(Municipality of Magangué) and which are the main means of transportation for the people living there. Additionally, a comparative analysis of the results is presented when the electrification of commercial propulsion units is considered, preserving the design parameters originally established for the combustion power head. The methodology allows comparing the optimum values with the result of keeping the standard parameters of the unit to be electrified. For this purpose, the standard propeller provided by the manufacturer is used. The graphs of the results of the other combinations (23 non-optimal combinations) are included in **Appendix A**. Finally, **Chapter 6** presents the conclusions of the research and future work.

Chapter 2

State of the Art

This section addresses the basic principles for the design of ship propulsion systems and presents a summary of the state of the art and the works developed around the area of interest. Under a theoretical framework, which exposes the basic principles, it is intended to provide clarity and theoretical tools for the development of this research proposal. A global vision of the methods that have been implemented in the design of these propulsion systems allows to better delimit the hypothesis and generate a better value proposal.

2.1 Theoretical framework

It is important to start with the definitions of the general concepts necessary to understand the principles that govern the behavior and the establishment of variables in the design process of a propulsion system. These are presented below:

2.1.1 General definitions

In order to clarify the basic concepts and to set the basis of what is going to be proposed, the following concepts and definitions will be clarified:

- **Hydrodynamic resistance:** The fluid (water) force acting on a moving body in such a way as to oppose its motion
- **Prime mover:** The function of the prime mover is to deliver mechanical energy by converting electric energy contained in the batteries into mechanical energy. In traditional boats the prime mover may be a gasoline or diesel engine (ICE) mainly due to i) the ease of access to this type of fuel, ii) the massification of this type of engines (in these and other applications) and iii)

their technological development throughout history (Klein Woud and Stapersma, 2019; Birk, 2019; Molland et al., 2017).

- **Transmission:** Is the set of components such as shafts, gearboxes and bearings. The main function of the transmission is to transfer the mechanical energy generated by the prime mover to the propeller. Several types of transmission are used: direct (The prime mover is coupled directly, through a gearbox a shaft, to the propulsor), geared (the coupling between the prime mover and the impeller is through a gearbox and a shaft. The function of the gearbox is to reduce the rotational speed of the motor until it matches the desired speed of the impeller. Consequently the torque generated by the prime mover is amplified at the same rate as the rotational speed is reduced. A gear drive has the advantage of allowing the prime mover to operate at a much higher speed, however the prime mover is intended to be small, light and economical. The gearbox increases the volume, cost and weight) (Klein Woud and Stapersma, 2019; Birk, 2019; Molland et al., 2017).

- **Propulsor:** The propulsor converts the rotating mechanical power delivered by the engine into translating mechanical power to propel ship. The most common propulsor is the propeller, generally fixed pitch. The figure 2.1 presents a general overview of the main components of a propulsion system(Klein Woud and Stapersma, 2019; Birk, 2019; Molland et al., 2017).

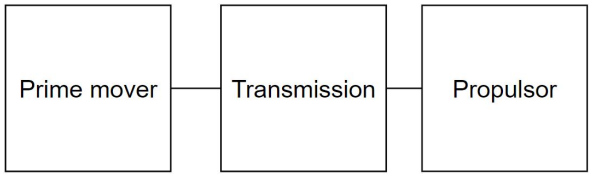

Figure 2.1: *Main components of a propulsion system*

- **Resistance:** Translation of a hull throught water requires a force.This force is called the resistance (Klein Woud and Stapersma, 2019; Birk, 2019; Molland et al., 2017).

- **Effective power (P_E)**: The effective power at any speed is defined as the power required to overcome the resistance of the bare hull at that speed. hull resistance at that speed, i.e., it is the energy required to tow the hull of the boat at a given speed and is the starting point for the speed and is the starting point for determining what the magnitude of the power requirements will be (Tupper, 2013).

- **Delivered power (P_D)**: The power delivered to the propeller $P_D = 2\pi TQn$ (Gillmer and Johnson, 1982).

- **Thrust power**: The power developed by the propeller thrust T at the speed of advance V_A. $P_T = TV_A$ (Harvald, 1992).

- **Speed of advance**: When a propeller behind a ship or model is producing the same thrust at the same rate of rotation as in open water the corresponding speed v A determined from the openwater propeller characteristics is termed the speed of advance of the propeller. This is usually less than the ship speed V_S (Lackenby, 1978).

- **Advance coefficient**: A parameter relating the speed of advance of the propeller V_A to the rate of rotation, given by $J = V_A/nD$, where D is the propeller diameter. The advance coefficient may also be defined in terms of ship speed V, in which case it is given by $J_V = V/nD$ (Lackenby, 1978).

- **Efficiency, hull (η_H)**: The ratio between the useful work done on the ship and the work done by the propeller or other propulsion devices in a given time that is effective power and thrust power respectively (Gillmer and Johnson, 1982; Molland, 2011; Birk, 2019).

- **Efficiency, propulsive or quasi-propulsive (η_D)**: The ratio between the useful or effective power and the power delivered to the propeller or the propulsion device P_D (Gillmer and Johnson, 1982; Molland, 2011; Birk, 2019).

- **Efficiency, propeller, behind hull (η_B)**: The ratio between the power developed by the thrust of the propeller and the power absorbed by the propeller when operating behind a model or ship (Gillmer and Johnson, 1982; Molland, 2011; Birk, 2019).

- **Efficiency, relative rotative (η_R)**: The relative rotative efficiency is the ratio of the propeller efficiencies behind the hull and in open water (Gillmer and Johnson, 1982; Molland, 2011; Birk, 2019).

- **Efficiency, propeller, open water (η_O)**: The ratio between the power developed by the thrust of the propeller and the power absorbed by the propeller when operating in open water with uniform inflow velocity.

2.1.2 Underlying principless

Throughout history, naval architects have striven to increase the speed of ships. Increasing speed allows, for example: i) a warship to get closer to its opponent or, conversely, to escape an attack, ii) merchant ships to reach port sooner and maximize the profit for their owner or iii) ship can make shorter voyages and increase its profit too. This provides comfort to users and makes possible to deliver goods that may need to be moved relatively quickly, such as perishable goods. Until the early 19^{th} century, wind was the force used to propel ships through the water and ships could only go as fast as the wind could propel them. In addition, because ships were built of wood, the structural limitations of wooden hull configurations meant that hull designs were primarily responsive to structural needs,

while hydrodynamics was only a secondary concern. Subsequently with the advent of steam propulsion in the early 1800s, and shortly thereafter in 1908, with internal combustion engines being incorporated not only as stationary propulsion units, but also as outboard combustion engines for small craft, naval architects realized that ship speeds were no longer limited by wind and began investigations into the power required to propel a hull through the water using these new means of propulsion (Santosh Raju and Niranjan Kumar, 2008; Łapko, 2019b; Siddall, 2019; Wells, 2007).

At this point it should be noted that steam engines and internal combustion engines caused a shift in the studies and research of naval architects to the study of the required power and electric propulsion systems for ships also made their appearance. The first experimental system of electric propulsion of ships appeared in the middle of the 19^{th} century and similarly, as in the case of the first electric cars, there was a possibility of wide dissemination of this propulsion system, thanks to the relatively simple construction of DC electric motors, their high efficiency and easy control, but unfortunately, this did not happen, because from the very beginning the main problem was the low capacity of batteries in relation to expectations (Łapko, 2019b).

In search of optimizing the efficiency of propulsion systems and the maximum use of the available energy, whether contained in a fossil fuel or in an electric energy storage unit such as batteries, hydrodynamic studies came to the forefront because the main way to reduce energy consumption in a vessel is to reduce its hydrodynamic resistance. This resistance determines, at the desired speed of displacement, the thrust required that must provide the propulsion device of the vessel. It is in this way that the concept of power is introduced in a vessel and is defined as the energy required to tow the vessel at the required speed. Its relationship is defined in Equation 2.1 where P is the effective power, R_t is the total resistance of the boat, and V_s is the boat's displacement speed.

$$P = R_t \times V_S \tag{2.1}$$

The electrical power at a given speed can be calculated using three different methods which allow for pre-estimation of performance and evaluation of design variables. The methods are listed below:

- Experimental: It includes real and reduced scale experiments with boats in open water, circulating water channels or towing tanks.
- Statistical methods: It groups all the equations derived from experiments aiming to relate the boat parameters and its operation variables with hydrostatic and hydrodynamic forces, such as drag and lift.
- Computational Fluid Dynamics (CFD): It is a more recent approach using computational resources to approximately solve the Navier-Stokes equations, which describe the behavior of water and air moving around the boat (Giraldo-Pérez et al., 2020).

Each of the methods has its advantages and disadvantages which focus on the time required for its development, costs and level of reliability, so it is usually used a comparison between the three to converge to a result. The CFD and statistical approaches have been extensively implemented in the resistance estimation of planing vessels and the high cost and high time consumption of experimental tests make both computational and statistical approaches more preferable in early design stage. The three methods seek to estimate the resistance or drag generated by the boat geometry and thus the force required to achieve its displacement. This force can be translated into effective thrust, required power and finally installed power. In particular the statistical model methods proposed by Crouch (Skene, 1973), Wyman (1998), Savitsky et al. (1964) and L. Blount and L. Fox (1976) have been in practical use for years (Giraldo Pérez et al., 2021). In the case of Savistky and Blount-Fox, the calculated drag leads to the effective power (P_E) to be delivered by the propeller. In contrast, Crouch relates the operating conditions to the power delivered and Wyman, in turn, uses the installed power (P_{EL}).

This is then the way in which naval architects can know the resistance of the ship and thus be able to iterate on the geometry of the hull in order to reduce the power required and therefore the energy consumption for its displacement. After knowing the power based on the calculated resistance of the vessel and the desired displacement speed, the naval architects move on to the design of the propulsion system. Each step of the design of this system and the establishment of variables is decisive to take maximum advantage, not only to the optimal design of the hull, but also to the use of the energy that will be available in the boat. Here, the different components that make up the propulsion unit (Motor–Transmission–Propeller) must be considered and how each of them influences the energy conversion. The energy, which in the case of an electric boat will come from batteries, is converted into mechanical energy to drive a propeller, and as each of the components comes into action there are energy losses due to friction, heat and slippage. These losses cause an increase in the energy demand to be installed, in order to obtain the desired parameters and operating points. Figure 2.2 illustrates the energy flow and the presence of energy losses as efficiencies, considering power converter losses, electric motor losses, transmission losses and finally propeller losses.

Typical values of efficiencies that can be found in the literature are summarized in Table 2.1, these can be used for preliminary unit calculations.

Due to those losses, the power delivered by the propulsion unit exceeds the effective power by virtue of the fact that the efficiency from the engine to the propeller is less than 100%. Thus (see equation 2.2),

$$\text{Effective power} < \text{Delivered power} \tag{2.2}$$

The total “installed power” will exceed the “delivered power” due to loss in the drive system

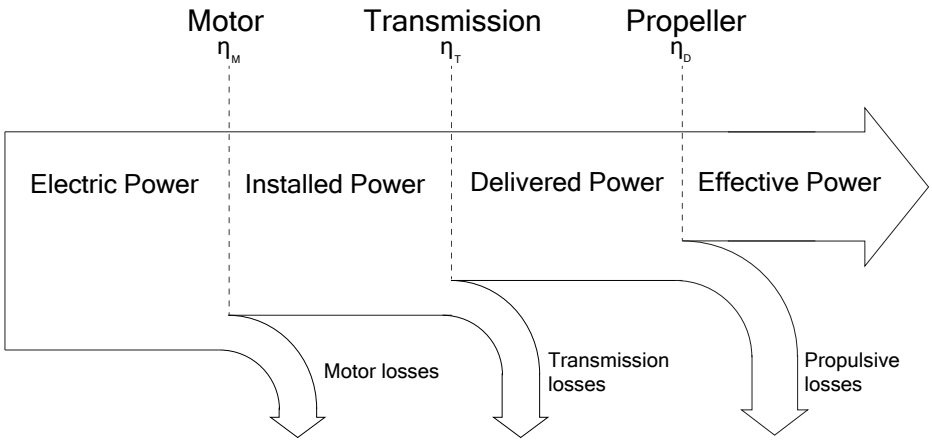

Figure 2.2: *Power losses due to efficiencies in the propulsion system.*

Table 2.1: *Typical range of efficiencies*

Component		Efficiency
	Power converter η_P (Lee, 2001)	98%
	Motor η_M (Lu, 2016a)	95%
Transmissions	Gears η_T (Molland, 2011; Ehsani et al., 2010)	95%
	Shaft η_H (Molland, 2011; Carlton, 2007; Birk, 2019)	98%
	Propeller (Molland, 2011)	70-75%

(shaft or gear losses), losses in the motor, and by an additional design power margin that takes into account random phenomena such as weather, wind, shallow water, and tides; this additional margin generally ranges from 15%-30% (Molland, 2011). Finally, the overall ratio of efficiencies for an electric propulsion system is shown in equations 2.3 and 2.4

$$\text{Installed Power } (PI) = \frac{\text{Effective power } (PE)}{\eta_D} \times \frac{1}{\eta_M} \times \frac{1}{\eta_T} \times \frac{1}{\eta_P} additional\ margin \tag{2.3}$$

$$\eta_D = \frac{\text{Effective power } (PE)}{\text{Delivered power } (PD)} \tag{2.4}$$

Where

η_D = is known as the quasi-propulsive coefficient

η_M = is the efficiency of the engine

η_T = is the efficiency of the transmission

η_P = is the efficiency of the power converter

This shows how the overall efficiency of a propulsion unit and the sizing of the power to be installed depends on each of the energy transformations carried out in each of the components of the unit. As shown in table 2.1, the propeller is the component that has the greatest commitment in the overall efficiency of the unit, since its efficiencies reach a maximum of 75%. A correct design or selection of this component is determinant in the performance of the unit, that is why the models and methods for the design of propulsion systems have this element and its design variables as a central axis. All propulsion devices operate on the principle of imparting momentum to a "working fluid" in accordance with Newton's laws of motion. The force required to produce the momentum change in the working fluid appears as a reaction force on the propulsion device, which constitutes the thrust produced by the device (Molland, 2011). Thrust is the result of change in momentum of the fluid from a point ahead of the propeller to a point astern of the propeller (Gillmer and Johnson, 1982). Suppose the fluid passing through the device has its speed increased from V_1 to V_2 by the device, and the mass flow per unit time through the device is $\dot{m}$, then the thrust T produced is given by the Equation 2.5,

$$T = \dot{m}(V_2 - V_1) \tag{2.5}$$

The momentum change can be produced in a number of ways, leading to the evolution of a number of propellant types. When a propellant is introduced at a location on the vessel it modifies the flow around the hull at the point of location, generally they are located at the stern (rear) of the vessel. This causes an increase in the drag experienced by the hull. It also changes the wake initially generated by the bare hull and therefore the average water speed through the propellant which will not be the same speed as the boat in the water. These two effects are taken together as a measure of hull efficiency. The other combination effect of the hull and propulsion unit is that the flow through the propeller (propeller or a variation thereof) is not uniform and is generally not directed along the propeller shaft. The ratio of the propeller efficiency in open water to the propeller located behind the ship is called the relative rotational efficiency. The aforementioned losses are quantified through the quasi-propulsive coefficient given in Equation 2.4 of this chapter. The values for the losses in the power transmission and between the main machinery and the propellant were summarized in Table 2.1 (Tupper, 2013). To estimate the quasi propulsive coefficient of the propeller it is then expressed as a function of the

components of efficiencies in equation 2.6 and 2.7 :

$$\eta_D = \eta_O \times \eta_H \times \eta_R \tag{2.6}$$

$$\eta_H = \frac{1-t}{1-w} \tag{2.7}$$

Where

η_O = is the open water propeller efficiency
η_H = is the hull interaction efficiency
η_R = is the relative rotational efficiency
t = is the thrust deduction factor
w = is the wake factor

The thrust deduction factor t accounts for the change in the drag of the vessel due to the presence of the submerged propeller or thruster and is understood as an increase in drag being an additional submerged appendage or surface that opposes the motion of the vessel, since some of the thrust from the propeller is used to compensate for the increased drag this effect is named thrust deduction. The w factor or wake fraction accounts for how much the propeller performance is affected by the presence of the hull ahead of it, which modifies the velocity of the fluid around it creating a wake that disturbs the fluid ahead of the propeller. The factors w and t are defined as shown in equations 2.8 and 2.9.

$$w = \frac{V_S - V_a}{V_S} \tag{2.8}$$

$$t = \frac{T - R_T}{T} \tag{2.9}$$

Where

V_S = is the displacement velocity of the vessel
V_a = is the average advance velocity of the propeller
t = is the thrust generated by the propeller
R_T = is the total drag

The average advance velocity of the propeller differs from the velocity of the vessel (V_a<V_S), and this difference in velocities is the result of the fluid shear caused by the acceleration towards the stern or rear of the vessel of the water mass ahead of the propeller and is known as the **Slip Ratio**.

Additionally the **Slip Ratio** is given by the Equation 2.10, where P is the pitch (fixed advance distance per turn) and n is the angular velocity of the propeller rotation (Gillmer and Johnson, 1982).

$$\text{Slip Ratio} = \frac{Pn - V_a}{Pn} \tag{2.10}$$

Thrust deduction and wake phenomena often have the opposite effect and tend to cancel each other out. There is a high degree of complexity in determining the deduction factors involved in calculating the effective power and efficiency of a propellant that is affected by the passage of fluid through it, many of these losses evade the possibility of accurate analysis and there is no completely satisfactory method of analysis for quantitative measurement of these factors (Gillmer and Johnson, 1982).

One approach for the designer is to use the best available figures from power tests of similar ships, based on experience and verifying where design differences exist. Self-propulsion model tests, where Ad-Hoc facilities are available, provide the required factors. These tests consist of fabricating a scale model of the ship together with its propulsion unit and instrumenting the model, to subsequently perform a scaling of the effects through relationships such as Reynols (Re) or Froude number (Fr). With the development of computation the current calculation methods focus on CFD analyses, that allow rapid processing of data providing substantially less opportunity for error.

Experimental models have also been developed for propellers, which consist of measuring the performance characteristics of the propellers in a tank by means of a towed mechanism or a cavitation tunnel, providing efficiency, thrust and torque curves. The most commonly tested propellers are the Wageningen B-series propellers and the Gawn series, making it possible to have a range of possibilities. The Wageningen B-Series is a general purpose series, was developed in the mid-20$^{\text{th}}$ century and is the most extensive propeller series, the name refers to the city of Wageningen, which is home to the Netherlands Ship Model Basin (NSMB), they are also known as Troost-Series in Birk (2019). The series comprises a total of 120 propellers with systematic variations of Blade Number (Z), Blade Area Ratio (A_E/A_O) and Pitch Ratio (P/D). The Wageningen B-Series propellers use aerofoil cross-sections. Ogival sections have been used from radius= 0.6 to the blade tip (Birk, 2019; Ekinci, 2011). The Gawn series is a set of 37 three-bladed propellers with (P/D) between 0.4 and 2.0 and expanded area ratios AE/AO from 0.2 to 1.1. Their extended blades are elliptical in shape and only ogival sections have been used. Although the geometry is old-fashioned, this series is important because its model propellers are exceptionally large at 20 in (508 mm) diameter, by this means many of the scale effects associated with the smaller diameter propeller series have been avoided (Birk, 2019; Carlton, 2018). This series also covers a wide range of P/D , making it applicable to high-speed craft (Carlton, 2007). Each of the propellers has a uniform face pitch, segmented blade sections, constant blade

thickness ratio (namely, 0.060), and a 0.2D overhang diameter. The propeller parameters for the different series, such as number of blades Z, propeller blade area ratio AE/AO and pitch ratio P/D are systematically modified in equations 2.11 and 2.12 in order to obtain the maximum efficiency for a given advance coefficient (J), equation 2.13.

$$K_T = \sum_{s,t,u,v} C^T_{s,t,u,v} \left(J\right)^s \left(P/D\right)^t \left(A_E/A_O\right)^u \left(Z\right)^v = \frac{T}{\rho n^2 D^4} \tag{2.11}$$

$$K_Q = \sum_{s,t,u,v} C^Q_{s,t,u,v} \left(J\right)^s \left(P/D\right)^t \left(A_E/A_O\right)^u \left(Z\right)^v = \frac{Q}{\rho n^2 D^5} \tag{2.12}$$

$$J = \frac{V_a}{nD} \tag{2.13}$$

The regression coefficients C^T , C^Q and the s, t, u and v terms are presented in Molland (2011). The large amount of accumulated data on performance characteristics, containing accurate trends of energy losses for a multiplicity of designs, now provides opportunities for much more comprehensive analyses. An additional degree of complexity encountered in designing the propulsion unit is the calculation of the power delivered to the propeller (because at this point the propeller shaft is outside the ship and it is impractical to make torque measurements under operating conditions). However, the designer can arrive at an estimate of the power delivered by the propulsion unit to the propeller, with only a slight decrease in confidence, by adding the best estimates of fluid losses through the propeller to the effective power and calculating: i) the support bearing or stern tube losses, ii) progressing through the inner shaft bearings and gear losses.

2.1.3 Architectures and configurations

As explained in the general definitions section, the propulsion system is composed of three elements: the prime mover, the transmission and the propeller. These three components can be configured under different types of architectures which preserve this structure and give designers, depending on the context, the possibility to generate multiple solutions to propel the vessel. Below is a description of each different type of architecture along with a comparative analysis of advantages and disadvantages.

2.1.3.1 Inboard

An inboard engine is the one installed inside the boat, in a fixed way, and whose transmission is also housed inside the boat (see Figure 2.3). In this type of transmissions the propulsion direction is given by the rudder, installed independently of the engine installation, something that differentiates them notably from inboard-outboard and outboard transmissions. Boats that are equipped with this architecture are very diverse. From conventional wooden boats used by fishermen for decades, to the

most modern boats for water sports such as skiing, to luxury yachts and large merchant ships. As can be deduced, this is the most common type of transmission and covers a wider range of possible vessels in which to be installed. That is why there are multiple variants, depending on the boat in which it can be found. These differences arise mainly between the propeller and the coupling that joins the inverter to the shaft.

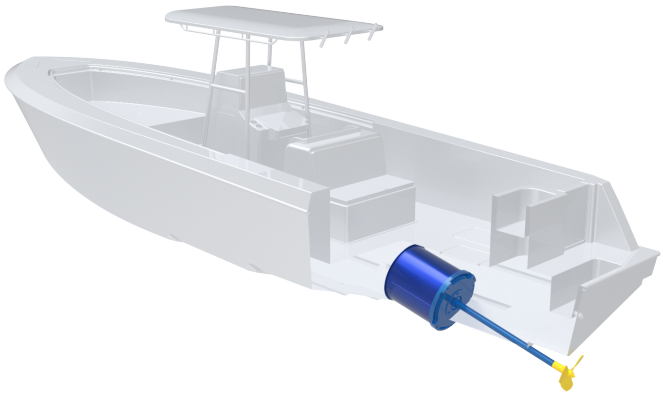

Figure 2.3: *Inboard configuration*

2.1.3.2 Outboard

Outboard engines are the most suitable choice for fishing boats and light to medium weight commercial vessels. Outboard engines are mounted on the outside of the boat, high on the transom, and can be tilted completely out of the water, making them very easy to service and, if necessary, replace (see Figure 2.4). With primarily positive attributes, outboards are limited to certain power ranges (50-250 HP). To obtain, or match, the power produced by an inboard motor, there must be several outboard motors mounted on the transom. To steer an outboard, the entire motor must be moved. On smaller boats, this is often done using a manual tiller, while on larger outboards a steering wheel adjusts the direction of the motor.

2.1.3.3 Water Jet

Water jet propulsion is often chosen instead of conventional propellers for boats that require high speeds, shallow water operation, protected propulsion, high maneuverability at all speeds, low noise emissions and low vibration (maritime affairs, 2019). This type of propulsion has become more common in recent years for high-speed boats. Water is drawn into the vessel and then pushed outward to the stern to develop thrust. The ejector unit can be steered to give direction to the thrust so it

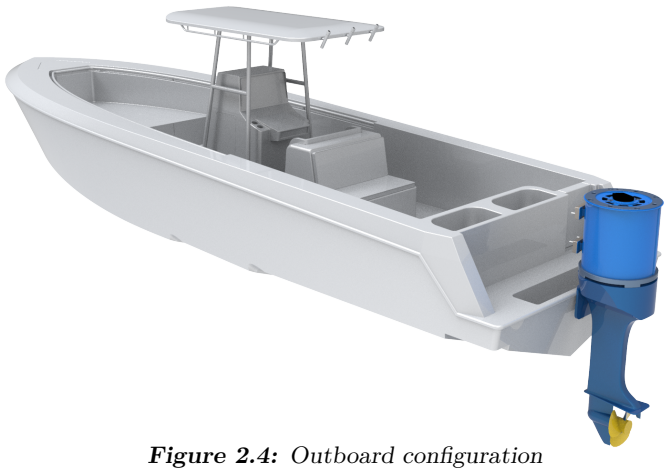

Figure 2.4: *Outboard configuration*

allows vectored thrust (see Figure 2.5). It is attractive for vessels where it is desirable to have no moving parts outside the hull. The Water jet can be discharged above or below the water (Tupper, 2013). The reason for the infrequent use of the Water jet, compared to the screw propeller, initially occurred because the propeller was generally considered to be a simpler, lighter and more efficient propulsion element. However, the introduction of more efficient pumps and increased commercial demand for higher speed craft are the main reasons for its rapid growth (Carlton, 2007).

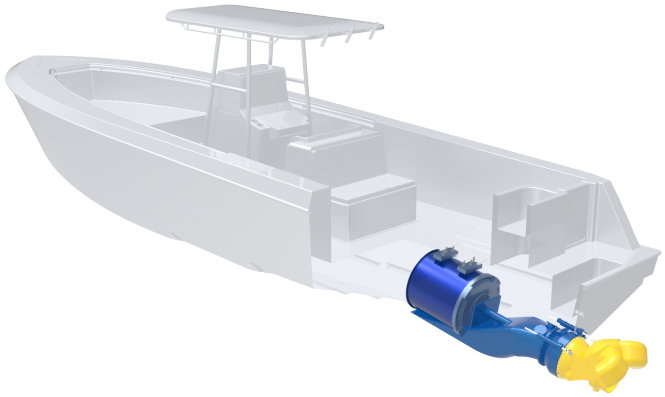

Figure 2.5: *WaterJet configuration*

Water jet propulsion has superior performance advantages over propeller propulsion for high-speed vessels at speeds of 30+ knots due to its high efficiency and good maneuverability characteristics. Unlike a propeller that transmits the force of its blade to the hull through the shaft, the principle of thrust generation and transmission for a Water jet drive is somewhat different. Thrust is not

only transmitted through the shaft: some of the thrust is also generated in the drive channel and transmitted directly to the hull body (Brown and Li, 2015).

The Water jets installed on multi-hull vessels are located in the compartment next to the transom and comprise a shallow, cone-shaped inlet duct, curved to a section of the pump and stator leading to a nozzle. The geometry of the duct is normally fixed, although some high-speed vessels have had a movable lower lip for the intake which achieves improved low-speed performance of the vessel. The intake is designed to take water from the bottom of the vessel and deliver it to the pump in such a way that as it enters the pump rotor, cavitation is avoided. The pump then accelerates the water to provide thrust. Depending on the speed and size of the vessel, the pump may be axial flow, mixed flow or, when speeds exceed 50 knots, a two-stage pump, where the first stage rotor is a helical inducer to raise the "static" pressure head of the main rotor. Unlike a free propeller, a water jet operates inside a fixed duct like a pump. The inlet duct sucks water from the flow under the hull and directs it into the pump impeller, where energy is added in a similar way to a free propeller, except that the blade tips cannot generate free vortices, so the blade acts more like a wing with an infinite span (Yun et al., 2018)

2.1.3.4 Azimuth-Podded

These are propellers mounted in a housing, or capsule, that can rotate 360° about their own axis to give thrust in any direction. Early applications were limited to tugs that require good maneuverability, today, a number of large ships, including cruise ships are equipped with azimuth electric propulsion, these are powered by diesel engines connected to a generator, this provides the possibility of mounting large capsules which are essentially electric motors submerged under a packing nose and driving a propeller connected directly onto the central shaft of the engine (see Figure 2.6).

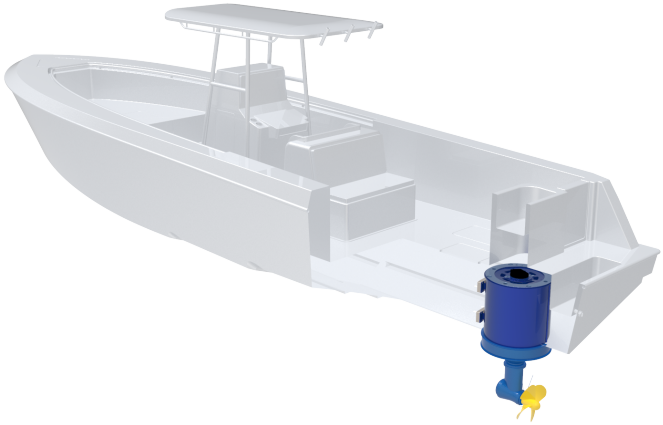

Figure 2.6: *Azimuth-Podded Configuration*

Units transmitting 5-8 MW of power are typical, but units of about 15 MW have been installed on large cruise ships. Large fast container ships are also candidates for the use of Azimuth-Podded units. As mentioned above the propeller is mounted on the rotor and sometimes two propellers are mounted on the same shaft, one forward and one aft of the pod, this allows a larger blade area. There is another configuration in which the two propellers are mounted independently, using two Azimuth-Podded motors (Tupper, 2013).

2.1.3.5 Rim-Thruster

The Rim-Thruster, a novel integrated propulsion system also called a shaftless rim thruster, is a marine propeller that does not require a shaft or gearbox for torque transmission (Tan et al., 2015). In this propulsion system a propeller-type impeller is structurally integrated into an electric motor system; the motor stator is mounted in the duct while the rotor forms a ring around the rim of the propeller (see figure 2.7). The rotor and stator are coated with epoxy material and sealed by a waterproof metal can respectively. The entire unit operates submerged and only the electrical cables pass through the hull of the ship. As a new type of electric propulsion for boats, the integrated propeller and electric motor in the Rim-Thruster make this a revolutionary and highly innovative system. The Rim-Thruster can be designed as fixed, retractable, and/or azimuthing (Yan et al., 2017).

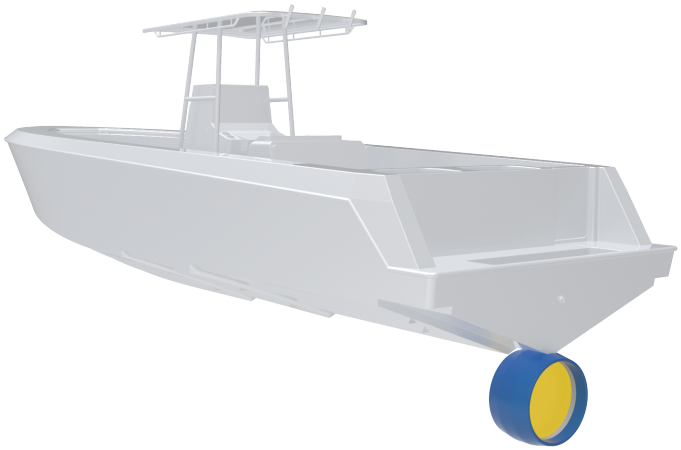

Figure 2.7: *Rim-Thruster configuration*

The Rim-Thruster does not require an engine cooling system and, therefore, it does not need power to run such a system. It uses water-lubricated bearings instead of oil-lubricated bearings. The energy consumption of the ship's lubrication systems is therefore reduced (Yan et al., 2017). This type of architecture is mostly used in side-thrust thrusters for ships as they provide high torque values (Yan et al., 2017). Some other advantages of the Rim-Thruster are:

- Compact design, which saves space inside the case and allows for greater flexibility in installation and layout.
- Increased motor efficiency (Van Blarcom et al., 2002)
- The motor rotor, which is usually of the permanent magnet configuration, is mounted on the rim around the propeller, allowing the motor to produce higher torque and thus operate at lower RPM. The low RPM results in a low relative speed over the blades, which contributes to good efficiency and mitigation of cavitation phenomena.
- Increased hydrodynamic efficiency (Lea et al., 2003), when scale comparisons are made with other models. The maximum open-water efficiency of a Rim-Thruster and is 67.2% (Yan et al., 2017).

2.1.3.6 Architectures analysis

Each type of propulsion engine and propellant has its own advantages and disadvantages, possibility of applications and also limitations, including those fundamental attributes such as size, cost and efficiency. All of the above propulsion options (Inboard, Outboard, Rim-Thruster, Azimuth-Podded, Water jet) are in use today and the choice of a particular propulsion engine and thruster will depend on the type of vessel, hull geometry and available space, together with design and performance requirements (Molland, 2011). Assuming electrical propulsion for these architecture alternatives, Figure 2.8 shows, for each type of architecture, the general configuration of the different constituent elements. This allows to clearly identify the number of components and internal mechanisms for each type of propulsion.

In order to summarize the different characteristics that qualify the different architectures in terms of advantages and disadvantages, a comparative table is prepared for the different alternatives described in the previous section (see Figure 2.9).

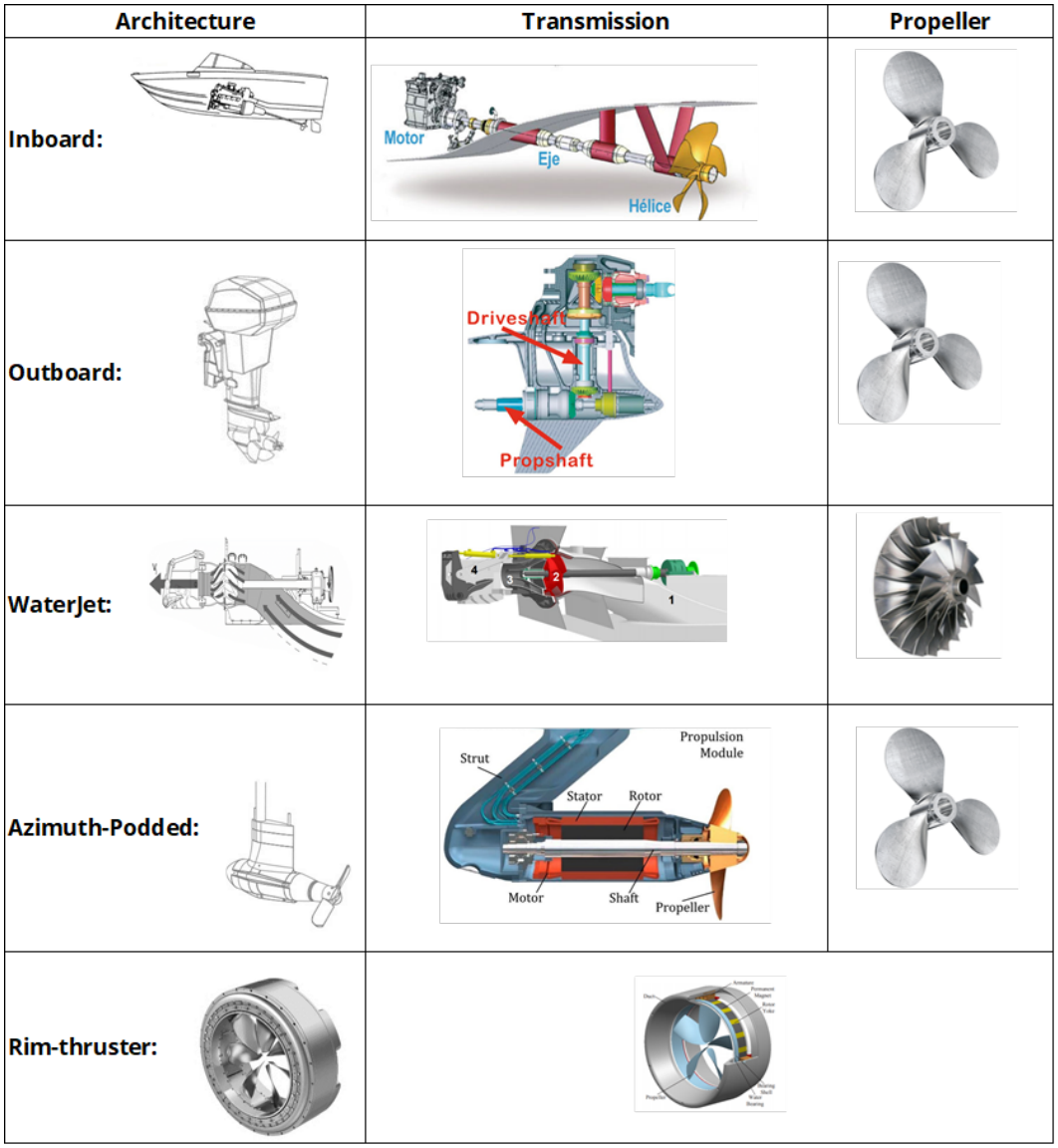

Figure 2.8: *Constructive elements of the different architectures (Pan et al., 2016; Chasiotis and Karnavas, 2019)*

Architectures Propulsion Unit					
	Outboard: 	**Inboard:** 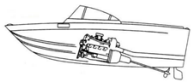	**Azimuth-Podded:** 	**WaterJet:** 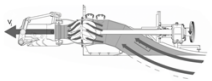	**Rim-Thruster:** 
Advantages	Easy access to the drive unit (M-T-H)	Possibility of incorporating large motors	Provides high manoeuvrability at low speeds (360° thrust vectoring - turns)	Shallow water operation	Designed to transmit high torque (more thrust, less drive)
	Vectorized Thrust	High power ranges		Protected drive element (impeller)	
	Possibility to rise completely out of the water	They serve as the vessel's ballast (CM)		High manoeuvrability at low speeds	Reduced energy losses due to fewer mechanical elements
	Simplicity of maintenance activities	Better weight distribution and control over the effects of this force on stability	Water cooling (no pumping subsystems required)	Absence of submerged appendages, thus reducing the resistance of the boat	
	Freeing up space inside the boat		Reduced energy losses due to fewer mechanical elements	Safety for people underwater around the boat	Unit Portability
	Unit Portability (Spare Parts)	Incorporates deeper propellers which reduces the risk of cavitation	The smallest space required inside the main hull	Low noise levels	Water cooling (no pumping subsystems required)
	Low draught (surface draft)		Greater freedom to position the propeller and develop the shape of the hull for greater efficiency	Reduced number of moving parts	
Disadvantages	The dimensions and thickness of a boat's transom will limit the size of the outboard that can be connected	Low portability (Spare)	High draught required	Difficulty of access to the unit	High cost of acquisition and repair
		Increased difficulty for maintenance activities	Increased difficulty in accessing the drive unit	High cost of acquisition and repair	Limited commercial power range
		Fire Risk Factor	Essential component of the boat exposed to a high risk of damage	Efficiency loss at low speeds (<30 knots)	Difficulty in accessing the motor unit
	Effect on weight distribution	Decrease in available space inside the boat		Possibility of obstruction due to river or marine elements	Complexity of maintenance activities
	Limited power ranges	Limited maneuverability (rudder required)	Complexity of maintenance activities and high intervention costs	They normally tend to be heavier than conventional propeller-based systems	Essential component of the boat exposed to a high risk of damage
	Propellers closer to the surface, which increases the risk of cavitation	Need for deeper draft			
own elaboration from: [Carlton, 2007; Molland, Turnock, & Hudson, 2011; nautical ventures, 2018; Statistical Surveys LCC, 2015; Tupper, 2013; Williams, 2017; world maritime affairs, 2019; Yun, Bliault, & Zong, 2019]					

Figure 2.9: *Comparative advantages and disadvantages for different propulsion architectures*

The result of this comparison is that the **Outboard** architecture is the one that provides more available space inside the boat. This is something that can be harness for battery storage, in the case of electric boats. Additionally, this architecture provides greater portability since it is an external unit that is easy to replace and facilitates maintenance activities. The disadvantage of this architecture is that being located at the rear of the boat can affect the weight distribution which can be compensated to some extent with the possibility of modifying the trim[1] of the boat by having the possibility of having vectored thrust, not only for turning maneuvers, but also for lifting the bow. Its power ranges are limited by the size.

On the other hand, the **Inboard** architecture allows the possibility of incorporating higher power engines that also serve as ballast for the boat. There is the possibility of having a better weight distribution and control of its effects on the stability of the boat with the use of this architecture. The disadvantages are the reduction of the available space inside the hull and the reduced maneuverability compared to other architectures, since a submerged rudder is required for steering.

On the other hand, the **Azimuth** architecture is the one that provides the widest range of maneuverability (360°). At low speeds it allows lateral displacement of the vessel. Being a fully submerged unit reduces the risk of cavitation and does not require cooling systems. The disadvantages are that, for shallow water applications, its use is limited since the essential component of the vessel would be at risk of damage due to collisions. Its maintenance activities are much more complex than the other architectures described so far and may involve high costs.

The **Water jet** architecture is the most appropriate for vessels operating in shallow waters and offers good maneuverability characteristics and can be easily reversed. There is an absence of submerged appendages which reduces the resistance of the vessel and has low noise levels. The main disadvantages of this architecture are that there is the possibility of obstruction by river debris and they tend to be much heavier than other propulsion architectures. For vessels traveling at speeds of less than 30 knots they are inefficient.

The final product of this comparison is the **Rim-Thruster** architecture. This architecture is the most modern of all, specifically designed to make use of an electric motor. Its advantages are its use in applications that demand high torques, which is why it is commonly used for the lateral movement of large ships. There is a decrease in energy losses due to the smaller number of parts. As disadvantages it has its high acquisition and maintenance costs along with the possibility of being affected by shallow draft operations.

Up to this point, the basic principles for the design of ship propulsion systems have been exposed

[1] **Trim**: When the boat is on a plane, the bow rise is known as the boat's trim. trimming results in less drag and greater stability and efficiency. Normally the keel line of the boat rises between 3 and 5 degrees (Yamaha Motor Co., 2002)

and how the studies developed around their design have been gaining more and more relevance. The following section presents the results of the analysis of the state of the art about the methods that seek to obtain the best Motor–Transmission–Propeller matching by means of information search strategies that allow to obtain the research gap.

2.2 Related works:information search strategy and analysis of state of the art

In order to identify the developed works in the literature, around the development of electric boats and their propulsion systems, in addition to the search of the optimal Motor–Transmission–Propeller configuration, two strategies of information search are proposed:

- The first strategy (see Figure 2.10) intends to understand a holistic approach about boats' developments, with emphasis on electric boats and their propulsion systems. Generic search terms were used, such as " Propulsion Systems Design", Electric Boats", " Electric Propulsion Systems" and " Motorboat Electric Mobility", This search strategy produces as main result the literature baseline of naval design and architecture. The search limits in terms of dates were set from 1870, when the first electric boat is recorded to have appeared, to the year 2021. The main sources of information were established as books, databases, journals and patents. This strategy allows the appropriation and clarification of the necessary knowledge for the development of this type of systems. As a result of this strategy, the comparative analyses presented in section 2.1.3.6 of this chapter, among others, were elaborated and allowed the design team of the ENERGÉTICA 2030 project to have more criteria when evaluating the different alternatives for the development of the propulsion prototype to be implemented.

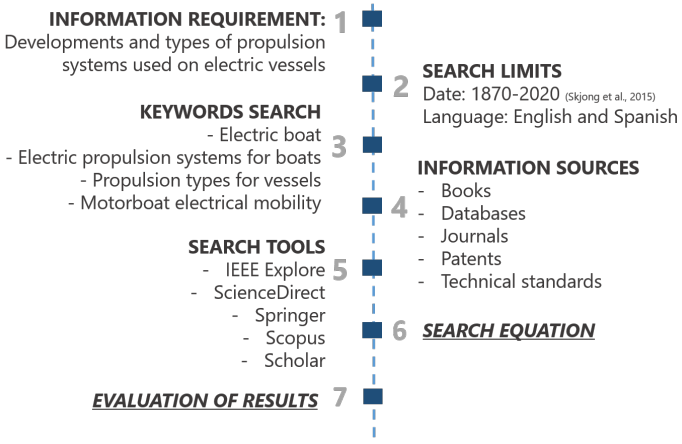

Figure 2.10: *Information search strategy # 1*

- The second search strategy (see Figure 2.11) explores specific results about methods developed for the estimation and calculation of efficiencies in the design of electric boat's PSs. With more specific search terms such as "Model", "Method", "Efficiency Analysis" and "Propulsion", this strategy focuses its information sources on databases and journals working on these topics. The search limits were established between 1990 and 2021, because between these years there was a record of an accelerated growth of the fleet of electric boats in the world, thanks to advances in power electronics. Scopus, IEEE Xplore and Google Scholar, among others, were defined as the main search tools.

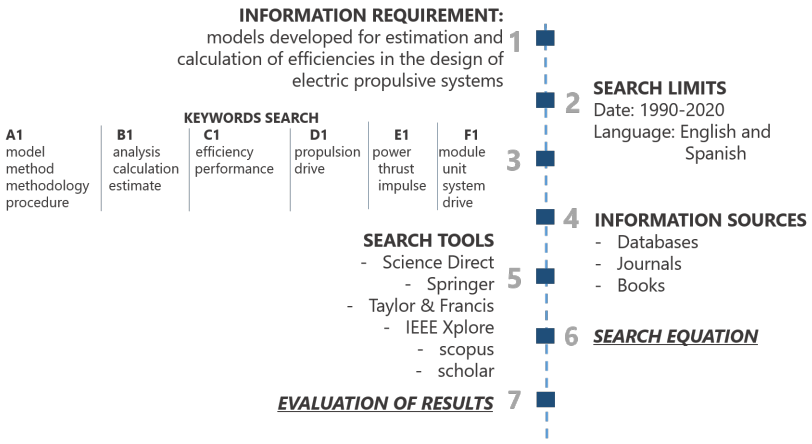

Figure 2.11: *Information search strategy # 2*

With the 18 defined search terms and making use of Boolean logical operators, 12 information search equations are proposed, which are listed in Table 2.2 and are run in primary information sources (books, current scientific journals, technical standards).

Table 2.2: *Search equations*

Item	Equation
1	model **AND** (analysis **OR** calculation **OR** estimate) **AND** (Efficiency **OR** performance) **AND** propulsion **AND** module **AND** electric vessel
2	methodology **AND** (analysis **OR** calculation **OR** estimate) **AND** (Efficiency **OR** performance) **AND** drive **AND** unit **AND** electric ship
3	method **AND** (analysis **OR** calculation **OR** estimate) **AND** (Efficiency **OR** performance) **AND** power **AND** system **AND** electric boat
4	procedure **AND** (analysis **OR** calculation **OR** estimate) **AND** (Efficiency **OR** performance) **AND** thrust **AND** drive **AND** vessel
5	model **AND** (analysis **OR** calculation **OR** estimate) **AND** (Efficiency **OR** performance) **AND** impulse **AND** module **AND** ship
6	methodology **AND** (analysis **OR** calculation **OR** estimate) **AND** (Efficiency **OR** performance) **AND** propelling force **AND** unit **AND** boat
7	method **AND** (analysis **OR** calculation **OR** estimate) **AND** (Efficiency **OR** performance) **AND** propulsion **AND** system **AND** vessel
8	procedure **AND** (analysis **OR** calculation **OR** estimate) **AND** (Efficiency **OR** performance) **AND** drive **AND** drive **AND** ship
9	model **AND** (analysis **OR** calculation **OR** estimate) **AND** (Efficiency **OR** performance) **AND** power **AND** unit **AND** boat
10	methodology **AND** (analysis **OR** calculation **OR** estimate) **AND** (Efficiency **OR** performance) **AND** thrust **AND** module **AND** vessel
11	method **AND** (analysis **OR** calculation **OR** estimate) **AND** (Efficiency **OR** performance) **AND** impulse **AND** unit **AND** ship
12	procedure **AND** (analysis **OR** calculation **OR** estimate) **AND** (Efficiency **OR** performance) **AND** propelling force **AND** module **AND** boat

A total of 120 references were obtained, including articles and books, that were filtered to 13

references that contains the most relevant advances in the area were selected. This was done by means of a systematic process of debugging that took into account the number of cross references, date of publication (giving priority to the most current ones), number of citations, publication ranking and basic methodology of the implementation. The information is subdivided in such a way that those references can be classified by type of vessel (focused on, whether displacement, semi-displacement and planing[2]) and also by type of propulsion architecture, as depicted in Figure 2.12.

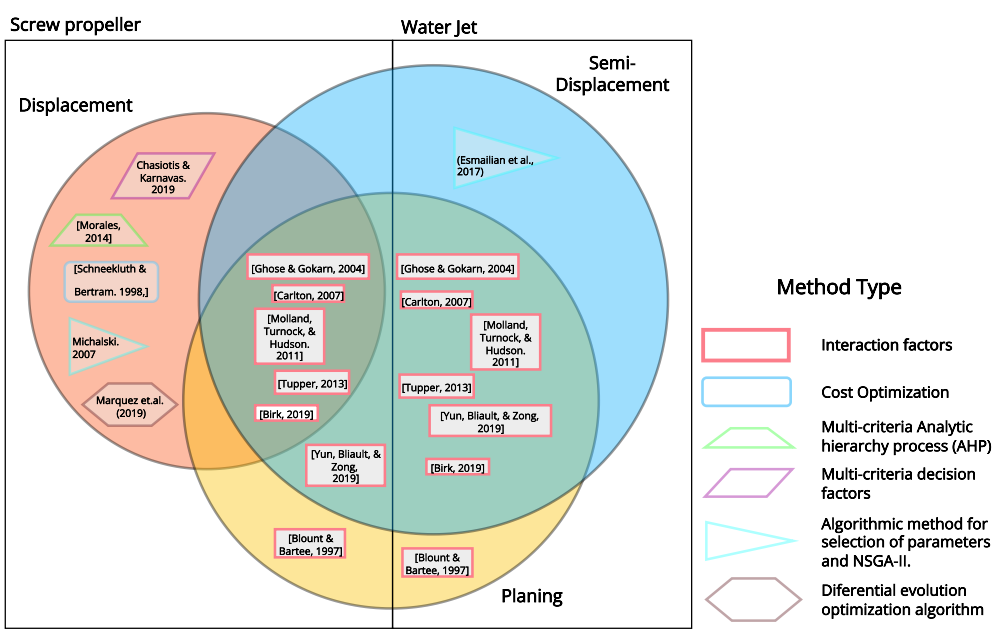

Figure 2.12: *Literature review chart*

Additionally, Figure 2.13 shows the different methods by number of citations.

As a summary, a compiled table with the literature review is presented in Table 2.3.

From those references it can be concluded that:

- Methods for the design of ship propulsion systems can be classified into five (5) major groups, those focused on the Calculation of Interaction Parameters, those focused on Cost Optimization, Multi-criteria Analytic Hierarchy Process (AHP) methods, Algorithms by parameter selection

[2]This classification is made according to the Froude number $Fn = \frac{v}{\sqrt{gL}}$.

Displacement: Vessels with an Fn < 0.6. Hydrodynamics is almost negligible and, the forces acting are mostly hydrostatic forces.

Semi-displacement: Those vessels with a $0.6 <$ Fn < 1.3. Hydrodynamic forces forces begin to play a more important role and the vertical center of gravity increases with speed. the speed.

Planing: Those vessels with an Fn > 1.3. In this case, the lift forces, the hydrodynamic forces, are very important. hydrodynamic forces, are very important and gain value as the Fn increases (Reche Tejero et al., 2019).

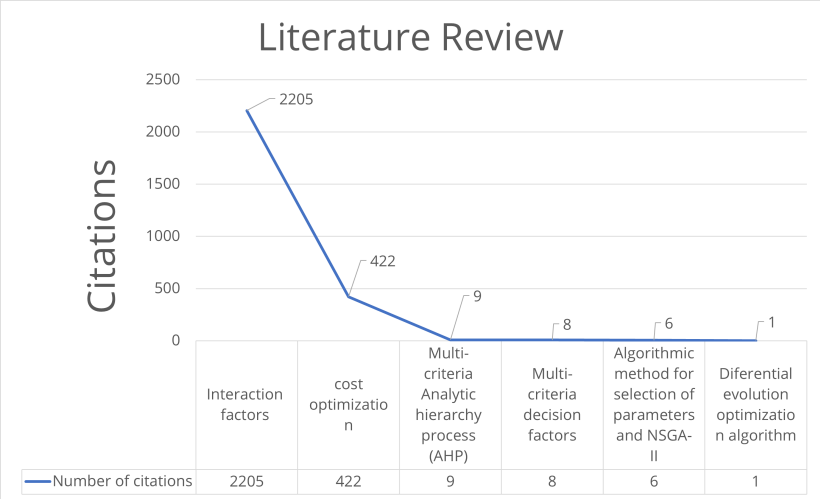

Figure 2.13: *Distribution by number of citations*

and Differential evolution optimization algorithm.

- The 40% of the methods found are focused on the design of propulsion systems for displacement vessels.
- The most used propeller is the screw propeller type with 65% of the methods.
- The most cited methods in the literature are those based on the Calculation of Interaction Parameters with a total of 2205 citations.
- The methods based on Cost Optimization are the second most cited in the literature with a total of 422 citations and are mainly used for the design of propulsion systems for large ships and merchant vessels.

With respect to the analyzed methods and their application, it was found that, in the case of electric vessels, these methods present some inaccuracies when it comes to establishing the required energy demand. This is because in their stages they make use of over-dimensioning estimates to cover energy losses and inefficiencies.

Regarding the design and selection of the propeller, in Chang et al. (2015), a mathematical model of the propeller is established in order to improve its performance. In this model the efficiency of propellers in open water is obtained for different speeds and the propeller pitch is optimized by means of a genetic algorithm. When authors compared the optimized propeller in water performance with the design, they verified that when only design conditions are considered, energy savings are not normally achieved, due to changes in the speed of the vessel. Therefore, multiple points around the design speed must be taken into account in the design process. In Gorter (2015), an increase up to

Table 2.3: *Summary table state of the art*

Title	Author/Year	Journal/publisher	Cites	Type vessel			Architecture Type		Method
				Displacement	Semi-displacement	Planing	Screw propeller (Inboard, Outboard, Azimuth-podded)	Water jet	
Marine Propellers and Propulsion	Carlton (2007)	Elsevier Butterworth-Heinemann	1420		X	X	X	X	Interaction factors
Ship Design for Efficiency and Economy	Schneekluth & Bertram (1998)	Elsevier Butterworth-Heinemann	422	X			X		cost optimization
Ship resistance and propulsion	Molland, Turnock, & Hudson (2011)	Cambridge University Press	343	X	X	X	X	X	Interaction factors
Introduction to naval architecture	Tupper (2013)	Elsevier Butterworth-Heinemann	287	X	X	X	X	X	Interaction factors
Basic ship propulsion	Ghose & Gokarn (2004)	Allied Publishers Pvt. Limited	85	X	X	X	X	X	Interaction factors
High Speed Catamarans and Multihulls	Yun, Bliault, & Zong (2019)	Springer	32		X	X	X	X	Interaction factors
Design of propulsion systems for high-speed craft	Blount & Bartee (1997)	Marine technology	16			X	X	X	Interaction factors
Influence of EEDI (Energy Efficiency Design Index) on Ship Engine Propeller Matching	Ren, H., Ding, Y., & Sui, C. (2019).	Journal of Marine Science and Engineering	13	X	X		X		Interaction factors
Fundamentals of ship hydrodynamics	Birk (2019)	Wiley	9	X	X	X	X	X	Interaction factors
A methodology to select the electric propulsion system for supply vessel (PSV)	Morales (2014)	Politécnica Universidade de Sao Paulo.	9	X			X		Multi-criteria Analytic hierarchy process (AHP)
Multi-criteria decision-making for marine propulsion: Hybrid, diesel electric and diesel mechanical systems from cost-environment -risk perspectives	Chasiotis & Karnavas (2019)	IEEE Transactions on Transportation Electrification	8	X			X		Multi-criteria decision factors
A method for selection of parameters of ship propulsion system fitted with compromise screw propeller	Michalski(2007)	Polish maritime research	6	X			X		Algorithmic method for selection of parameters
Marine propeller parametric optimisation and matching to electric motor	Marquez et.al. (2019)	Journal of the Brazilian Society of Mechanical Sciences and Engineering	1	x			x		Diferential evolution optimization algorithm

15% in the efficiency of a photovoltaic powered racing boat is reported by taking firstly into account the amount of energy available in the boat and considering then the hull resistance to determine the efficiency points of the motor. Thus, the appropriate design parameters for the propeller are selected. In the work of Windyandari et al. (2018), a procedure to determine the optimum design parameters for a B-series propeller is presented, therefore improving the vessel performance. Similarly, Mulyana et al. (2020), presented also a methodology to optimize the efficiency of a B-series propeller for a known value of the hydrodynamic resistance. Since in this work the case of study was a fishing vessel, for which it is not usual to make a proper sizing for the selection of the propellers rather than to opt for those available in the market, the authors verified that by selecting the optimal propeller instead an increase of 6% in the total efficiency of the vessel can be obtained. Finally, Bacciaglia et al. (2020), presented a methodology to design and optimize a controllable pitch propeller by means of a particle swarm algorithm seeking to minimize the energy consumption of the motor.

On the other hand, different authors have proposed to optimize the energy efficiency of different components of the vessel simultaneously, as the work reported in Esmailian et al. (2017), in which, a methodology to optimize the propeller-hull system all together is presented. By taking into account different design parameters for both hull and propeller, the system performance is optimized using an evolutionary algorithm based on NSGA-II. The features obtained for 60-series vessels and B-series propellers result in appropriate efficiency of the propeller-hull system. Another example of the optimization of the system from an unified perspective is presented in Marques et al. (2019b). In this work, an optimization methodology for B-series propellers by means of a differential evolutionary algorithm is presented. The optimization algorithm takes into account comprehensively the design requirements of the boat and adapts to an electric motor, seeking to decrease the power required for the electric motor and thus selects the design parameters of the B-series propellers. The authors also proved, by means of the aforementioned algorithm, that the worst individual presented an objective function increased by 25% and finally propeller designs has an open water efficiency between 36.18% and 40.49%.

In the reviewed works, none of them presents a methodology that optimize the triad Motor–Transmission–Propeller taking into account the gear ratio required to set both propeller and motor in the best operational point, improving the overall efficiency of the boat.

Chapter 3

Proposal

This chapter is an extension of the presented in Mira et al. (2021).

3.1 Characterization of propulsion architectures: Chain efficiencies

Once evidencing the opportunities in the literature review, the first step to develop the proposed method, is to identify the energy conversion points of a propulsion system for a vessel, characterizing a chain of efficiencies with emphasis on the three main types of architectures: inboard, outboard and Water jet. The objective is to identify the energy conversion points, what are the associated losses, their reduction potential, and what are the main variables that govern the functional performance of each of the components and influence the overall system performance.

It must first be understood that a ship is an autonomous system whose power is generated by a power source and an onboard "converter". That converter is the PS and, in the case of an electric boat, the energy comes from the batteries and it is the source of the required energy that needs to be converted. The different types of energy conversions are listed in Table 3.1.

Table 3.1: *Energy conversions table*

TO → **FROM ↓**	**Mechanical energy**	**Electric energy**	**Hydraulic energy**	**Heat**
Mechanical energy	GearBox and Propeller	E-Generator	Hydraulic Pump	Cooling System
Electric energy	Electric Motor	Converter		Heater
Hydraulic energy	Hydraulic motor and steering system hand pump		Hydraulic Transformer	
Heat	Shafts and bearings			Heat Exchanger

The next step was to model the energy transfers and conversions in diagrams, on order to facilitate their understanding. This enables to define a scope by components, allowing a subdivision and grouping of energy by transformation steps. For each architecture, the following flow diagrams are described.

3.1.1 Inboard

An analysis of the chain of efficiencies implicit in this type of propulsion architecture identifies 3 points of energy conversion: Motor, Transmission (which can be of the linear shaft or shaft-gear type when the installation of a gearbox is required) and the Propeller or Thruster. A total of five characteristic powers of the system can be associated which are: i) the brake power or power delivered by the engine, ii) the shaft power delivered by the reduction system, iii) the power delivered to the propeller, which is typically a screw propeller, iv) the thrust power delivered by the propeller and, finally, v) the effective power, which accounts for how much of the final thrust power is converted into effective thrust of the vessel. The efficiency and power parameters will be determinant for the characterization of the final solution to be installed in a vessel. They will allow the estimation of the values and types of associated losses and the identification of energy conversion points in order to reduce as much as possible from the design conception the values of these losses. A schematic diagram specifying the above estimates was prepared and can be consulted in the figure 3.1.

3.1.2 Outboard

An analysis of the chain of efficiencies implicit in this type of propulsion architecture was carried out in the same way as for the inboard architecture. It was found the same similarity in the energy conversion points and powers involved in the characterization of the unit. There is an important

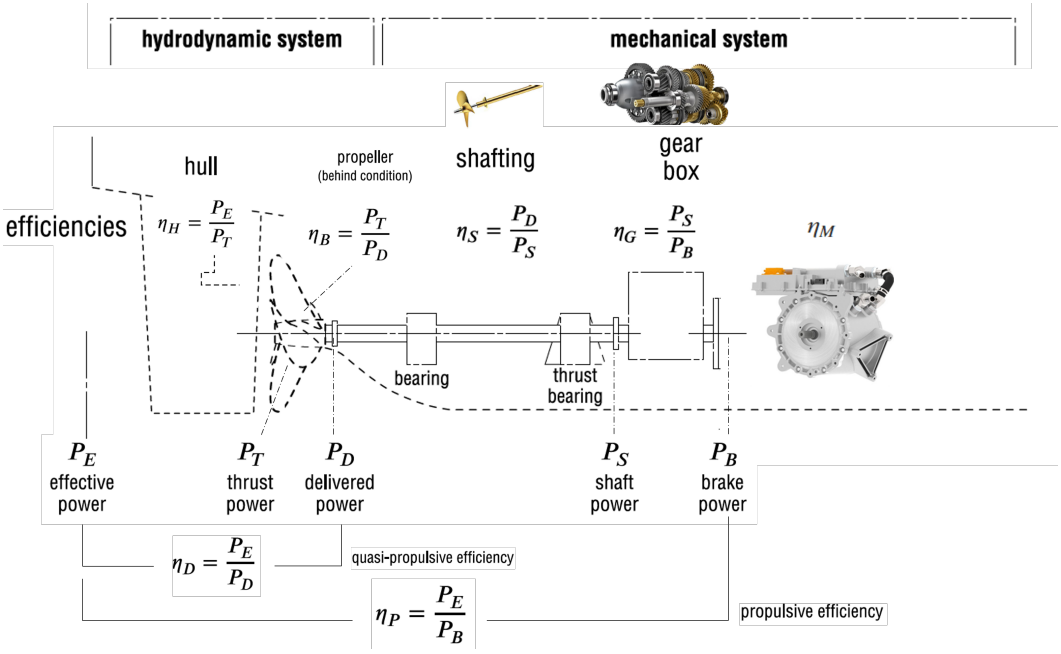

Figure 3.1: *Inboard Architecture Analysis. Elaborated from:Burcher (1988); Larsson and Eliasson (2000); Molland (2011); Siddall (2019); Yun et al. (2018); Birk (2019); Ghose (2004)*

difference and it is the transmission system in this type of architecture, which is based on the use of helical bevel gears that allow the transmission of motion at 90°either for L or L-Drive configurations or Z or Z-Drive geometries. A schematic diagram specifying the above estimates was prepared and can be consulted in figure 3.2.

3.1.3 Water jet

Likewise, an equivalent analysis of the chain of efficiencies eas also carried out for this propulsion architecture. The main difference found, was a new point of energy losses, which is the duct that shapes the jet. Due to the presence of this duct and the mandatory passage of water through this channel, there will be losses associated with the passage of fluid through it. Consequently, a new term of efficiencies must be included in the calculations, called “Jet efficiency”. Additionally, the type of impeller varies from propeller to impeller, so the way of calculating the efficiencies associated with this element, is different because data used for analyzing efficiencies is no longer from series of propellers operating in open water, but from pumps operating under conditions of uniform flow. A schematic diagram specifying the above estimates was prepared and can be consulted in figure 3.3.

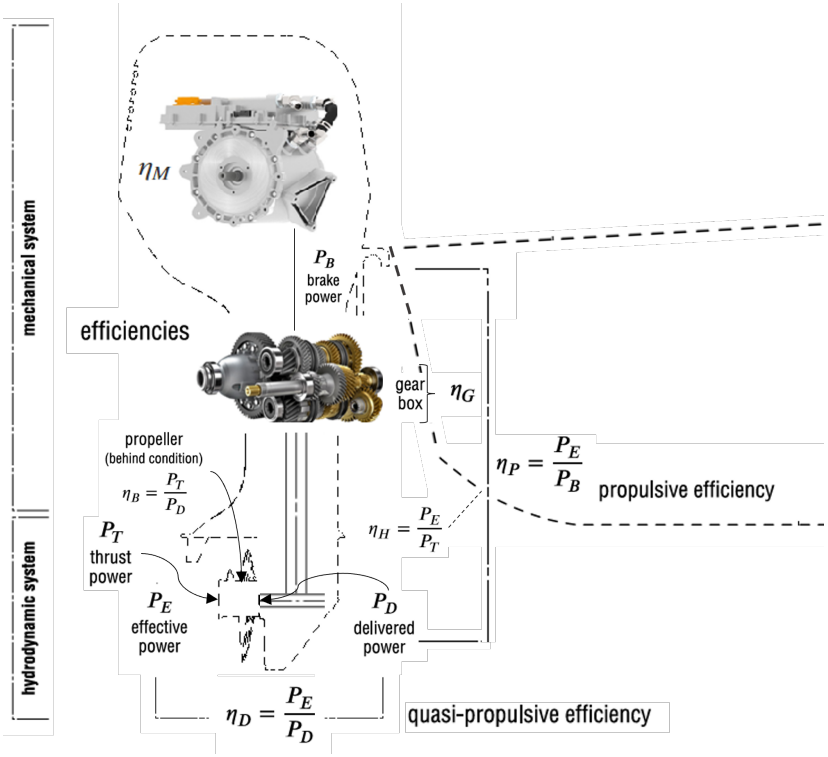

Figure 3.2: *Outboard Architecture Analysis. Elaborated from:Mira et al. (2021), Burcher (1988); Larsson and Eliasson (2000); Molland (2011); Siddall (2019); Yun et al. (2018); Birk (2019); Ghose (2004)*

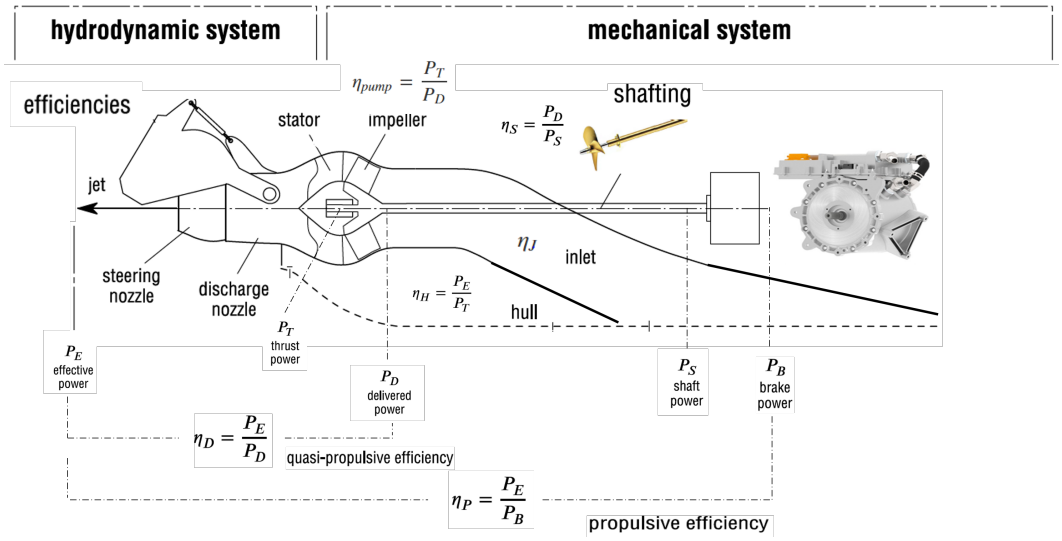

Figure 3.3: *WaterJet Architecture Analysis. Elaborated from: Burcher (1988); Larsson and Eliasson (2000); Molland (2011); Siddall (2019); Yun et al. (2018); Birk (2019); Ghose (2004)*

3.1.4 Analysis of the architecture's efficiencies chain

With the aforementioned analysis, the efficiency chains schematics allow to identify the following aspects:

- The thrust required to propel the bare hull of the vessel is generally increased when the propeller is added to the vessel resulting in an interaction known as propeller-hull and quantified by the term "Hull Efficiency (η_H)". The main reason for this difference is that the propeller draws its water along the hull and rudders (in case of inboard architectures) creating additional resistance. The efficiency of the hull itself depends on two other factors. The "Thrust deduction factor (t)" and the "Wake fraction (w)". The thrust deduction factor t accounts for how the vessel's resistance is increased by the presence of an additional submerged appendage such as the propeller. The wake fraction accounts w for how the efficiency of the propeller is affected by the wake generated by the hull of the vessel when it is ahead of it, which modifies the water velocity at the location of the propeller. The boundary layer at the stern of the ship has a considerable thickness and, usually, the propeller is within the region where the water is affected by the presence of the hull.

- To deliver thrust at a certain translation speed, power must be delivered to the propeller in the form of torque and rotational speed $P = 2\pi Qn$. This torque comes from the electric motor and will depend on the reduction ratio values that are set, which gives the designer the possibility to mechanically control the operating point of the drive.

- The "Open Water Efficiency (η_O)" refers to the fact that propellers are usually tested in an open water tank or tunnel. During the open water test the flow ahead of the propeller is uniform.

- In reality the power actually delivered to the propeller, when it is behind the boat, is different as a result of the non-uniform velocity field. The difference between the power in open water and the actual power delivered is quantified by means of the parameter "relative rotational efficiency (η_R)".

- All effects on the overall efficiency concerning the hull and the propeller are covered by the here called quasi-propulsive coefficient $\eta_D = \frac{1-t}{1-w} \cdot \eta_O \cdot \eta_R$

- During the process of energy conversion in the propeller a lot of energy is lost. Although the propeller has been in use for more than 150 years (Klein Woud and Stapersma, 2019), today much research is focused on improving its efficiency. It is, together with the reduction ratio, the most determinant component in the overall efficiency and where the design can make major interventions oriented to energy optimization.

- The transmission is responsible for power losses caused by friction in bearings, gears and other mechanisms used (pulleys, belts, chains, clutches). There is also a component of losses due to the fluid friction of the lubricants used. Despite the losses, its efficiency levels are superior to the other components. The establishment of a correct reduction ratio value will positively influence the behavior of the other components of the propulsion system (motor-propeller) since it will establish the operating points of these in both transient and steady state. The losses generated by shafts and their deformations do not exceed 0.5–1% of the nominal power to be transmitted. Gearbox losses are moderate, around 1–5% depending on the number of reduction stages, which increases inefficiency by the same amount. Multiple reduction stages are commonly used in multi-motor configurations or motors that have high rated speeds. Total drive efficiency is defined as power delivered and brake power.

As a result, Figure 3.4 presents the global energy transformation chain that goes from a ship's resistance to the electrical power to be installed.

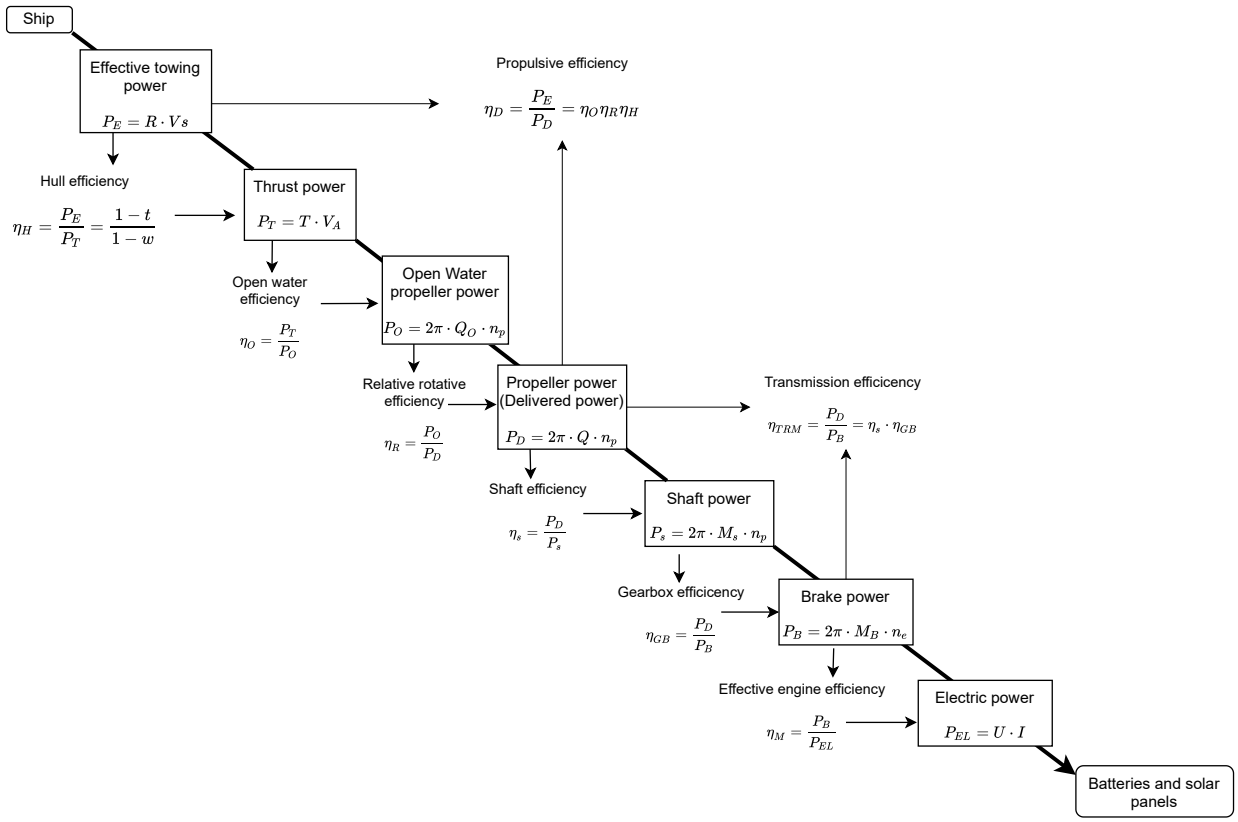

Figure 3.4: *Propulsion chain: overview of power and efficiencies from resistance to brake power (adapted from: Klein Woud and Stapersma (2019))*

3.2 Formulation of the optimality problem

3.2.1 Mechanical performance

The propulsion system design process aims to maximize the propulsive efficiency (Birk, 2019). Achieving the optimum overall efficiency depends on fully understanding how the individual performance of each component is featured and which variables of the system contribute to the collective performance of the unit. The efficiency of a propulsion system ($\eta_{overall}$) is commonly defined as the ratio of the effective Output Power to the Input Power (eq. 3.1). Being the Output Power lower than the Input Power due to heat, friction and slip losses, so the overall Efficiency always is less than one ($\eta_{overall} < 1$) in compliance with the principle of conservation of energy for closed systems (Birk, 2019).

$$\text{Efficiency} = \frac{\text{Output Power}}{\text{Input Power}} = \frac{\text{Usable Power}}{\text{Total Power Spent}} \tag{3.1}$$

A fundamental requirement of any propulsion system is the efficient conversion of the energy supplied into effective thrust power ($P_E = T_E \times V_S$) as it is demanded. In the case of ships or vessels, the power needed to travel at the different speeds at which the ship can move is defined as the power required to overcome the resistance of the bare hull as mentioned above. That speed is the starting point for sizing the Electric Power (P_{EL}) to be installed on the ship (Tupper, 2013; Hudson et al., 2014). Thus, the electrical power to be installed will be the product between the effective power and the overall efficiency of the propulsion system (see Eq. 3.2).

$$P_{EL} = P_E \times \frac{1}{\eta_{overall}} \tag{3.2}$$

The power is transmitted from the power head to the propeller through the components Motor-Transmission[1]-Propeller. The efficiency in the intermediate stages, as seen in Figure 3.4, from the effective power to the electric power, are usually described as follows (Tupper, 2013):

- P_E/P_T = Hull efficiency = $\frac{R_T \times V_S}{T \times V_a} = \frac{1-t}{1-w} = \eta_H$
- P_T/P_D = Propeller efficiency = $\eta_O\, \eta_R$
- P_D/P_B = Transmission efficiency = η_T
- P_B/P_{EL} = Motor efficiency = η_M

Therefore, the overall propulsive efficiency can be written as seen in Eq. 3.3 (Birk, 2019):

$$\begin{aligned} \eta_{overall} = \frac{P_E}{P_{EL}} &= \frac{P_E}{P_T} \times \frac{P_T}{P_D} \times \frac{P_D}{P_B} \times \frac{P_B}{P_{EL}} \\ &= \eta_H \times \eta_O \times \eta_R \times \eta_T \times \eta_M \end{aligned} \tag{3.3}$$

[1] Gear and/or Shaft

Then, each factor composing the overall propulsive efficiency $\eta_{overall}$ is properly described according to the definitions presented in previous sections and chapters. By taking the ratio between the effective power, required to tow the bare hull of the vessel (without the propulsion unit), and the power delivered by the propeller, or thrust power, the hull efficiency (η_H) is obtained. For a single screw vessel the efficiency takes values typically into the range from 1.05 to 1.1. and for ships with two propellers it is between 0.95 and 1.05 approximately (Propulsion, 2006; Birk, 2019). This value can be greater than 1, since two different systems are being compared again each other, instead of using only one closed system. The hull efficiency can be expressed as a function of the parameters t and w (see eq. 3.4). These parameters quantify the interaction between the hull and the propeller by estimating the increasing in the boat drag due to the presence of the propeller and the decreasing in performance due to the wake disturbing fluid ahead of the propeller, respectively (Molland et al., 2017; Gillmer and Johnson, 1982; Birk, 2019; Ghose, 2004).

$$\eta_H = \frac{1-t}{1-w} \qquad t = \frac{T - R_T}{T} \qquad w = \frac{V_S - V_a}{V_S} \tag{3.4}$$

There is no method that provides satisfactory results for the quantitative measurement of t and w. Consequently, it is necessary to perform experimental estimations under a hull-propeller configuration on a mechanism towed in a test tank (ITTC, 2002). These systematic tests are carried out on sets of propellers considered as standard. Their results are widely disseminated providing a database that allows designers to understand better the effects of these factors on propeller performance. In the following sections, the use of such results in the proposed methodology, in the present work, will be discussed in detail (Mira et al., 2020a).

The ratio of thrust power ($P_T = T \times V_a$) to power delivered to the propeller ($P_D = 2\pi nQ$) is a measure of the efficiency of the propeller when working astern of the ship and is sized by comparison with propeller performance values in open water. For a propeller in the behind hull condition the thrust generated and torque required is likely to be different in open water as it is affected by the wake of the hull. Efficiency η_O, or open water efficiency, is related to a propeller working in undisturbed parallel flow instead of the wake of the ship. This depends on the speed of advance (V_A), thrust force (T), rate of revolution (n), diameter (D) and on the design parameters of the propeller: number of blades (Z), BAR, and pitch ratio (P/D). The open water efficiency is estimated by means of open water tests (see Kim et al. (1970)) by systematically varying the advance coefficient J defined as in eq. 3.5 (Birk, 2019; AA, 1983; Molland et al., 2017; Tupper, 2013):

$$J = \frac{V_a}{nD} \tag{3.5}$$

The relationship between thrust and torque when the propeller operates in open water is called relative rotational efficiency (η_R). This efficiency differs from the one when the propeller operates

behind the hull as the water flowing towards the propeller, in this case, does not travel perpendicular to the propeller disc area, but it has a rotational flow instead. Therefore, compared to open water, the efficiency of the propeller is affected by η_R. When a vessel has a single propeller, η_R is usually about 1.0 to 1.07. When it has two propellers it will be lower, about 0.98, while for a twin-keel ship with two propellers η_R will be the same (Gillmer and Johnson, 1982; AA, 1983). The efficiencies described up to this point size the performance of the hydrodynamic system and is defined as quasi-propulsive efficiency (η_D). Concerning the transmission system (η_T), the use of shafts coupled by means of gearboxes is necessary in the propulsion architecture since the rotational speeds of the engines do not allow a direct coupling to obtain the best performance of the propeller. Losses in the transmission system are usually between 2–5% and are centered on friction in the bearings and gears that reduce the delivered power (Birk, 2019; Propulsion, 2006; Molland et al., 2017).

Transforming the motor angular velocity into an optimum n value for the propeller depends on the reduction ratio and is the key design parameter in the process of getting the driving machinery and the load synchronized. Equilibrium is achieved when the P_B and the power demanded by the propeller are equal, which makes the system operate in stationary conditions, giving rise to the so-called operating points (Marques et al., 2019b). An operating point is found whenever the load curve intersects the drive curve under stationary conditions (Klein Woud and Stapersma, 2019).

Figure 3.5 presents a typical efficiency map provided by electric motor suppliers, where the designer can visually determine the efficiency as a function of angular velocity and torque. This information provides an overall idea of how the motor will behave for a given operating point. The manufacturers usually do not provide more information than the one described in this type of graphs. Typical efficiency values for permanent magnet electric motors such as those used in electric vehicles are around 95% (Gieras, 2002; Lu, 2016b).

The optimal design and adaptation in an electrification problem depends on the above described efficiencies, which as it turns out are a function of the parameters modeling the behavior of each of the components of the triad (Motor–Transmission–Propeller). For the propellers, the performance parameters are presented as the dimensionless coefficients K_T, K_Q, and J and which are typically presented in the form of charts and regression polynomials for standard series (see Eqs. 3.5, 3.6, 3.7).

$$K_T = \sum_{s,t,u,v} C^T_{s,t,u,v} \left(J\right)^s \left(P/D\right)^t \left(A_E/A_O\right)^u \left(Z\right)^v = \frac{T}{\rho n^2 D^4} \tag{3.6}$$

$$K_Q = \sum_{s,t,u,v} C^Q_{s,t,u,v} \left(J\right)^s \left(P/D\right)^t \left(A_E/A_O\right)^u \left(Z\right)^v = \frac{Q}{\rho n^2 D^5} \tag{3.7}$$

A propeller series is a set of propellers in which key propeller characteristics have been systematically varied (Birk, 2019). The standard series data are widely spread in the literature where the most widely used propellers series are the Gawn and the B-Wageningen series, and the values of the

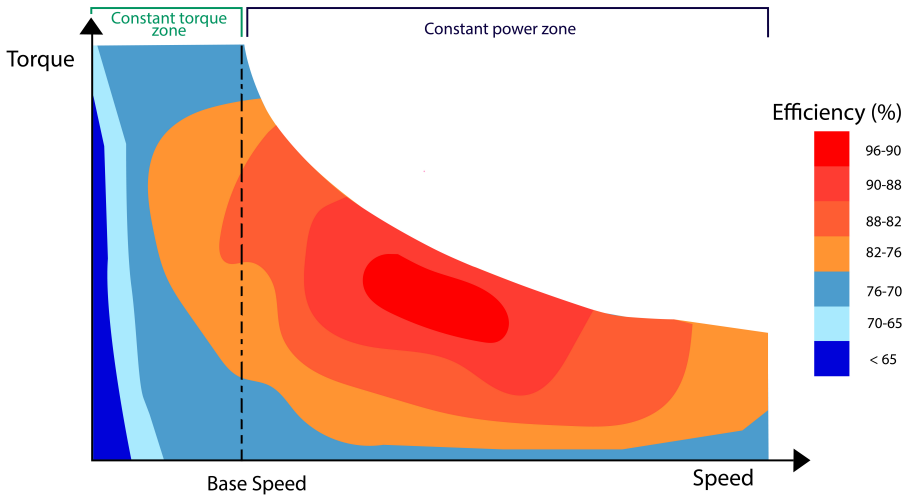

Figure 3.5: *Typical efficiency performance map for an electric motor.*

regression coefficients C^T, C^Q and the terms s, t, u and v are as presented in Ghose (2004); Birk (2019). Finally, the open water efficiency η_O can be described as in eq. 3.8:

$$\eta_O = \frac{TV_a}{2\pi nQ} = \frac{J}{2\pi}\frac{K_T}{K_Q} \tag{3.8}$$

3.2.2 Optimality Problem

The optimization objective is to establish the Motor–Transmission–Propeller matching, that increases the boat autonomy. That is, to decrease the energy consumption of the propulsion. This problem is equivalent to the problem of maximizing the overall efficiency $\eta_{overall}$ when generating the thrust required for the displacement of the vessel at a desired speed. In order to properly define the optimality problem that derives in the maximization of the autonomy by maximizing the overall efficiency, each of the parameters involved in the design/electrification of a propulsion unit for an electric boat (22 in total), are now summarized and grouped into the parameters ζ_i as defined as follows:

$$\begin{aligned}
\zeta_{boat} &= \{T, V_S\} \\
\zeta_{Motor} &= \{\omega, \tau\} \\
\zeta_{Trans} &= \{t_r, \eta_T\} \\
\zeta_{propeller} &= \{D, P, Z, A_e/A_0, A_p, A_d, n, V_a, J, K_T, K_Q, \eta_R, \eta_H\} \\
\zeta_{battery} &= \{V_n, I_n, C_n\}
\end{aligned} \tag{3.9}$$

Therefore, the optimality problem that seeks to increase autonomy can be written as:

$$\max_{(\omega^*, t_r^*, \zeta^*_{propeller})} \eta_{overall}(\rho)$$

$$\begin{aligned} s.t.\ & (3)-(8) \\ & \omega^{(l)} \leq \omega \leq \omega^{(u)} \\ & 1 \leq t_r \\ & D, P \in \psi_{pll-set} \end{aligned} \tag{3.10}$$

Where

ρ = is the density of the water $[slug/ft^3]$
$\psi_{pll-set}$ = is a suitable set of commercial available propellers
$\omega^{(\cdot)}$ = are the lower and upper and limits of the angular speed

Thus, the optimality problem to solve, stands as follows: The optimum $(\omega^*, t_r^*, \zeta^*_{propeller})$ has to be found in order to `maximize` the overall efficiency and the boat autonomy. The problem constraints are mainly due to the motor RPMs operating range, limited between a minimum and maximum value that will depend on the manufacturer's construction parameters. The second constraint is the range of reduction ratios, their min and max limits are established by the designer under the manufacturing constraints and admissible values for the power and propeller diameters available. For this, it is recommended to make use of the Diameter–HP–RPM [2] chart presented by Gerr (1989) (See Figure 3.6) .

Geometrical specifications of diameter and pitch are constrained by the characteristic values of commercially available propellers. The main difficulties of the overall efficiency optimization problem in Eq. 3.10 are mainly due to the fact that ζ_{Motor} and $\zeta_{propeller}$ are compiled in discrete databases. In addition, the mathematical expressions of the propeller performance parameters K_T, K_Q are nonlinear. Besides, evaluating the behavior of the different parameters under sequential optimization implies not finding a compromise on the values of common variables, which also implies that changes in these variables due to the compromise may worsen the performance levels.

In the following section, an unified framework to solve Eq. 3.10, and that deals with the nonlinearties and co-depence in the selection of the solutions paramaters is fully described.

[2] These charts, derived from Formula $D = \frac{632.7 \times SHP^{0.2}}{RPM^{0.6}}$, plot propeller diameter against maximum rated shaft horsepower and RPM at the propeller, and can be applied to most installations.

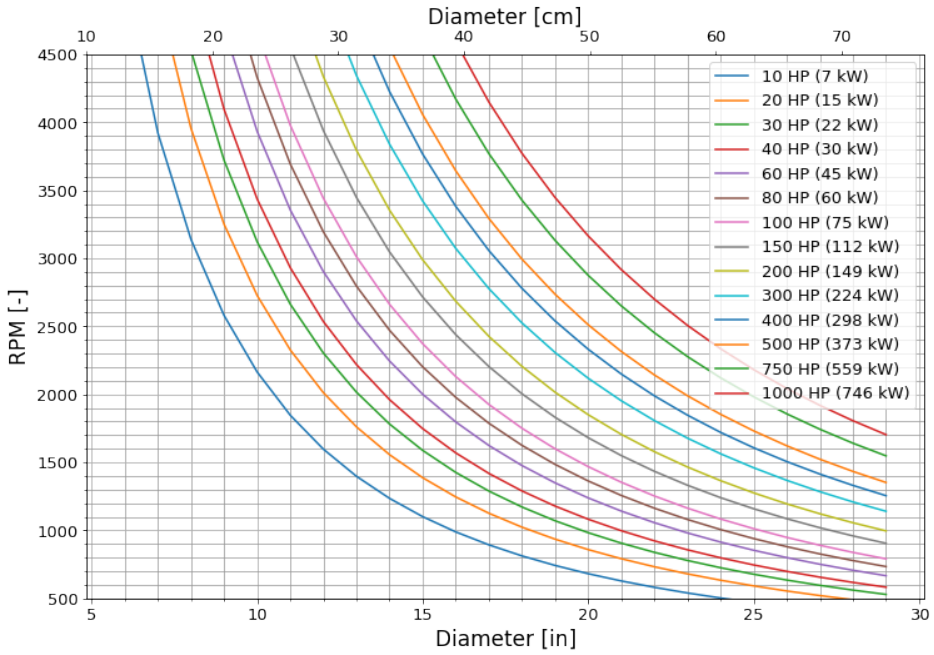

Figure 3.6: *RPM-DIAMETER-POWER chart*

3.3 Overall Efficiency Optimization Methodology

In order to solve Eq. 3.10, an **Exhaustive Search Optimization Algorithm** has been developed with a holistic approach (Rudolf et al., 2021; Miranda et al., 2016). A flowchart of the optimization process is presented in Figure 3.7. The process starts when variables take a first initial value to enter a simulation process where the physical models of each component are strategically included, simulating their behavior simultaneously. An iterative cycle is generated where each and every one of the members that make up the mesh of individuals on which the optimization strategy is run and the best solution is reported.

The optimal Motor–Transmission–Propeller configuration is found by characterizing all possible operating points, until achieving a desired cruise speed that defines the stationary conditions. This is achieved by systematically varying the values of ω, t_r and the propeller characteristics (P and D) from a given set of possible combinations. The number of combinations is obtained from the number of alternatives for each component (Motor, transmission and propeller) that the designer has to consider for the electrification. Combinations are then generated by means of a combinations-tree, as shown in Figure 3.8, and that are executed one by one by the algorithm, thus generating all possible solutions.

The possibility of varying the gear ratio $t_{r(i)}$ is the variable that makes the iteration possible and establishes the operating conditions and performance of the other components mechanically linked by means of this variable. Variable $t_{r(i)}$ is the main contribution of the present work allowing the

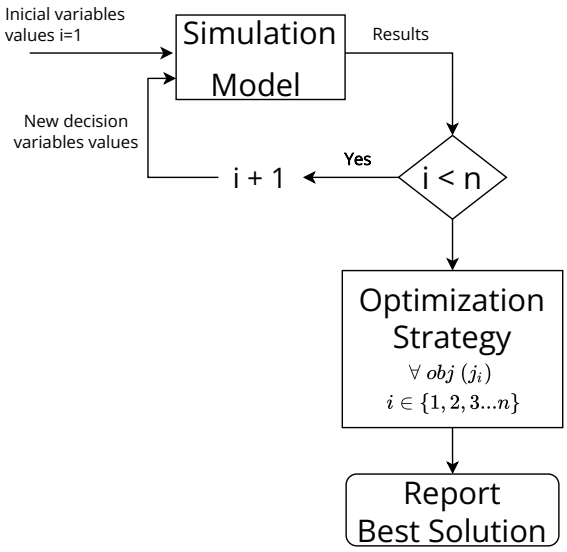

Figure 3.7: *Optimization loop*

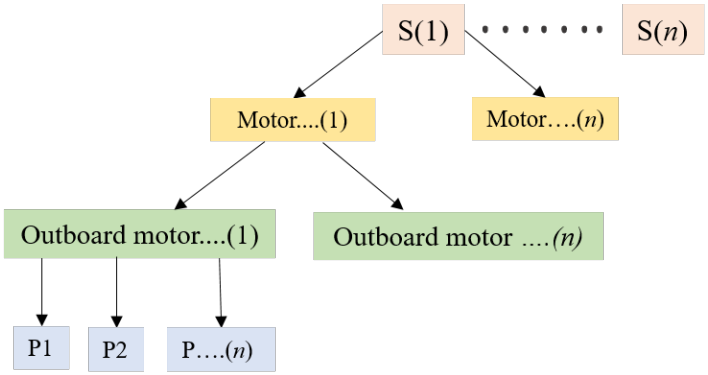

Figure 3.8: *Combination tree*

designer to know which is the value to use in his design to achieve the optimum operation conditions of the Motor–Transmission–Propeller configuration that will be implemented in the boat. Once the whole mesh of operating points is obtained, the global efficiency of the system is maximized and the result values for the design parameters are extracted. Figure 3.9 shows the iterative approach of the implemented multivariable optimization algorithm and summarizes the proposed methodology covering the three stages into which it is divided and which are described below.

3.3.1 Step 1: Vessel and electric motor inputs

Vessel requirements are set and the electric motor efficiency diagram is mapped in this step. The characteristic parameters of the vessel to be electrified must be established, the desired V_s in combi-

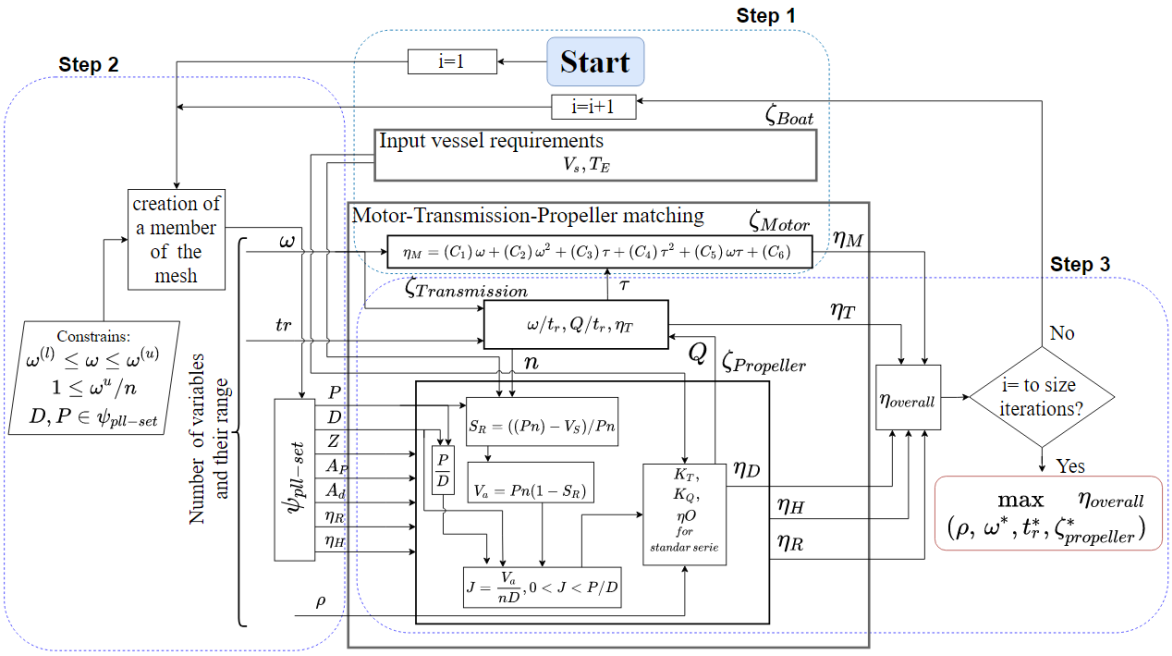

Figure 3.9: *Multivariable optimization algorithm and methodology steps diagram.(Mira et al., 2021)*

nation with the hull construction geometry allows the T_E demand requirements for the vessel. The estimation of the hydrodynamic resistance of the vessel can be performed by applying the methods presented by Savitsky et al. (1964), Wyman (1998), Crouch (Skene, 1973), Keith (Sponberg, 2011), and L. Blount and L. Fox (1976).

The steady-state thrust value at the desired speed is the main output of this stage and will be used in subsequent steps to establish the thrust to be delivered by the propeller. Additionally, at this stage the regression of the motor performance information contained in the efficiency map is proposed. This is possible by means of the derivation of a characteristic polynomial for the map, which is generated by means of a multivariable linear regression and establishing ω and τ as generic variables and η_M as response variable. The characterization of the information contained in these maps allows the evaluation of the engine behavior under different operating points and enables the generation of computational models where the motor performance can be evaluated.

The strategy proposed here, for the processing of the efficiency map image, consists of identifying the RGB color combination of each pixel that makes up the image with the support of a segmentation tool. Each color in the image is associated to a specific efficiency value, defining “iso-efficiency” zones. This is why by creating a dictionary type data structure, is possible to associate each pixel to a specific engine performance value. Once the color segmentation is executed, and a category is assigned to each pixel of the image, it is possible to identify the location coordinates of each pixel, knowing the resolution of the image. The dimension in width and height of the image can be compared with the

dimension of the X and Y axes of the map, which allows a scaling of the axes, providing each pixel with the information contained in these axes: torque coordinates and angular velocity of the motor. The proposed strategy is presented in Figure 3.10 which summarizes in four steps what is described above:

- **Step 1**: Image provided by the supplier
- **Step 2**: Color segmentation process
- **Step 3**: Digitization
- **Step 4**: Regression surface

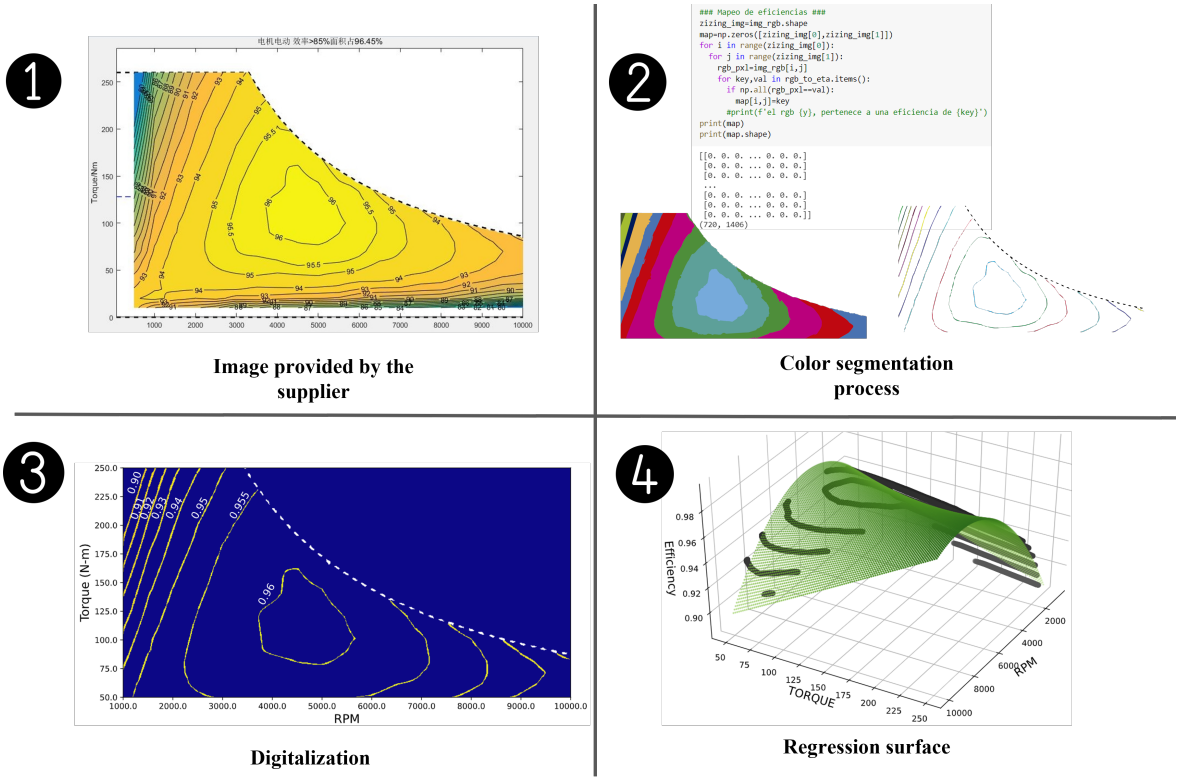

Figure 3.10: *Efficiency mapping process by image segmentation*

All this information can be extracted from the image and stored in a correspondence dataframe with columns as shown in Figure 3.11.

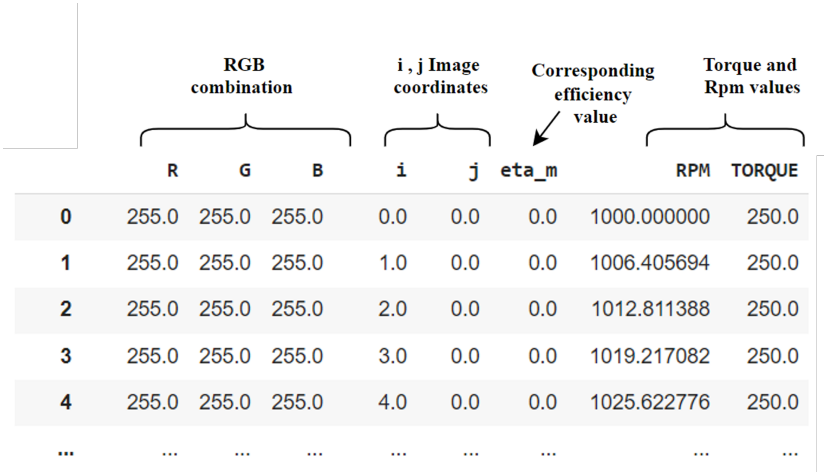

	R	G	B	i	j	eta_m	RPM	TORQUE
0	255.0	255.0	255.0	0.0	0.0	0.0	1000.000000	250.0
1	255.0	255.0	255.0	1.0	0.0	0.0	1006.405694	250.0
2	255.0	255.0	255.0	2.0	0.0	0.0	1012.811388	250.0
3	255.0	255.0	255.0	3.0	0.0	0.0	1019.217082	250.0
4	255.0	255.0	255.0	4.0	0.0	0.0	1025.622776	250.0
...	...	...	...	...	...	...	...	...

Figure 3.11: *Dataset heat*

With the information contained in this dataframe it is possible to train a **Machine Learning Algorithm** that predicts the curve that best fits the data map. This provides computable engine information, through a multivariate polynomial of 2nd order, as presented in Equation 3.11.

$$\eta_M = (C_1)\, w + (C_2)\, w^2 + (C_3)\, \tau + (C_4)\, \tau^2 + (C_5)\, w\tau + (C_6) \tag{3.11}$$

Where

w = is angular velocity

τ = is torque

C_i = are each of the coefficients of the regression.

3.3.2 Step 2: Constraints definition

The second step consists of defining the ranges for the design variables under the existing constraints. This having as objective of the present methodology, not only to design, but also the electrification of traditional propulsion units. Therefore, a set of electric motors, and a set of commercial candidate propellers ($\psi_{pll-set}$) must be defined in this step. In addition to the geometrical parameters (P, D), the number of blades Z and their developed area A_d are required to fully describe each propeller. The blades' area must be sized according to their shape and width, since this area is directly related to the amount of thrust and power that the propeller is capable of absorbing, as well as influencing the cavitation phenomenon. There can be propellers with the same diameter but with a different number of blades, having different cross sections, different contours and even a greater or lesser thickness (Gerr, 1989). The designer must rely on different tools for area estimation, tools that range from using CAD software, to carefully fitting a piece of paper flush against the surface of the blade, cutting it to match the contour of the blade and finally placing it on the plan (see Figure 3.12).

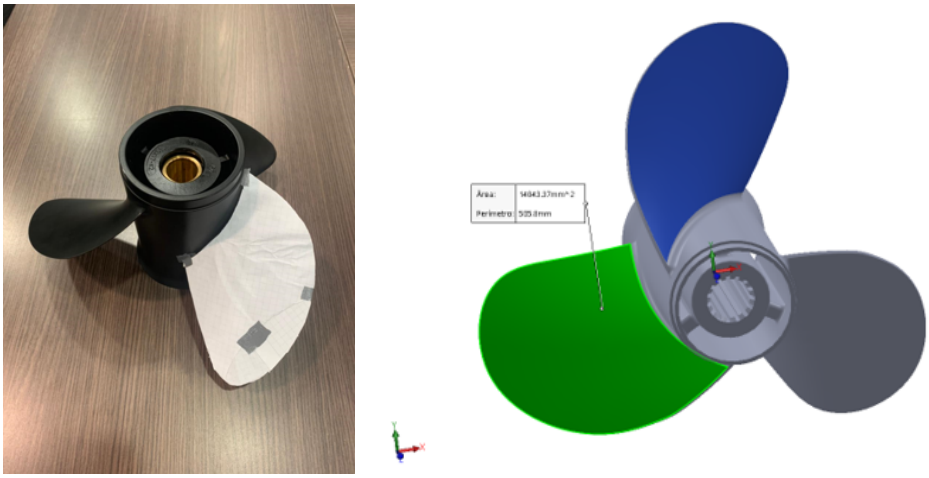

(a) Manual method (b) CAD method

Figure 3.12: *Estimation of blade area*

Two different types of blade area can be used, the "Projected Area" and the "Developed Area" (see Figure 3.13), where Equation 3.12 presents the relationship between them. This gives the designer the possibility to indirectly estimate the developed area once the projected area is available (Gerr, 1989).

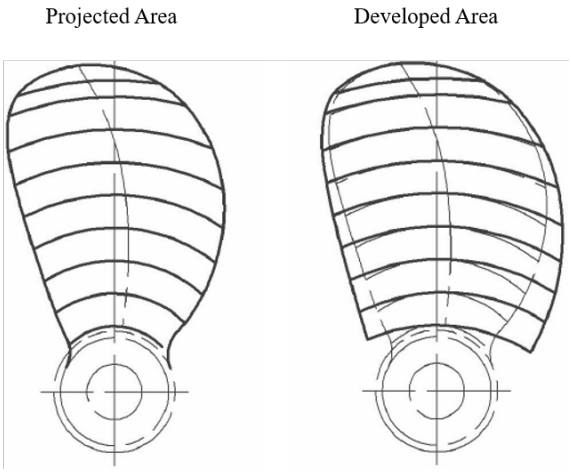

Figure 3.13: *Two diferent types of BAR*

$$\frac{A_p}{A_d} = 1.0125 - (0.1 \times \frac{P}{D}) - (0.0625 \times \frac{P^2}{D^2}) \tag{3.12}$$

Once the constraints are evaluated and the characteristic values associated with the area of the blades are established, the designer narrows down the ranges for each parameter. The algorithm

proceeds to generate the design individual $(\omega_i, t_{r_i}, \zeta_i)$ by means of a nested for cycle (see eq.3.13) which is executed for the entire set of Motor–Transmission–Propeller combinations.

$$\begin{aligned} &\text{for; } P, D \ \in \ \psi_{pll-set} : \\ &\qquad \text{for } t_r \ \in \ 1 \leq t_r \leq t_{r_{max}} : \\ &\qquad\qquad \text{for } \omega \ \in \ \omega^{(l)} \leq \omega \leq \omega^{(u)} : \end{aligned} \tag{3.13}$$

For each of these individuals the propulsion parameters and the values of η_i will be evaluated simultaneously, thus creating the result element that conforms the grid. The final size of the candidates grid will be given by the number of iterations, which is dependent on the amplitude and pitch values of the previously established ranges, in addition to the number of combinations to be evaluated. For which the elaboration of a combinations-tree is proposed (as seen in Figure 3.8). The tree routes are traveled by a combination of boat, speed, electric motor, mechanical unit (to be electrified) and the propeller. The fulfillment of the constraints when generating the ranges for each variable guarantees that the input values are feasible. Finally, the design variable's values, that maximize the global efficiency, are considered as the "optimal design".

3.3.3 Step 3: Optimization

In the final step the performance factors of the Motor–Transmission–Propeller triad are computed for each individual $(\omega_i, t_{r_i}, \zeta_i)$ generated in Step 2 (see Sec. 3.3.2) by means of Equations 3.5 to 3.8, applied on a standard propeller series database. It is recommended to use the B-Wageningen series for displacement craft and large vessels and the Gawn series for warships, small craft and higher speed craft (Molland et al., 2017). The mechanical equations of the reduction system (see eq. 3.14) are applied for angular velocity and torque, both demanded by the propeller (n, Q) and delivered by the motor (ω, τ). All the performance values corresponding to the individuals being generated are simultaneously evaluated on the characteristic polynomial of the electric motor efficiency map obtained in Step 1 (see Sec. 3.3.1).

$$t_r = \frac{\omega}{n} = \frac{Q}{\tau} \tag{3.14}$$

For η_H and η_R values are taken from Molland et al. (2017); Birk (2019); Ghose (2004); Tupper (2013); Carlton (2018); Gillmer and Johnson (1982) as discussed in the Section 3.2.1. The factors are computed simultaneously, simulating the interaction of the triad components and their mutual effects on the efficiency behavior under the common variables, thus iterating over the different operating points of the system. The results of the thrust demand of the section 3.3.1 and the water density are also taken as inputs. Once all possible combinations that shape the grid are executed, the algorithm

proceeds to maximize the results by identifying the individual that provides the optimum global efficiency. The holistic execution of the optimization method, which is one of the main novelties of the proposed approach, is possible thanks to the polynomial representation of the efficiency maps of electric motors (by means of the proposed image segmentation algorithm), together with the iteration cycles, that simulate the simultaneous behavior of the components (by giving values to the variable $t_{r(i)}$).

The results obtained for the intermediate gear ratio ($t_{r(i)}$) to be used in the electrification design should be compared with the commercial options available (this when custom manufacturing is not possible) in order to select the commercial gear that provides the closest value to the optimum obtained. Once selected, the effects on the overall efficiency of the PS can be evaluated on the maps presented in Figure 5.3(c). The commercial transmission systems by gears, chain, commercial synchronous belt facilitate the manufacture and are standardized by the manufacturers of this type of mechanisms in catalogs such as the one presented in Intermec (2021).

In order practically see the proposed method, the following section describes a case study consisting of the electrification of a river boat. In this case study, the proposed optimization methodology is fully developed in order to better illustrate the proposed algorithm.

Chapter 4

Case Study: Electric River Boat PS Design

This chapter is an extension of the presented in Mira et al. (2021).

4.1 Overall Efficiency Optimization

In order to clarify the proposed approach, it will be applied for **the design of an electrically powered propulsion system for an Electric River Boat**. The context of use for this vessel is for passenger's public transport operation in the Magdalena River in Colombia, as seen in Figure 4.1. This passenger transport operation is part of the ENERGETICA 2030 objectives, where traditional ICE vessels are under study, and an Electro-Solar Catamaran[1] has been proposed to shift to sustainable transport in the region.

The context of use and design requirements were analyzed in Mira et al. (2020b). From those requirements and a conceptual design phase (Giraldo-Pérez et al., 2020; Giraldo Pérez et al., 2021), the general parameters of the boat, which will be a Catamaran with Outboard architecture, as well as a energy storage unit (composed of NCM-type lithium battery cells) are presented in Table 4.1.

Consequently, and in terms of PS design (which is the focus of this project), the proposed Vessel's design will be powered by making use of the outboard architecture, and for the calculated energy demand, two outboard engines will be needed. In order to define the electrically powered PS, the alternatives for electrification are presented in Table 4.2. Here, two options of traditional outboard units, that can be electrified, are available: YAMAHA® of F100BETX reference or SUZUKI® of

[1] A catamaran is a multihull boat, in which two semi-hulls are joined by a central bridge. This configuration provides greater stability and more internal space than a monohull boat (Yun et al., 2018).

(a) Typical ICE vessel (b) Passengers river port

Figure 4.1: *Boat's context of public transport in the Magdalena River*

Table 4.1: *General parameters for the case study (Mira et al., 2021)*

Parameter	Value
Catamaran boat	
Boat mass [kg]	4324
Mean chine beam [m]	1.84
Dead rise angle [deg]	13
Lenght	7.9
Longitudinal center of gravity	3.16
Battery Cells	
Nominal voltage [V]	3.65
Nominal capacity [Ah]	87.5
Number of series [-]	92
Number of parallel [-]	4

DF90 reference. In addition, there are two electric motor options that can be implemented: Wolong EG80® or Alpha APEV528®. Each outboard unit will be adapted to replace the ICE with an electric motor.

Table 4.2: *Alternatives for the optimization process.(Mira et al., 2021)*

Outboard YAMAHA F100BETX	
Original gear ratio stage [-]	2.15:1
Length [in]	25
Original transmitted power [kW]	74.57
Weight [kg]	188

Alpha APEV528 Electric Motor	
Rated voltage [VDC]	400
Max current [Arms]	450
Peak power [kW]	120
Peak torque [Nm]	260
Peak speed [rpm]	10000

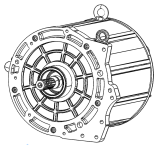

Outboard SUZUKI DF90	
Original Gear Ratio Stage [-]	2.59:1
Length [in]	25
Original transmitted power [kW]	67.11
Weight [kg]	155

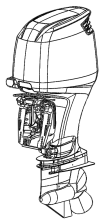

Wolong EG80 Electric Motor	
Rated voltage [VDC]	360
Max current [Arms]	470
Peak power [kW]	130
Peak torque [Nm]	300
Peak speed [rpm]	12000

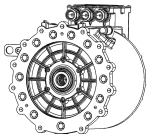

With these alternatives, what is the most suitable design combination to improve PS's efficiencies?. The starting point is to know: i) the hydrodynamic resistance (extracted by Savitsky's method (Savitsky et al., 1964; Giraldo-Pérez et al., 2020)), and ii) the electric motors' power and efficiency curves. With this information, the methodology proposed in this work (See Sec. 3) may now be implemented. Consequently, in order to optimize the triad Motor–Transmission–Propeller, the methodology will help to find a commercial propeller, the matching transmission ratio and rotational speed that optimize the efficiency of the energy flow of the outboard unit, according to the selected electric motor, as presented in Figure 4.2. This efficiencies optimization will lead to a less energy consumption and, as a consequence, it enables to improve the autonomy of the boat. The analyses carried out for the implementation of the methodology and the obtained results, will be described below.

4.1.1 Step 1: Vessel and electric motor inputs

An estimation of the hydrodynamic resistance of the vessel is performed by implementing the method presented in Giraldo-Pérez et al. (2020). This method is based on the statistical model of resistance estimation proposed by Savitsky et al. (1964) with the vessel parameters presented in Table 4.1. By this method, and according to design specifications, the vessel needs to move at speeds between 10–15m/s. The result may be observed in Figure 4.3, that shows Drag vs Speed for the vessel under study. That is how a hydrodynamic resistance (R_T) is obtained, being of 6.18 kN and 7.74 kN for speeds of 47km/h (13m/s) and 55km/h (15m/s), respectively. These speeds are average speeds reached by the ICE boats that operate in the area of interest, being a fast alternative of transportation for the

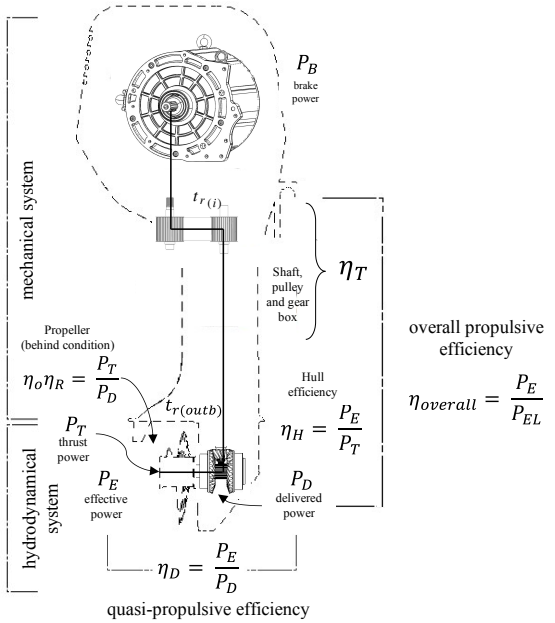

Figure 4.2: *Power and efficiencies chain of an outboard propulsion system.(Mira et al., 2021)*

people who live near the river.

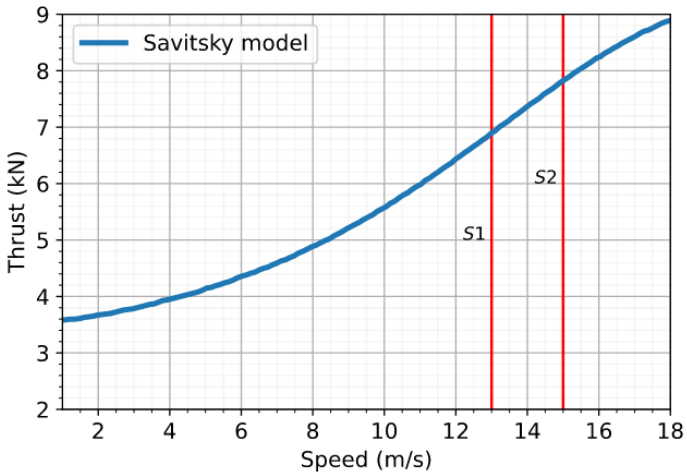

Figure 4.3: *Hydrodynamic Resistance (R_T) Vs Speed, for the Catamaran Case Study.(Mira et al., 2021)*

Then, from the electric motor's efficiency curves supplied by the manufacturers (like the one from Figure 3.5), the regression model is obtained in order to make this information "computer processable". For this purpose, it was proposed to use OpenCV-Python® library for image processing and segmentation. Through the use of the zones of constant efficiency values (identified by the same color in the resulting image), it is possible to determine the Torque and rpm coordinates for each pixel. This is done by associating the efficiency value of each color to an RGB combination, through

the creation of a dictionary type data structure. By mapping the image matrix generated in OpenCV, pixel by pixel, a dataframe is generated with τ,ω, and η_M coordinates. τ and ω coordinates of the pixel are obtained by scaling the size $[n \times m]$ given by the resolution of the image with the minimum and maximum value intervals for the motor. With the resulting database, a multivariable ordinary least squares regression is performed and the polynomial parameters obtained for each engine are as presented in Table 4.3. Finally, Figures 4.4(a) and 4.4(b) depicts the resulting surfaces. The corresponding polynomials for each motor are written in the equations 4.1 and 4.2.

Table 4.3: *Electric motors Coefficient results for the multivariable ordinary least squares regression method.(Mira et al., 2021)*

Wolong EG80						
Dep. Variable:			$\eta_{Overall}$			
Model:			OLS			
R-squared:			0.821			
Adj. R-squared:			0.821			
Prob (F-statistic):			0			
Df Model:			5			
	C_i	$\sigma_{\bar{x}}$	t	$P > \|t\|$	[0.025	0.975]
Int	0.9335	0.002	487.497	0.000	0.930	0.937
ω	7.831e-06	4.56e-07	17.156	0.000	6.94e-06	8.73e-06
ω^2	-1.255e-09	2.76e-11	-45.446	0.000	-1.31e-09	-1.2e-0
τ	-5.489e-05	1.8e-05	-3.057	0.002	-9.01e-05	-1.97e-05
τ^2	-5.62e-07	4.28e-08	-13.121	0.000	-6.46e-07	-4.78e-07
$\omega\tau$	4.745e-08	1.69e-09	28.131	0.000	4.41e-08	5.08e-08

Alpha APEV528						
Dep. Variable:			$\eta_{Overall}$			
Model:			OLS			
R-squared:			0.913			
Adj. R-squared:			0.913			
Prob (F-statistic):			0			
Df Model:			5			
	C_i	$\sigma_{\bar{x}}$	t	$P > \|t\|$	[0.025	0.975]
Int	0.9426	0.001	1809.433	0.000	0.942	0.944
ω	1.33e-05	1.4e-07	95.212	0.000	1.3e-05	1.36e-05
ω^2	-2.004e-09	9.48e-12	-211.297	0.000	-2.02e-09	-1.98e-09
τ	-0.0004	5.59e-06	-64.284	0.000	-0.000	-0.000
τ^2	3.859e-08	1.51e-08	2.547	0.011	8.9e-09	6.83e-08
$\omega\tau$	7.958e-08	6.63e-10	119.961	0.000	7.83e-08	8.09e-08

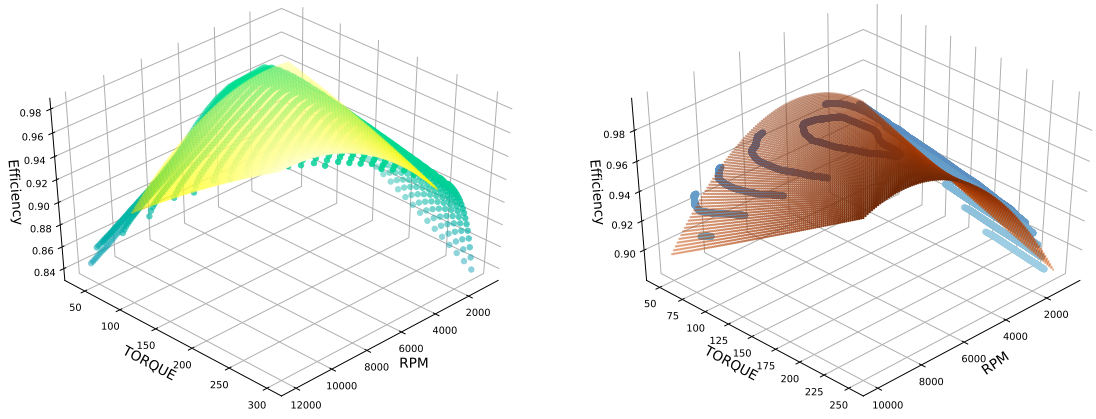

(a) Wolong EG80 surface

(b) Alpha APEV528 surface

Figure 4.4: *Motors efficiency adjustment surfaces.(Mira et al., 2021)*

$$\eta_{M_{wolong}} = 7.831e{-}06\ w - 1.255e{-}09\ w^2 - 5.489e{-}05\ \tau - 5.62e{-}07\ \tau^2 + 4.745e{-}8\ w\tau + 0.9335 \quad (4.1)$$

$$\eta_{M_{wolong}} = 1.33e-05\ w - 2.004e-09\ w^2 - 0.0004\ \tau + 3.859e-08\ \tau^2 + 7.958e-8\ w\tau + 0.9426 \quad (4.2)$$

4.1.2 Step 2: Constraints definition

To define the candidate propellers, the diameter and pitch constraint were established for the different commercial propellers. Finally the propellers that can be seen in the Table 4.4 were selected.

Table 4.4: *Candidate propeller parameters.(Mira et al., 2021)*

Parameter	Units	Propeller 1: 13.5" x 14-K	Propeller 2: 13.5" x 16-K	Propeller 3: 13" x 17-K2
D	$[in]$	13.5	13.5	13
P	$[in]$	14	16	17
Z	$[-]$	3	3	3
P/D	$[-]$	1.03	1.2	1.3
A_p	$[in^2]$	20.66	19.85	20.97
A_p/A_d	$[-]$	0.90	0.89	0.87
A_d	$[in^2]$	68.50	67.08	71.94
DAR	$[in^2]$	143.14	143.14	132.73
BAR	$[in^2]$	0.48	0.47	0.54

For each of the propellers, the procedure described in the methodology (section 3.3.2) was carried out to establish the BAR from images provided by the propeller supplier and CAD files. These results for each propeller can be seen in Figures 4.5(a), 4.5(b) and 4.5(c).

We proceed to define what will be the range of variation for the transmission ratio. This range is established using the chart presented by Gerr (1989) as described in Section 3.2.2. By making use of this map (known as Crouch's Propeller Method) it is possible to define and present graphically which is the operating range considered by this method as "ideal" for the proposed propellers (for the case of 13" and 13.5" diameter propellers). In the Figure 4.6 we see that for the estimated power (107 Hp@13 m/s -155 Hp@ 15m/s) the method establishes that the candidate propellers should operate between 2800 rpms - 3400 rpms. If we consider the angular velocity (ω) ranges at which the motors can deliver these estimated powers (this by analyzing the information provided by the supplier) we see that they are bounded between 4000 rpms - 8000 rpms as shown in Figure 4.7, where the operating range or area of interest for each engine is highlighted. By comparing the extreme values of these ranges (ideal

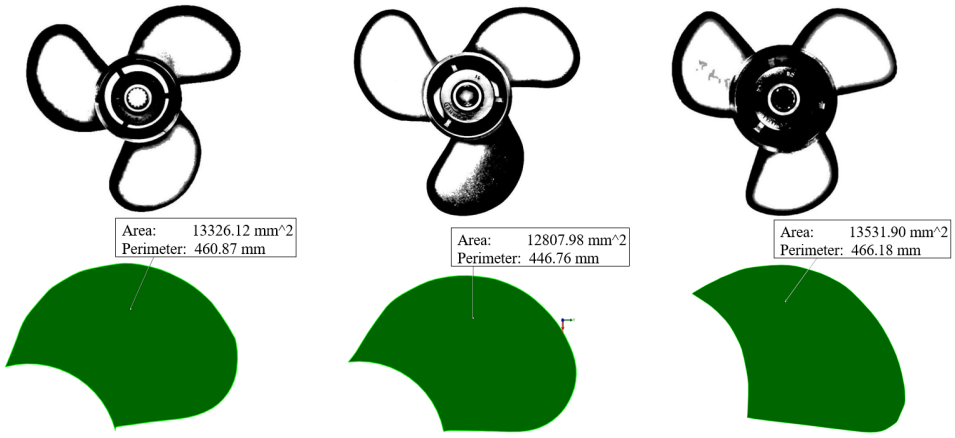

(a) **Propeller 1 (P1):** 13.5"x14"-K. (b) **Propeller 2 (P2):** 13.5"x16"-K. (c) **Propeller 3 (P3):** 13"x17"-K2.

Figure 4.5: *Projected area for propellers*

propeller turning range and engine angular speed range) it is possible to determine the ranges in which the reduction ratio may vary to ensure the power demand delivery conditions of the vessel. In this case, this range is between 1.17 and 2.85 which is refined by integrating manufacturing constraints. These constraints are centered on the use of power transmission elements such as sprockets, chains, pulleys and timing belts and the geometrical constraints associated with their manufacturing process. These constraints are gear modulus, pitch and number and profile of teeth. In this case we will make use of a transmission system by pulleys and synchronous belt whose limitations and standard commercial systems are presented in Intermec (2021). Considering the above, a range between 1 and 2.5 is defined as the ideal range of variation. It is possible that space restrictions to install the intermediate drive system may also become a limiting factor, so this must be taken into account.

The angular velocity a range between 0 and 12000 rev/min was selected, based on the speeds that the Wolong EG80 and Alpha APEV 528 motors can reach (see Figure 4.7).

4.1.3 Step 3: Optimization

The number of combinations evaluated were $n = 24$ and they are presented in the combination tree Figure 4.8, where two speeds of interest (47km/h and 55km/h) are evaluated, being these the average speeds developed by similar combustion boats that operate in the area.

With the set of candidates propellers, and by using the parameters presented in Table 4.4, the open water efficiency η_O, and the Thrust (K_T) and Torque (K_Q) Coefficients are calculated, for each propeller, through Equations 3.6,3.7, 3.8. Next, the curves depicted in Figures 4.9(a) to 4.9(c), are obtained for each propeller, in terms of the advance coefficient J.

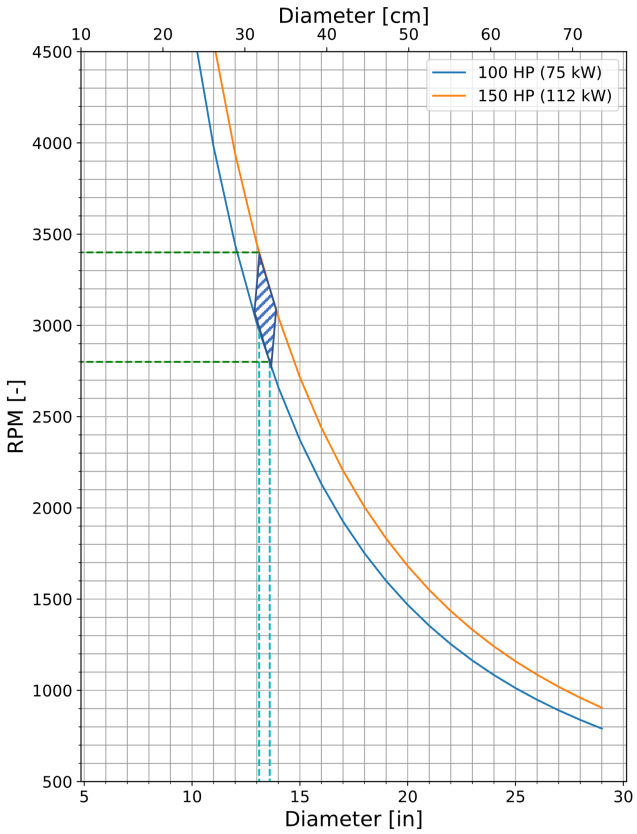

Figure 4.6: *RPM-DIAMETER-POWER chart*

These curves provide a graphical analysis of the efficiency and performance of each propeller. It can be seen in Figure 4.9(c) that although the **P3** has the highest thrust and torque delivery values, its efficiency is below the **P1** and **P2** propellers, and its performance decay rate is much higher than the others. Propeller **P1** on the other hand has the performance curves with a much lower decay rate but its performance values are below those of propeller **P2** for equal values of J, which allows to infer preliminarily a better performance when using propeller **P2**.

Varying the advance coefficient means, not only to go through the performance curves or maps for the propellers which have been presented here, but, in practice, to go through different operating speeds of the boat until reaching the cruising speed point, these speeds implied a variation in the rotational speed of the propeller, which in turn demanded an increase in the angular velocity of the engine. How quickly the stationary operating point is reached, and once there, how the overall performance of the components determines what the energy efficiency of the unit will be. The reduction ratio governs this behavior.

With all previous information, the whole proposed model was run to find the general efficiency of the outboard unit, in the different range of angular speed and transmission ratio, for each of the 24

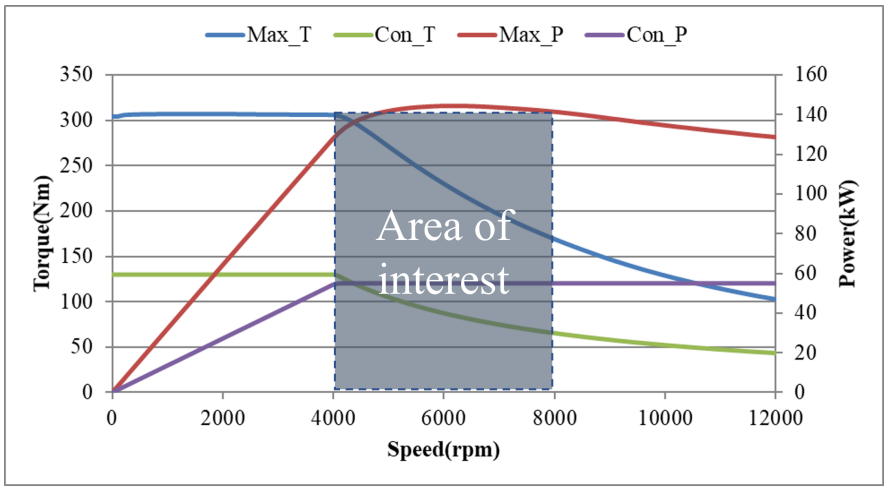

(a) Wolong EG80: Area for t_r range definition

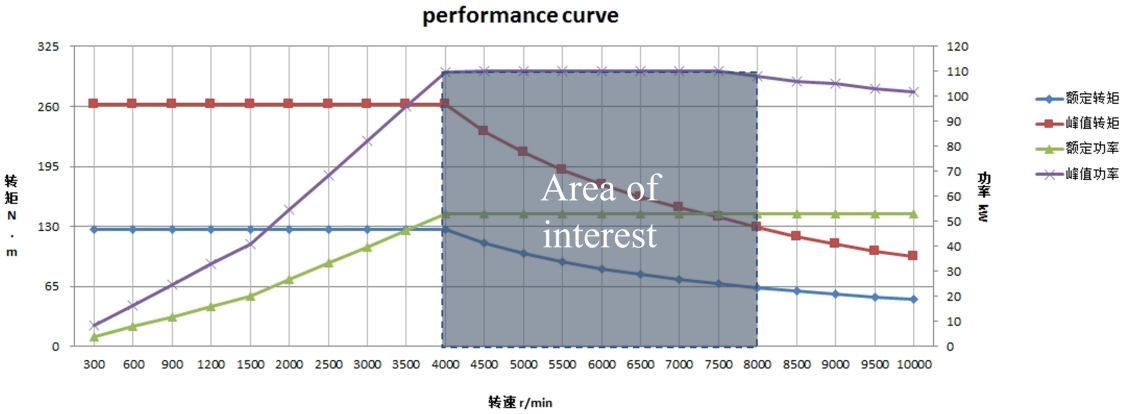

(b) Alpha APEV528: Area for t_r range definition

Figure 4.7: *Operation area of motors for t_r range definition (from supplier).*

possible matches. This is possible by using the polynomial approximation to calculate the efficiency of the motor (as a function of the angular speed and the required torque), and also by using the efficiency curves of the propellers.

As a result, different efficiency curves were obtained for each evaluated speed (47 and 55 km/h). An example of this can be observed in Figures 4.10 and 4.11 for each of the evaluated speeds and engines, when using the optimum propeller with the engine. For each matching the main performance values t_r, $t_{r(i)}$, $\eta_{overall}$, P_E, and *Autonomy* (resulting from the optimization run) can be observed in Table 4.5. The following Chapter 5 presents an analysis and discussion of these obtained results.

For more details, all graphical results obtained from the 24 combinations are presented in Appendix A together with the extended table of values Table A.1 from that Appendix.

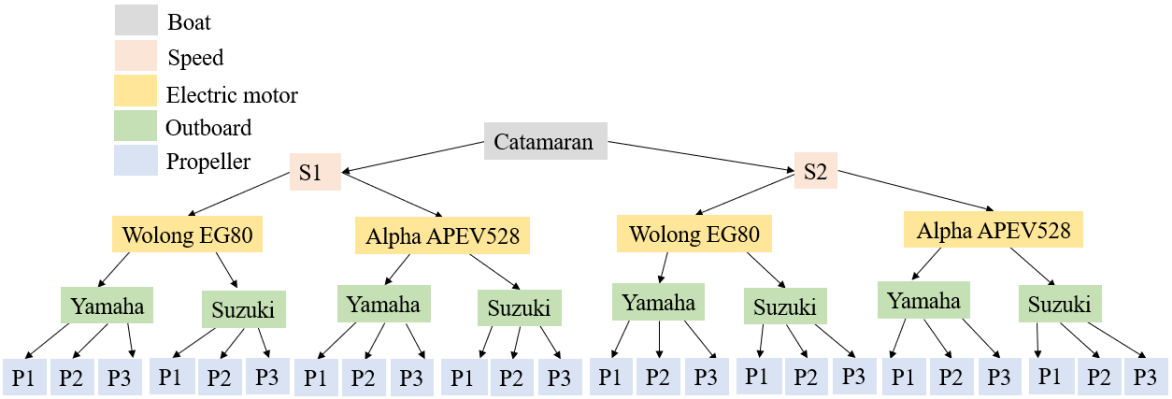

Figure 4.8: *Combination tree.(Mira et al., 2021)*

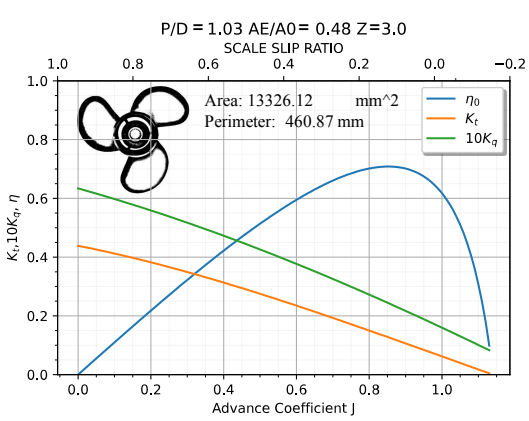

(a) **P1:** Open water performace chart

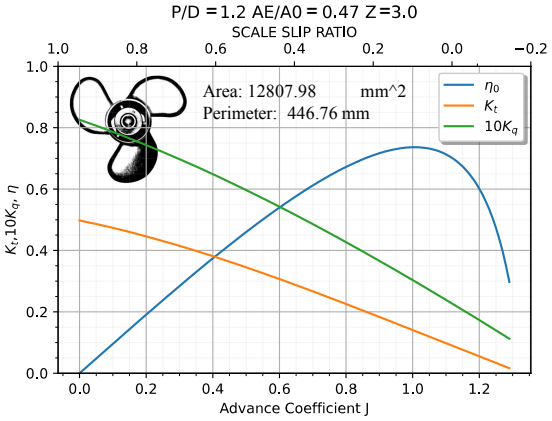

(b) **P2:** Open water performace chart

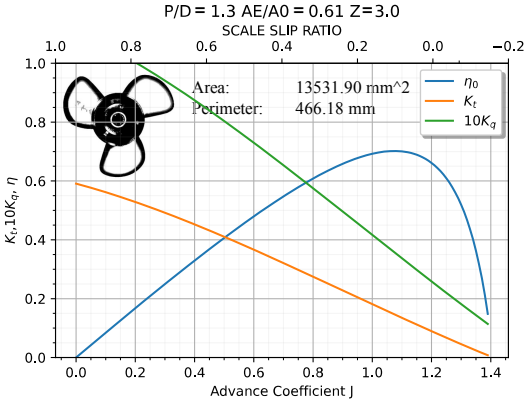

(c) **P3:** Open water performace chart

Figure 4.9: *Projected area and Open water performace charts for propellers.(Mira et al., 2021)*

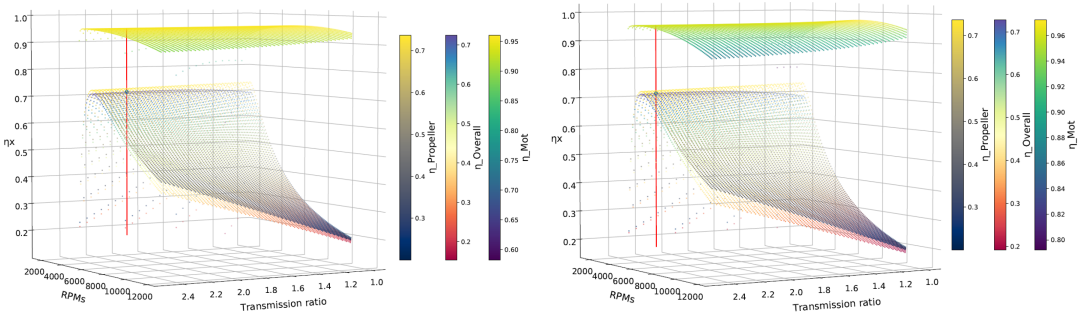

(a) **Wolong EG80:** Motor–Transmission–Propeller matching

(b) **Alpha APEV528:** Motor–Transmission–Propeller matching

Figure 4.10: *Motor–Transmission–Propeller matching for the Speed 1 (47 km/h)*

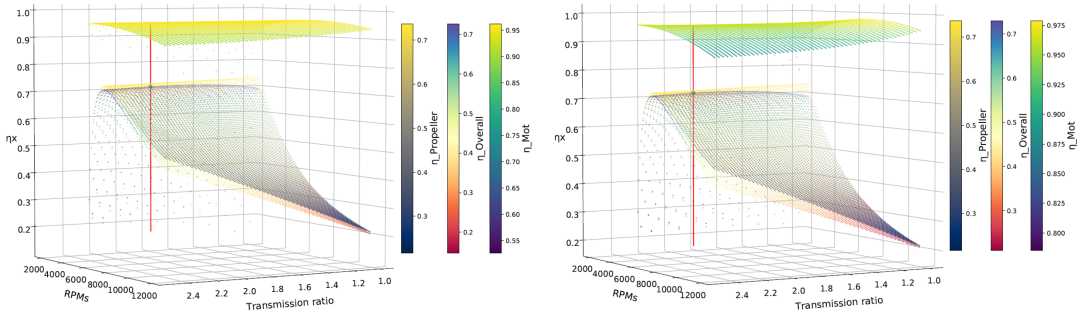

(a) **Wolong EG80:** Motor–Transmission–Propeller matching

(b) **Alpha APEV528:** Motor–Transmission–Propeller matching

Figure 4.11: *Motor–Transmission–Propeller matching for the Speed 2 (55 km/h).(Mira et al., 2021)*

Table 4.5: *Catamaran case study results: Direct electrification vs Proposed optimization method.(Mira et al., 2021)*

		Parameter	Units	**Speed 1:** 47 km/h				**Speed 2:** 55 km/h			
Baseline Results	Original Propeller Provided: 13"x 17	**Electric motor :**		Wolong EG80		Alpha APEV528		Wolong EG80		Alpha APEV528	
		Outboard :		Yamaha	Suzuki	Yamaha	Suzuki	Yamaha	Suzuki	Yamaha	Suzuki
		$t_{r(outboard)}$	[-]	2.15	2.59	2.15	2.59	2.15	2.59	2.15	2.59
		$\eta_{overall}$	[-]	0.650	0.639	0.690	0.692	0.691	0.680	0.694	0.692
		P_E	[kW]	68.00	68.60	67.40	67.40	89.40	89.47	89.49	85.52
		Autonomy	[km]	38.1	38.1	39.2	39.3	34.5	34.4	34.7	34.6
Optimization Results	Propeller 1: 13.5" x 14-K	t_r	[-]	1.86	1.86	2.01	2.01	1.74	1.74	1.86	1.86
		$t_{r(i)}$	[-]	1.14	1.28	1.06	1.22	1.19	1.32	1.13	1.30
		$\eta_{overall}$	[-]	0.696	0.696	0.699	0.699	0.697	0.697	0.701	0.701
		P_E	[kW]	66.83	66.83	66.83	66.83	88.67	88.67	88.66	88.66
		Autonomy	[km]	39.5	39.5	39.7	39.7	34.8	34.8	35.1	35.1
	Propeller 2: 13.5" x 16-K	t_r	[-]	2.19	2.19	2.38	2.38	2.07	2.07	2.13	2.13
		$t_{r(i)}$	[-]	0.98	1.15	0.90	1.08	1.04	1.20	1.01	1.17
		$\eta_{overall}$	[kW]	0.723	0.723	0.727	0.727	0.725	0.725	**0.728**	**0.728**
		P_E	[km]	64.28	64.28	64.28	64.28	85.26	85.26	85.27	85.27
		Autonomy	[-]	41.0	41.0	**41.2**	**41.2**	36.3	36.3	36.5	36.5
	Propeller 3: 13" x 17-K2	t_r	[-]	2.31	2.31	2.44	2.44	2.16	2.16	2.27	2.27
		$t_{r(i)}$	[-]	0.92	1.11	0.88	1.06	0.99	1.16	0.94	1.13
		$\eta_{overall}$	[kW]	0.690	0.690	0.693	0.693	0.691	0.691	0.694	0.694
		P_E	[km]	67.45	67.45	67.45	67.45	89.47	89.47	89.47	89.47
		Autonomy	[-]	39.1	39.1	39.3	39.3	34.5	34.5	34.7	34.7

Table 4.6: *Performance features of optimal results.(Mira et al., 2021)*

Parameter	**Electric motor:**	**Alpha APEV528**			
	Speed:	47 km/h		55 km/h	
	Outboard:	Yamaha	Suzuki	Yamaha	Suzuki
$t_{r(outboard)}$	[-]	2.15	2.59	2.15	2.59
t_r	[-]	2.38	2.38	2.13	2.13
$\boldsymbol{t_{r(i)}}$	**[-]**	**0.90**	**1.08**	**1.01**	**1.17**
ω	[rev/min]	5400	5400	5700	5700
n	[rev/min]	2270	2270	2669	2669
$\boldsymbol{D}$	**[in]**	**13.5**	**13.5**	**13.5**	**13.5**
$\boldsymbol{P}$	**[in]**	**16**	**16**	**16**	**16**
S_R	[-]	0.15	0.15	0.15	0.15
V_a	[ft/s]	42.83	42.83	50.12	50.12
η_H	[-]	1.05	1.05	1.05	1.05
η_R	[-]	0.98	0.98	0.98	0.98
J	[-]	1.006	1.006	1.001	1.001
P_D	[-]	1.20	1.20	1.20	1.20
A_E/A_0	[-]	0.47	0.47	0.47	0.47
Z	[und]	3	3	3	3
η_o	[-]	0.736	0.736	0.736	0.736
η_D	[-]	0.757	0.757	0.757	0.757
τ	[N.m]	113.67	113.67	142.85	142.85
η_{motor}	[-]	0.959	0.959	0.961	0.961
$\boldsymbol{\eta_{overall}}$	**[-]**	**0.727**	**0.727**	**0.728**	**0.728**
$\boldsymbol{P_E}$	[kW]	**64.28**	**64.28**	**85.27**	**85.27**
Autonomy	**[km]**	**41.2**	**41.2**	**36.5**	**36.5**

4.2 Electrically-Powered Outboard Unit Prototype Design

As a result of the methodology applied to the case study, it was possible to analyse the optimal combinations for motor, transmission and propeller. Thanks to this work, it is possible to know not only the optimal combination and its performance, but also the performance for other alternatives, which the designer can use according to the design, manufacturing and component procurement context. For the practical application in the case study, although the combination that makes use of the Wolong EG80 engine is not the one that generates the most favorable results, under the context of the development of the ENERGÉTICA 2030 project it is necessary to make use of this engine. However, the parameters that maximize energy efficiency for this combination are known. The prototype that is developed is designed under these parameters, which are listed in Table 4.7.

Table 4.7: *Design parameters: Optimum result for Matching Wolong EG80-Yamaha F100BETX*

Propeller for Matching:	Propeller 2: 13.5" x 16-K	
Parameter	**Electric motor:**	**WOLONG EG80**
	Speed:	55 km/h
	Outboard:	Yamaha
$t_{r(outboard)}$	[-]	2.15
t_r	[-]	2.07
$\boldsymbol{t_{r(i)}}$	**[-]**	**1.04**
ω	[rev/min]	5500
n	[rev/min]	2651
$\boldsymbol{D}$	**[in]**	**13.5**
$\boldsymbol{P}$	**[in]**	**16**
S_R	[-]	0.14
V_a	[ft/s]	50.12
η_H	[-]	1.05
η_R	[-]	0.98
J	[-]	1.008
P_D	[-]	1.20
A_E/A_0	[-]	0.47
Z	[und]	3
η_o	[-]	0.736
η_D	[-]	0.758
τ	[N.m]	148.04
η_{motor}	[-]	0.956
$\boldsymbol{\eta_{overall}}$	**[-]**	**0.725**
$\boldsymbol{P_E}$	[kW]	**85.26**
Autonomy	**[km]**	**36.3**

Even though the full design process is not the focus of this research, the design activities will be generally described here, in order to guide the actions towards the final result. The PS design starts from the product design specifications, where a total of 19 needs were identified for the case study. Those specifications are grouped into 8 categories: weight, ergonomics, environment, standardization, performance, safety, size and usability. These needs are extracted from the study carried out in Magangué as part of the ENERGÉTICA 2030 project and are completed with those specified by the Hydrodynamic and Mechanical Propulsion design team (Mira et al., 2020b).

Needs such as the vessel's displacement speed, the minimum generation of pollutants and the possibility of maneuvering at different speeds and in different places and spaces along the routes are categorized as "demands" or indispensable characteristics that must be met and without which the solution is not acceptable. In addition, requirements mandated by standards, current legislation and safety regulations are included in this category. Commercial construction elements,low noise levels and the possibility to dock in different directions are categorized as "Desires" considering the inclusion in the development of the unit design of features that are not necessarily essential. Technical features and requirements that constrain the design of the propulsion unit were categorized as Constraints.

A Functional Analysis was performed, identifying as main function of the propulsion unit "to provide effective thrust". 19 function carriers were identified in the internal functional analysis. Other design considerations such as maneuverability and regulatory economics are also listed, such as Law 1242 of 2008, "*whereby the National Code of Navigation and River Port Activities is established and other provisions are issued*", where among others, it is established that vessels must have redundant systems in case of emergency. As part of the conceptual design, a morphological matrix was also developed, which served as input to the design team to establish the ideal configuration. A weighting analysis was performed on a total of 14 designs with a team of expert consultants.

Afterwards, the detailed design was carried out, where special emphasis was placed on the need for an intermediate transmission system, that allows modification of the original reduction ratio of the Yamaha engine that is being electrified. Detailed calculations were developed for a synchronous belt and pulley drive system, along with stress analysis and material selection for the different components of the system supported by Finite Element Analysis (FEA). A selection of commercial elements such as bearings, retaining rings and bolts was also made. A detailed design of the cooling system was developed, using two working fluids, in this case river water and glycol, which run through an open and a closed circuit respectively for heat exchange. The heat transfer calculations were developed by means of the simulation of a concentric tube liquid-liquid exchanger, designed by the logarithmic mean temperature method presented in Çengel et al. (2011).

Finally, Figure 4.12 presents the final design of the propulsion unit and Figure 4.13 a picture of the entire developed system in the Physical Prototype Implementation.

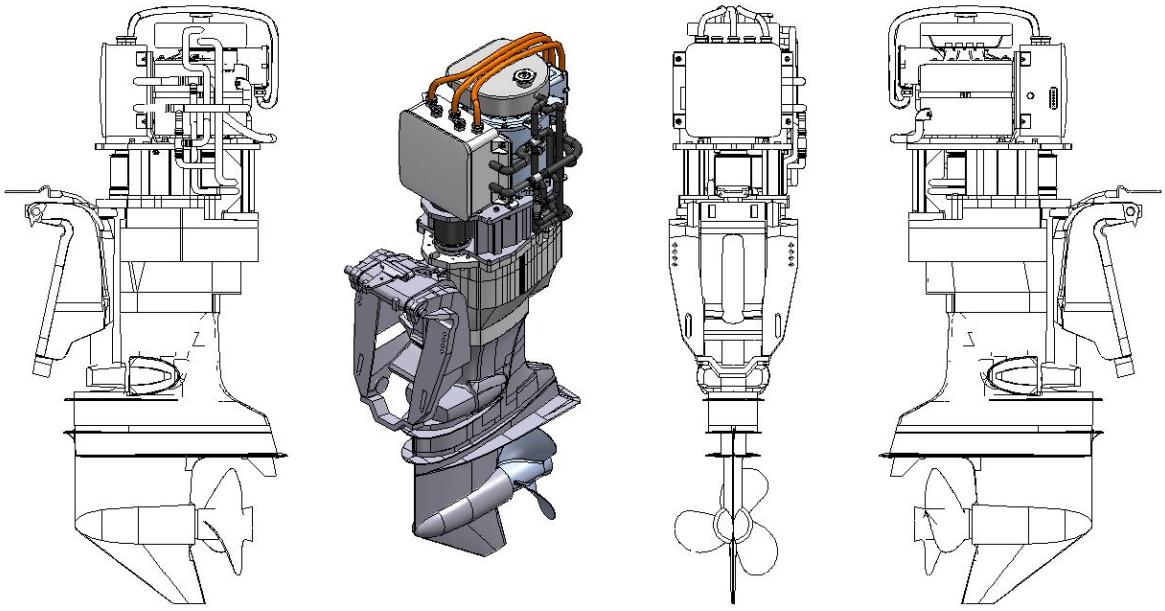

Figure 4.12: *Outboard Electrical Unit Design*

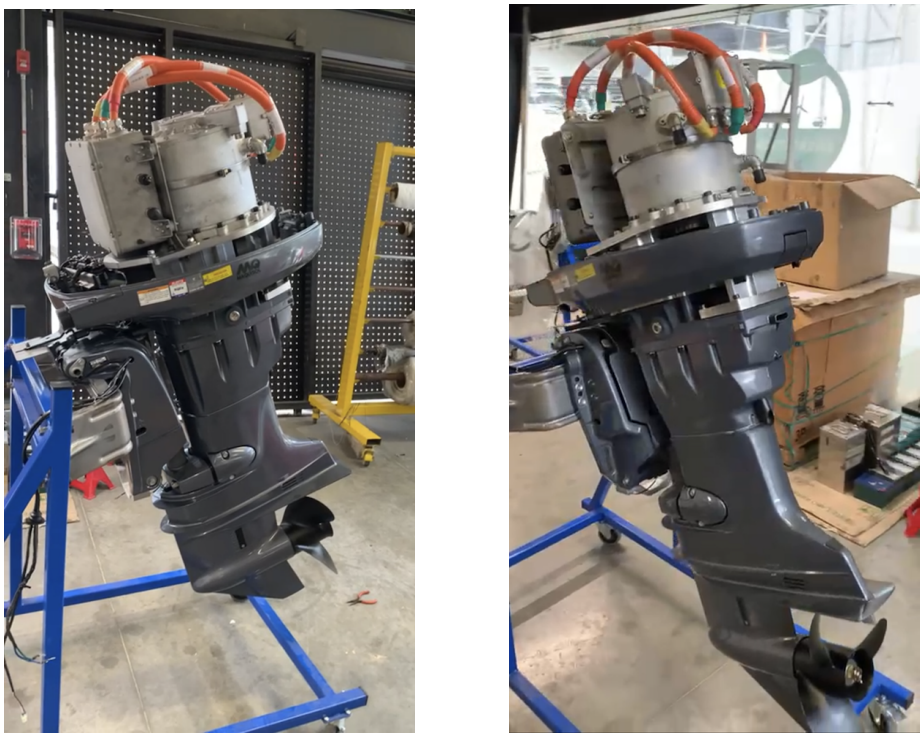

Figure 4.13: *Outboard Electrical Unit: Physical Prototype Implementation*

Chapter 5

Analysis of the Results

From the general results presented in Table 4.5, the Alpha APEV528 engine and propeller 2: 13.5" x 16-K are identified as the matching components that provide the highest efficiency of the propulsion unit and the maximum range of the boat. Table 4.6 presents an in-depth analysis of the specific results for this combination at the speeds of 47 km/h and 55 km/h.

The maximum overall efficiency is 0.728 at an operating speed of 55 km/h and is achieved by using a reduction ratio t_r of 2.13 with a reduction stage t_{r_i} of 1.01 for the Yamaha F100BETX outboard and 1.17 for the Suzuki DF90 outboard. The maximum range is 41.2 km which is achieved by operating at the speed of 47 km/h and the use of a reduction ratio t_r of 2.38 with a reduction stage t_{r_i} of 0.90 for the Yamaha F100BETX outboard and 1.08 for the Suzuki DF90 outboard. The operating points for both speeds are presented in Figure 5.1 where for each speed the coordinates of the ω, τ and P_E demanded from the motor are specified.

These graphs show in dotted–line the load demand curve generated by the ship in terms of power and torque, which the installed engine must supply from zero speed to cruising speed. This allows to observe the behavior, compared to the performance values established by the manufacturer[1] for these two variables (continuous lines in the figure). The manufacturer presents the performance curves for the maximum and nominal values for which the engine was designed. Other curves such as the current curve where the current is related to the motor speed may be useful. In order to give greater clarity to the parameters of interest, this is not presented.

The analysis of these graphs allows identifying that there will always be a positive starting torque[2] when comparing the torque demand curves, versus the maximum performance curves of the motor. If it is compared the load demand behavior with the nominal engine performance curve, it can be seen that, for the desired cruising speeds of 47km/h and 55km/h, the starting torque will be negative.

[1] known as torque-speed and power-speed curves

[2] difference between the maximum torque and the demanded torque

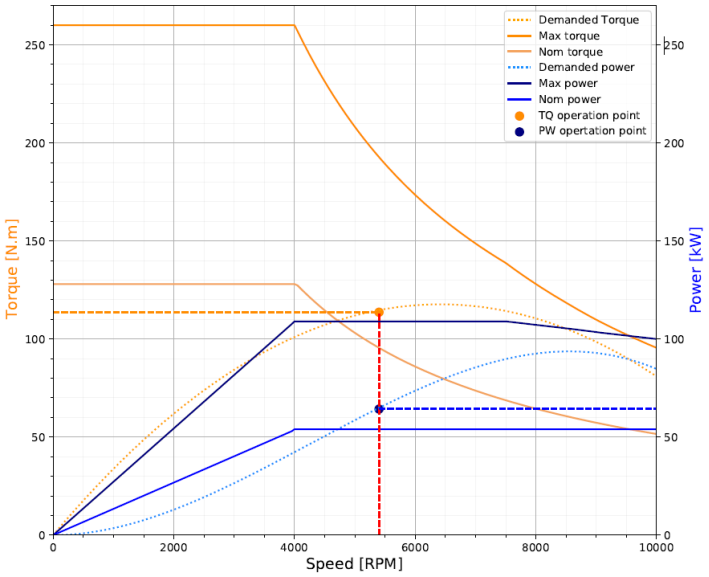

(a) **Optimal operation point for Speed 1:** 47 km/h

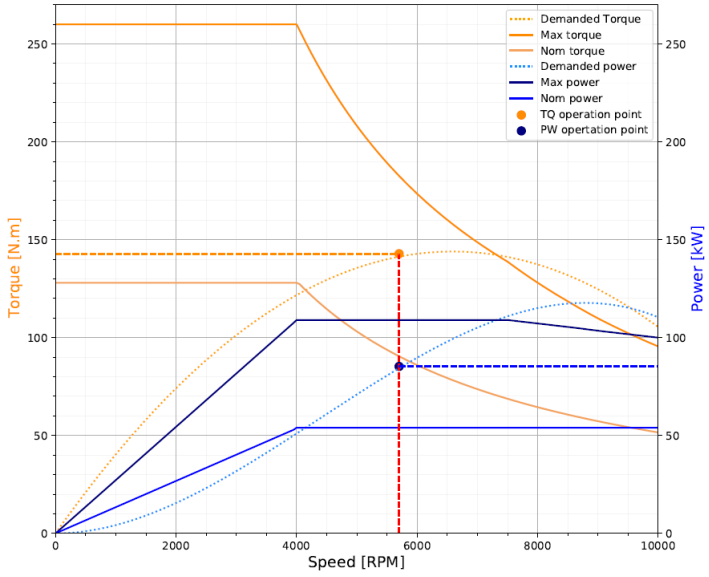

(b) **Optimal operation point for Speed 2:** 55 km/h

Figure 5.1: *Operation point for optimal Motor-Transmission-Propeller matching.(Mira et al., 2021)*

Specifically for the 47 km/h speed there is a difference of 18.67 Nm. This can be interpreted as an overdemand to the nominal values of 16.4% for that speed, which could perhaps generate an increase in the operating temperature of the engine. If the power is analyzed the difference is 9.28 kW (14.4%). A similar analysis for the 55 km/h speed shows an over demand of 52.8 Nm (36.9%) in torque and 30.27 kW (35.5%) in power. Figures 5.3 and 5.4 show the mesh plots generated from the iterations. Here, it can be seen the local maximum for the global efficiency and the local minimum for the power and autonomy of the matching, discriminated by speed. Other values of interest to the designer were listed in Table 4.6 as n, η_D and η_{motor}.

Finally, a comparison is proposed considering the electrification of commercial propulsion units (retaining the design parameters originally established for the combustion power head). The methodology makes it possible to compare the optimal values with the result of preserving the standard parameters of the unit to be electrified. The standard propeller provided by the manufacturer is used (REF: 13"X 17). Then, the operating point of the electric motor is established maintaining the constructive t_r value of the original outboard motor and placing it in the ω coordinate where it operates at its highest efficiency point. The result values are presented in the first rows of Table 4.5 (baseline). As a result, less autonomy of the boat is obtained with respect to the optimization results due to the displacement of the triad operating point with respect to the optimum result obtained in the model. Figure 5.2 presents a comparative statistical analysis of the values obtained. Therefore, **an improvement in overall efficiency is evidenced** when using the method proposed here vs. the baseline **obtaining an improvement of 5.1% in efficiency and 7.3% in autonomy** vs. the worst case scenario. The data set is analyzed for each of the speeds that constitutes the study.

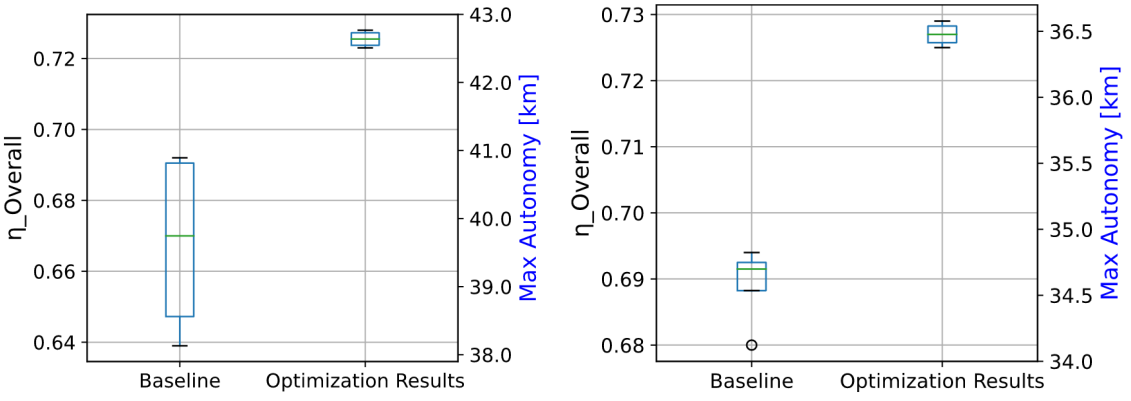

(a) **Comparative results for Speed 1:** 47 km/h (b) **Comparative results for Speed 2:** 55 km/h

Figure 5.2: *Optimization model vs direct electrification(Mira et al., 2021)*

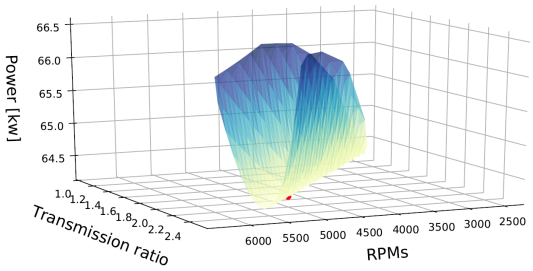

(a) **Speed 1 and Wolong EG80:** Power graph

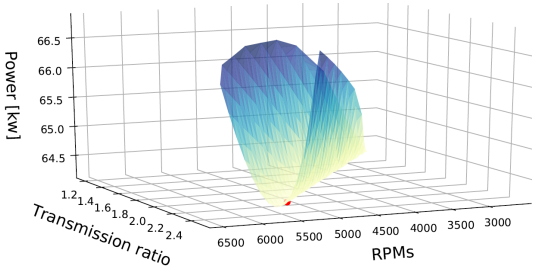

(b) **Speed 1 and Alpha APEV528:** Power graph

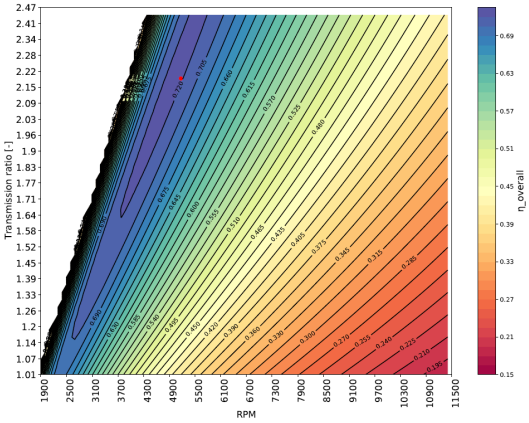

(c) **Speed 1 and Wolong EG80:** Transmission ratio efficiency map

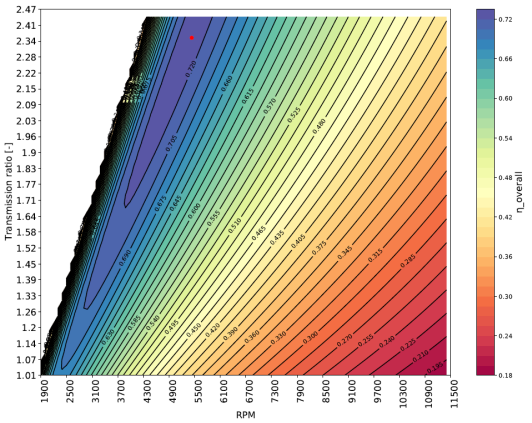

(d) **Speed 1 and Alpha APEV528:** Transmission ratio efficiency map

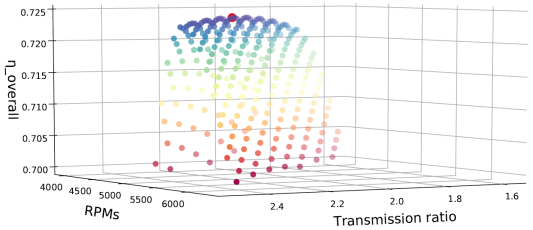

(e) **Speed 1 and Wolong EG80:** Overall efficiency

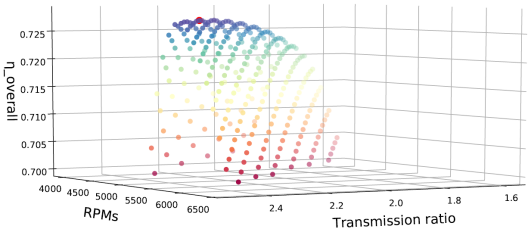

(f) **Speed 1 and Alpha APEV528:** Overall efficiency

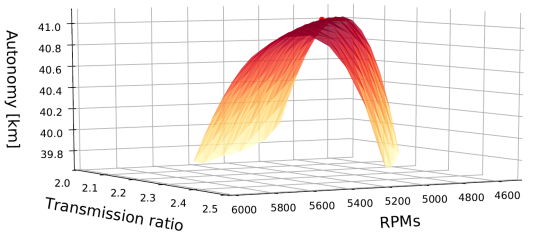

(g) **Speed 1 and Wolong EG80:** Autonomy

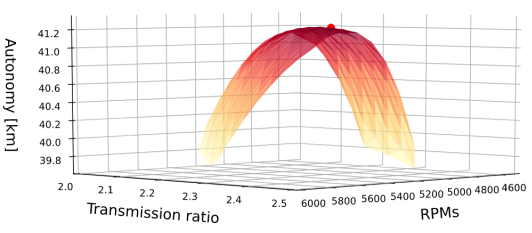

(h) **Speed 1 and Alpha APEV528:** Autonomy

Figure 5.3: *Analysis of the results of Optimal Motor-Transmission-Propeller matching for Speed 1*

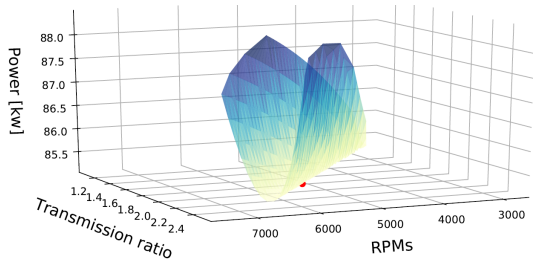

(a) **Speed 2 and Wolong EG80:** Power graph

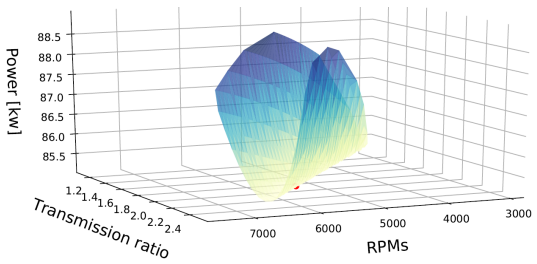

(b) **Speed 2 and Alpha APEV528:** Power graph

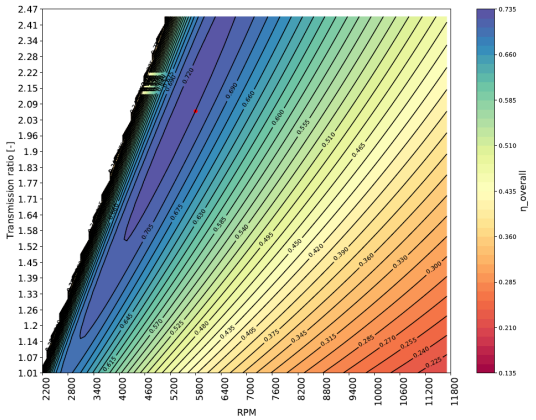

(c) **Speed 2 and Wolong EG80:** Transmission ratio efficiency map

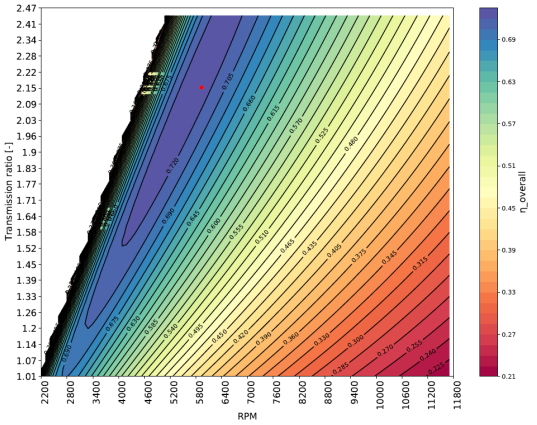

(d) **Speed 2 and Alpha APEV528:** Transmission ratio efficiency map

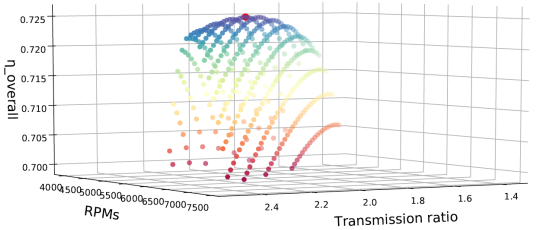

(e) **Speed 2 and Wolong EG80:** Overall efficiency

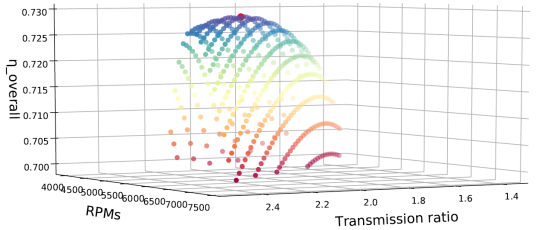

(f) **Speed 2 and Alpha APEV528:** Overall efficiency

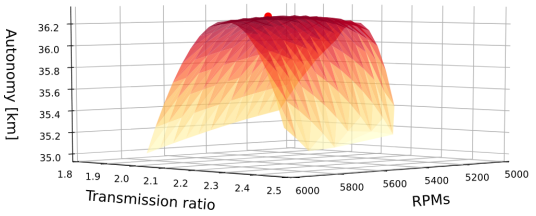

(g) **Speed 2 and Wolong EG80:** Autonomy

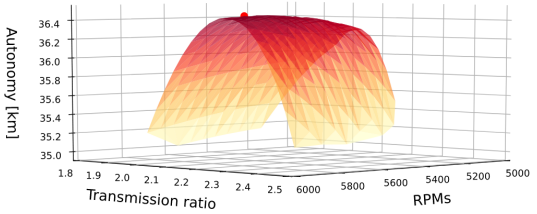

(h) **Speed 2 and Alpha APEV528:** Autonomy

Figure 5.4: *Analysis of the results of Optimal Motor-Transmission-Propeller matching for speed 2.(Mira et al., 2021)*

Chapter 6

Discussion and Conclusions

As a result of this research, a methodology was proposed to improve autonomy of electrically-powered vessels, by maximizing the overall efficiency. The optimization has been done from a Motor–Transmission–Propeller matching point of view. A case study about an electrically powered Propulsion System (PS), for an Electric River Boat, was addressed to evidence the results.

The context of use for this vessel is for passenger's public transport operation in the Magdalena River in Colombia, and by properly including the key variables into a optimality problem, the proposed methodology allowed to achieve an autonomy gain up to 2.9 km (7%) in the most favorable case (See Table A.2). Besides, an increment in autonomy was obtained, being a gain of 2 km (4.8%) for speed 1 (47 km/h) and 1.9 km (5.2%) for speed 2 (55 km/h), with respect to the direct electrification of a boat (with no modifications on transmission or propellers). This gain could represent the successful arrival to destination, or even the possibility to extend the length of the navigation routes or opening new routes to sites nearby the operating area. The optimum matching is given with the Alpha APEV528 motor, propeller 2 (13.5" x 16-K) and a t_{r_i} of 1.01 for Yamaha® outboard and 1.17 for Suzuki® outboard.

The total weight may also be reduced in 21 kg for one hour trips and cells with an energy capacity of 319.3 Wh/kg. The above by requiring an installed power of 85.27 kw compared to 89.47 kW in the worst configuration and operating in the situation of highest energy demand (speed 2). Less weight translates into less sinking of the boat and therefore less drag. Additionally, this result can be capitalized in increasing the passengers or luggage capacity. Failure to smartly modify the mechanics of the original design will result in system inefficiency.

The efficiency maps presented in Figures 5.3(c),5.3(d), 5.4(c) and 5.4(d), and become a useful tool for the designer to predict the behavior of this variable for the range of reduction ratios from 1.01 to 2.47, identifying the zones of higher efficiency bounded by the black contours and predicting changes in range and installed power as they move within the range that make up the design constraints.

A 45% efficiency gain is obtained with respect to an internal combustion engine.

Further Research: This method can be complemented by including other elements that make up the system and that influence the efficiency chain such as power electronics, conductor losses and the design of the power supply system. As a future work, the execution of a cycle of experimental tests with the outboard propulsion unit prototype that has been developed is proposed, where through the instrumentation, values of energy efficiency of the unit are obtained indirectly by means of the acquisition of data in operation of torque delivered by the motor, torque delivered to the propeller, current consumption, voltage, displacement speed and acceleration of the boat. This cycle provides greater robustness and offers the possibility of testing the validity and feasibility of the ideas through the implementation of a verifiable instance such as the prototype and will allow a better understanding and the formulation of improvement possibilities.

References

AA, S. (1983). Harvald. *Resistance and Propulsion of Ships*, pages 133–215.

Aponte, L. A. G. and Fragozo, C. A. Q. (2017). Geografía económica de los municipios ribereños del magdalena. *Revista del Banco de la República*, 90(1081):17–57.

ARCADIS Nederland BV and JESYCA S.A.S (2015). Plan Maestro Fluvial de Colombia 2015. Technical report, Ministerio de Transporte.

Bacciaglia, A., Ceruti, A., and Liverani, A. (2020). Controllable pitch propeller optimization through meta-heuristic algorithm. *Engineering with Computers*.

Birk, L. (2019). *Fundamentals of Ship Hydrodynamics: Fluid Mechanics, Ship Resistance and Propulsion*. John Wiley & Sons.

Brown, M. and Li, D.-Q. (2015). Advanced tools for waterjet performance prediction. *SSPA Highlights*, 60:12–13.

Burcher, R. K. (1988). Naval architecture. *Underwater Technology*, 14(4):26–28.

Carlton, J. (2018). *Marine propellers and propulsion*. Butterworth-Heinemann.

Carlton, J. S. (2007). *Marine Propellers and Propulsion*. Elsevier Ltd.

Çengel, Y. A., Ghajar, A. J., and DBorneville, E. J. H. (2011). *Transferencia de calor y masa: fundamentos y aplicaciones*. McGraw-Hill.

Central Intelligence Agency (CIA) (2020). The World Factbook - Central Intelligence Agency.

Chang, X., Sun, S., Wang, C., and Mo, T. (2015). Optimal design of propellers considering beyond-design conditions. *Harbin Gongcheng Daxue Xuebao/Journal of Harbin Engineering University*, 36(12):1544–1548.

Chasiotis, I. D. and Karnavas, Y. L. (2019). A generic multi-criteria design approach toward high power density and fault-tolerant low-speed pmsm for pod applications. *IEEE Transactions on Transportation Electrification*, 5(2):356–370.

Edenhofer, O. (2015). *Climate change 2014: mitigation of climate change*, volume 3. Cambridge University Press.

Ehsani, M., Gao, Y., and Emadi, A. (2010). *Modern electric,hybrid electric and fuel cell vehicles*. CRS Press, Florida, 2 edition.

Ekinci, S. (2011). A practical approach for design of marine propellers with systematic propeller series. *Brodogradnja: Teorija i praksa brodogradnje i pomorske tehnike*, 62(2):123–129.

Eliasson, R., Larsson, L., and Orych, M. (2014). *Principles of yacht design*. A&C Black.

Esmailian, E., Ghassemi, H., and Zakerdoost, H. (2017). Systematic probabilistic design methodology for simultaneously optimizing the ship-hull-propeller system. *International Journal of Naval Architecture and Ocean Engineering*, 9(3):246–255.

Galindo, N. (2010). *Impacto de la incorporación del vehículo eléctrico en la integración de energías renovables en el sistema eléctrico*. PhD thesis, Universidad Carlos III de Madrid.

Gerr, D. (1989). *Propeller handbook*. International Marine Publishing.

Ghose, J. (2004). *Basic ship propulsion*. Allied publishers.

Gieras, J. F. (2002). *Permanent magnet motor technology: design and applications*. CRC press.

Gillmer, T. C. and Johnson, B. (1982). *Introduction to naval architecture*. Naval Institute Press.

Giraldo-Pérez, E., Gaviria, G., Betancur, E., Osorio-Gómez, G., and Mejía-Gutiérrez, R. (2020). Influence of energy consumption on battery sizing of electric fluvial vessels: a colombian case study. In *2020 Fifteenth International Conference on Ecological Vehicles and Renewable Energies (EVER)*, pages 1–8. IEEE.

Giraldo Pérez, E. S. et al. (2021). *A comparative study of the hydrodynamic performance of planing boats through experimental and statistical approaches*. PhD thesis, Universidad EAFIT.

Gorter, T. (2015). Design Considerations of a Solar Racing Boat: Propeller Design Parameters as a Result of PV System Power. In *Energy Procedia*, volume 75, pages 1901–1906.

Hansen, J. F. and Wendt, F. (2015). History and state of the art in commercial electric ship propulsion, integrated power systems, and future trends. *Proceedings of the IEEE*, 103(12):2229–2242.

Harvald, S. A. (1992). *Resistance and propulsion of ships*.

Horváth, I. et al. (2007). Comparison of three methodological approaches of design research. In *DS 42: Proceedings of ICED 2007, the 16th International Conference on Engineering Design, Paris, France, 28.-31.07. 2007*, pages 361–362.

Hudson, D. A., Molland, A. F., and Turnock, S. R. (2014). *Ship Resistance and Propulsion: Practical Estimation of Propulsive Power*. Cambridge University Press.

Intermec (2021). Transmisiones por correas dentadas de tiempo y sincrónicas. *Intermec.com*.

IPCC (2014). Climate Change 2014: Mitigation of Climate Change. Summary for Policymakers and Technical Summary. Technical report, IPCC.

ITTC (2002). Recommended procedures and guidelines 7.5-02-03-01.1. *Testing and extrapolation methods propulsion, performance propulsion test, Revision*, 1.

Jaimurzina, A. and Wilmsmeier, G. (2017). La movilidad fluvial en américa del sur: avances y tareas pendientes en materia de políticas públicas. *Serie recursos naturales e infraestructura-Naciones Unidas*.

Kim, K., Turnock, S., Ando, J., Becchi, P., Minchev, A., Semionicheva, E., Van, S., Zhou, W., and Korkut, E. (1970). The propulsion committee: final report and recommendations to the 25th ittc. *Proceedings of 25th ITTC Volume I*.

Klein Woud, H. J. and Stapersma, D. (2019). Design of propulsion and electric power generations systems, revised edition. *Published by IMarEST, The Institute of Marine Engineering, Science and Technology. ISBN: 1-902536-47-9*.

L. Blount, D. and L. Fox, D. (1976). Small-Craft Power Prediction. *Marine Technology*, 13:14–45.

Lackenby, H. (1978). *ITTC Dictionary of Ship Hydrodynamics*. Royal institution of naval architects.

Łapko, A. (2019a). Is it time for motorboat e-mobility? *Transportation Research Procedia*, 39(2018):280–289.

Łapko, A. (2019b). Is it time for motorboat e-mobility? *Transportation Research Procedia*, 39:280–289.

Larsson, L. and Eliasson, R. (2000). Principles of Yacht Design.

Lea, M., Thompson, D., Van Blarcom, B., Eaton, J., Friesch, J., and Richards, J. (2003). Scale model testing of a commercial rim-driven propulsor pod. *Journal of ship production*, 19(2):121–130.

Lee, E. C. (2001). Review of Variable Speed drive technology. page 13.

Lu, S. M. (2016a). A review of high-efficiency motors: Specification, policy, and technology. *Renewable and Sustainable Energy Reviews*, 59:1–12.

Lu, S.-M. (2016b). A review of high-efficiency motors: Specification, policy, and technology. *Renewable and Sustainable Energy Reviews*, 59:1–12.

maritime affairs, W. (2019). Learn about Waterjet Propulsion System - A Maritime industry Affairs.

Marques, C. H., Belchior, C. R. P., and Caprace, J. D. (2019a). An early-stage approach to optimise a marine energy system for liquefied natural gas carriers: Part a-developed approach. *Ocean Engineering*, 181:161–172.

Marques, C. H., Carlos, ·., Belchior, R. P., and Caprace, J.-D. (2019b). Marine propeller parametric optimisation and matching to electric motor. *Journal of the Brazilian Society of Mechanical Sciences and Engineering*, 41(3):119.

Michalski, J. (2007). A method for selection of parameters of ship propulsion system fitted with compromise screw propeller. *Polish Maritime Research*, 14(4):3–6.

Minambiente (2019). *Estrategia Nacional de Movilidad Eléctrica. Definición de la meta.*

Minas-Energia, M. (2021). Transición energética: un legado para el presente y el futuro de Colombia. Technical report.

Minciencias (2020). Convocatoria Energía Sostenible y su Aporte a la Planeación Minero Energética-2020. Technical report, Minciencias, Bogotá.

Mira, J.-D., Gómez-Oviedo, S., Betancur, E., and Mejía-Gutiérrez, R. (2020a). Preliminary sizing of a propulsion unit for an electrically-powered vessel using a screw propellers performance comparison tool. In *Workshop on Engineering Applications*, pages 465–476. Springer.

Mira, J.-D., Mendoza, F., Betancur, E., Manrique, T., and Mejía-Gutiérrez, R. (2021). A propulsion system design methodology based on overall efficiency optimization for electrically powered vessels. *IEEE Transactions on Transportation Electrification*, pages 1–1,DOI:10.1109/TTE.2021.3104763.

Mira, J.-D., Valderrama, S., Londoño, M.-J., Giraldo-Pérez, E., Betancur, E., Osorio-Gómez, G., and Mejía-Gutiérrez, R. (2020b). Preliminary design tools applied to a solar powered vessel design: A south american river analysis. In *2020 Fifteenth International Conference on Ecological Vehicles and Renewable Energies (EVER)*, pages 1–9. IEEE.

Miranda, I., Silva, N., and Leite, H. (2016). A holistic approach to the integration of battery energy storage systems in island electric grids with high wind penetration. *IEEE Transactions on Sustainable Energy*, 7(2):775–785.

Molland, A. F. (2011). *The maritime engineering reference book: a guide to ship design, construction and operation*. Elsevier.

Molland, A. F., Turnock, S. R., and Hudson, D. A. (2017). *Ship resistance and propulsion*. Cambridge university press.

Mulyana, D., Koeshardono, F., Sudradjat, A., and Widiatmoko, R. Y. (2020). Optimization of B-series propeller geometry dimension to improve traditional fishing ship performance. *IOP Conference Series: Materials Science and Engineering*, 830(4):2–8.

Nykvist, B. and Nilsson, M. (2015). Rapidly falling costs of battery packs for electric vehicles. *Nature climate change*, 5(4):329–332.

Pachauri, R., Meyer, L., and Stocker, T. (2014). Ipcc 2014: Cambio climático 2014: Informe de síntesis. *Contribución de los Grupos de Trabajo I. II y III al Quinto Informe de evaluación del panel intergubernamental sobre el cambio climático. IPCC, Ginebra, CHE*.

Pan, G., Cheng, B., Zhang, P., and Cao, Y. (2016). Coupling design and performance analysis of rim-driven integrated motor propulsor. In *OCEANS 2016-Shanghai*, pages 1–6. IEEE.

Papanikolaou, A. (2014). *Ship design: methodologies of preliminary design*. Springer.

Pestana, H. (2015). Future trends of electrical propulsion and implications to ship design. *Maritime Technology and Engineering - Proceedings of MARTECH 2014: 2nd International Conference on Maritime Technology and Engineering*, pages 797–806.

Propulsion, S. (2006). Basic principles of ship propulsion. *Presentado por: Man B&W Diesel*.

Reche Tejero, J. et al. (2019). Propuesta de modificación de diseño y materiales de una embarcación con motores eléctricos y energía solar. B.S. thesis, Universitat Politècnica de Catalunya.

Ren, H., Ding, Y., and Sui, C. (2019). Influence of eedi (energy efficiency design index) on ship–engine–propeller matching. *Journal of Marine Science and Engineering*, 7(12):425.

Roberts, A., Brooks, R., and Shipway, P. (2014). Internal combustion engine cold-start efficiency: A review of the problem, causes and potential solutions. *Energy Conversion and Management*, 82:327–350.

Rudolf, T., Schürmann, T., Schwab, S., and Hohmann, S. (2021). Toward holistic energy management strategies for fuel cell hybrid electric vehicles in heavy-duty applications. *Proceedings of the IEEE*, 109(6):1094–1114.

Santosh Raju, G. and Niranjan Kumar, N. (2008). STUDY ON DIFFERENT ESTIMATION METHODS OF PROPULSION POWER FOR 60 mts OFFSHORE SUPPLY VESSEL. *International Research Journal of Engineering and Technology*.

Savitsky, D. et al. (1964). Hydrodynamic design of planing hulls. *Marine Technology and SNAME News*, 1(04):71–95.

Siddall, J. (2019). *Mechanical Design: Reference Sources*. University of Toronto Press.

Skene, N. L. (1973). *Skene's elements of yacht design, 8th ed.* Dodd, Mead.

Sponberg, E. W. (2011). The design ratios. *A Naval ArchitectÂ´s Dozen (or thereabouts). Revised*.

Tan, W., Yan, X., Liu, Z., et al. (2015). Technology development and prospect of shaftless rim-driven propulsion system. *Journal of Wuhan University of Technology*, 39(3):601–605.

The Economist (2017). After electric cars, what more will it take for batteries to change the face of energy?

Tupper, E. C. (2013). *Introduction to naval architecture*. Butterworth-Heinemann.

Tupper, E. C. and Rawson, K. (2001). *Basic Ship Theory Volume 2*, volume 2. Elsevier.

UPME (2017). Mapa de ruta para la transición hacia el uso de vehículos de bajas y cero emisiones.

UPME (2020). Plan Energético Nacional 2020-2050. page 215.

Van Blarcom, B., Hanhinen, J., and Mewis, F. (2002). The commercial rim-driven permanent magnet motor propulsor pod. In *Ship Production Symposium, Boston MA, USA, Sept*, volume 25, page 26.

Wells, C. W. (2007). The Road to the Model T: Culture, Road Conditions, and Innovation at the Dawn of the American Motor Age. *Faculty Publications*.

Windyandari, A., Haryadi, G., Suharto, and Zakki, A. (2018). Optimization procedure to determine the optimum propeller of traditional purse seine boat. *International Journal of Mechanical Engineering and Technology*, 9(13):1519–1526.

Wyman, D. B. (1998). Wyman's Formula.

Yamaha Motor Co., L. (2002). MANUAL DEL PROPIETARIO F100B.

Yan, X., Liang, X., Ouyang, W., Liu, Z., Liu, B., and Lan, J. (2017). A review of progress and applications of ship shaft-less rim-driven thrusters. *Ocean Engineering*, 144:142–156.

Yang, T., Cox, T., Degano, M., Bozhko, S., and Gerada, C. (2016). History and recent advancements of electric propulsion and integrated electrical power systems for commercial & naval vessels.

Yun, L., Bliault, A., and Rong, H. Z. (2018). *High Speed Catamarans and Multihulls: Technology, Performance, and Applications*. Springer.

Acronyms

BAR Blade Area Ratio. x, 52, 61, 70

CFD Computational Fluid Dynamics. 24, 25, 29

DNP National Planning Department. 3

EV Electric Vehicle. 10

GHG Greenhouse Gas. 3

ICE Internal Combustion Engine. ix, 4, 7, 11–13, 16, 21, 65–67

IPCC Intergovernmental Panel on Climate Change. 2

PMSM Permanent Magnet Synchronous Motor. 14

PS Propulsion System. viii, 10, 11, 13–17, 40, 45, 63, 65–68, 70, 72, 74, 76, 78–80

RiDC Research in Design Context. 17

Appendix A

Engine-Transmission-Propeller Matching Simulations Results

Table A.1: *Results for catamaran case study*

Catamaran-type hull geometry																											
Parameter	Units	Propeller 1: 13.5' x 14-K								Propeller 2: 13.5' x 16-K								Propeller 3: 13' x 17-K2							
Boat Velocity		Speed 1: 47 km/h				Speed 2: 55 km/h				Speed 1: 47 km/h				Speed 2: 55 km/h				Speed 1: 47 km/h				Speed 2: 55 km/h			
Electric motor		Wolong EG80		Alpha APEV528		Wolong EG80		Alpha APEV528		Wolong EG80		Alpha APEV528		Wolong EG80		Alpha APEV528		Wolong EG80		Alpha APEV528		Wolong EG80		Alpha APEV528	
	Outboard	Yamaha	Suzuki	Yamaha	Suzuki	Yamaha	Suzuki	Yamaha	Suzuki	Yamaha	Suzuki	Yamaha	Suzuki	Yamaha	Suzuki	Yamaha	Suzuki	Yamaha	Suzuki	Yamaha	Suzuki	Yamaha	Suzuki	Yamaha	Suzuki
$t_{r(outboard)}$	[-]	2.15	2.59	2.15	2.59	2.15	2.59	2.15	2.59	2.15	2.59	2.15	2.59	2.15	2.59	2.15	2.59	2.15	2.59	2.15	2.59	2.15	2.59	2.15	2.59
t_r	[-]	1.86	1.86	2.01	2.01	1.74	1.74	1.86	1.86	2.19	2.19	2.38	2.38	2.07	2.07	2.15	2.15	2.31	2.31	2.44	2.44	2.16	2.16	2.27	2.27
$t_{r(i)}$	[-]	1.14	1.28	1.06	1.22	1.19	1.32	1.13	1.30	0.98	1.15	0.90	1.08	1.04	1.20	1.00	1.17	0.92	1.11	0.88	1.06	0.99	1.16	0.94	1.13
ω	[rev/min]	5000	5000	5400	5400	5500	5500	5800	5800	5000	5000	5400	5400	5500	5500	5700	5700	5100	5100	5400	5400	5600	5600	5900	5900
n	[rev/min]	2686	2686	2681	2681	3161	3161	3115	3115	2276	2276	2270	2270	2651	2651	2669	2669	2200	2200	2213	2213	2586	2586	2579	2579
D	[in]	13.5	13.5	13.5	13.5	13.5	13.5	13.5	13.5	13.5	13.5	13.5	13.5	13.5	13.5	13.5	13.5	13	13	13	13	13	13	13	13
P	[in]	14	14	14	14	14	14	14	14	16	16	16	16	16	16	16	16	17	17	17	17	17	17	17	17
S_R	[-]	0.18	0.18	0.17	0.17	0.18	0.18	0.17	0.17	0.15	0.15	0.15	0.15	0.14	0.14	0.15	0.15	0.17	0.17	0.18	0.18	0.17	0.17	0.18	0.18
V_a	[ft/s]	42.83	42.83	42.83	42.83	50.12	50.12	50.12	50.12	42.83	42.83	42.83	42.83	50.12	50.12	50.12	50.12	42.83	42.83	42.83	42.83	50.12	50.12	50.12	50.12
η_H	[-]	1.05	1.05	1.05	1.05	1.05	1.05	1.05	1.05	1.05	1.05	1.05	1.05	1.05	1.05	1.05	1.05	1.05	1.05	1.05	1.05	1.05	1.05	1.05	1.05
η_R	[-]	0.98	0.98	0.98	0.98	0.98	0.98	0.98	0.98	0.98	0.98	0.98	0.98	0.98	0.98	0.98	0.98	0.98	0.98	0.98	0.98	0.98	0.98	0.98	0.98
J	[-]	0.850	0.850	0.852	0.852	0.845	0.845	0.857	0.857	1.003	1.003	1.006	1.006	1.008	1.008	1.001	1.001	1.078	1.078	1.071	1.071	1.073	1.073	1.076	1.076
P_D	[-]	1.03	1.03	1.03	1.03	1.03	1.03	1.03	1.03	1.20	1.20	1.20	1.20	1.20	1.20	1.20	1.20	1.30	1.30	1.30	1.30	1.30	1.30	1.30	1.30
A_E/A_0	[-]	0.48	0.48	0.48	0.48	0.48	0.48	0.48	0.48	0.47	0.47	0.47	0.47	0.47	0.47	0.47	0.47	0.61	0.61	0.61	0.61	0.61	0.61	0.61	0.61
Z	[und]	3	3	3	3	3	3	3	3	3	3	3	3	3	3	3	3	3	3	3	3	3	3	3	3
η_o	[-]	0.708	0.708	0.708	0.708	0.708	0.708	0.708	0.708	0.736	0.736	0.736	0.736	0.736	0.736	0.736	0.736	0.701	0.701	0.701	0.701	0.701	0.701	0.701	0.701
η_D	[-]	0.728	0.728	0.728	0.728	0.728	0.728	0.728	0.728	0.757	0.757	0.757	0.757	0.758	0.758	0.757	0.757	0.722	0.722	0.722	0.722	0.722	0.722	0.722	0.722
τ	[N.m]	127.64	127.64	118.18	118.18	153.94	153.94	145.97	145.97	122.76	122.76	113.67	113.67	148.04	148.04	142.85	142.85	126.30	126.30	119.28	119.28	152.56	152.56	144.81	144.81
η_{motor}	[-]	0.955	0.955	0.960	0.960	0.956	0.956	0.962	0.962	0.955	0.955	0.959	0.959	0.956	0.956	0.961	0.961	0.955	0.955	0.960	0.960	0.957	0.957	0.962	0.962
$\eta_{overall}$	[-]	0.696	0.696	0.699	0.699	0.697	0.697	0.701	0.701	0.723	0.723	0.727	0.727	0.725	0.725	0.728	0.728	0.690	0.690	0.693	0.693	0.691	0.691	0.694	0.694
P_E	[kW]	66.83	66.83	66.83	66.83	88.67	88.67	88.66	88.66	64.28	64.28	64.28	64.28	85.26	85.26	85.27	85.27	67.45	67.45	67.45	67.45	89.47	89.47	89.47	89.47
Autonomy	[km]	39.5	39.5	39.7	39.7	34.8	34.8	35.1	35.1	41.0	41.0	41.2	41.2	36.3	36.3	36.5	36.5	39.1	39.1	39.3	39.3	34.5	34.5	34.7	34.7

Table A.2: *Catamaran case study results: Direct electrification vs Proposed optimization method (Mira et al., 2021)*

		Parameter	Units	**Speed 1:** 47 km/h				**Speed 2 :** 55 km/h			
Baseline Results	Original Propeller Provided: 13"x 17	**Electric motor :**		Wolong EG80		Alpha APEV528		Wolong EG80		Alpha APEV528	
		Outboard :		Yamaha	Suzuki	Yamaha	Suzuki	Yamaha	Suzuki	Yamaha	Suzuki
		$t_{r(outboard)}$	[-]	2.15	2.59	2.15	2.59	2.15	2.59	2.15	2.59
		$\eta_{overall}$	[-]	0.650	0.639	0.690	0.692	0.691	0.680	0.694	0.692
		P_E	[kW]	68.00	68.60	67.40	67.40	89.40	89.47	89.49	85.52
		Autonomy	[km]	38.1	38.1	39.2	39.3	34.5	34.4	34.7	34.6
Optimization Results	Propeller 1: 13.5" x 14-K	t_r	[-]	1.86	1.86	2.01	2.01	1.74	1.74	1.86	1.86
		$t_{r(i)}$	[-]	1.14	1.28	1.06	1.22	1.19	1.32	1.13	1.30
		$\eta_{overall}$	[-]	0.696	0.696	0.699	0.699	0.697	0.697	0.701	0.701
		P_E	[kW]	66.83	66.83	66.83	66.83	88.67	88.67	88.66	88.66
		Autonomy	[km]	39.5	39.5	39.7	39.7	34.8	34.8	35.1	35.1
	Propeller 2: 13.5" x 16-K	t_r	[-]	2.19	2.19	2.38	2.38	2.07	2.07	2.13	2.13
		$t_{r(i)}$	[-]	0.98	1.15	0.90	1.08	1.04	1.20	1.01	1.17
		$\eta_{overall}$	[kW]	0.723	0.723	0.727	0.727	0.725	0.725	**0.728**	**0.728**
		P_E	[km]	64.28	64.28	64.28	64.28	85.26	85.26	85.27	85.27
		Autonomy	[-]	41.0	41.0	**41.2**	**41.2**	36.3	36.3	36.5	36.5
	Propeller 3: 13" x 17-K2	t_r	[-]	2.31	2.31	2.44	2.44	2.16	2.16	2.27	2.27
		$t_{r(i)}$	[-]	0.92	1.11	0.88	1.06	0.99	1.16	0.94	1.13
		$\eta_{overall}$	[kW]	0.690	0.690	0.693	0.693	0.691	0.691	0.694	0.694
		P_E	[km]	67.45	67.45	67.45	67.45	89.47	89.47	89.47	89.47
		Autonomy	[-]	39.1	39.1	39.3	39.3	34.5	34.5	34.7	34.7

A.1 Results maps for speed 1 (47 km/h)

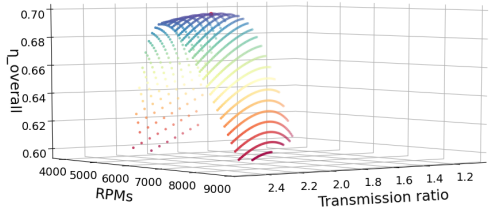

(a) **S1-W-Y-P1**: Maximum overall efficiency graph

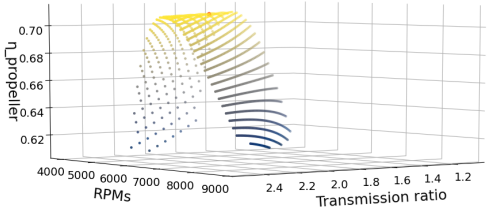

(b) **S1-W-Y-P1**: Maximum propeller efficiency graph

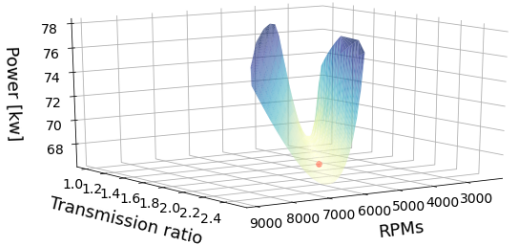

(c) **S1-W-Y-P1**: Minimum power graph

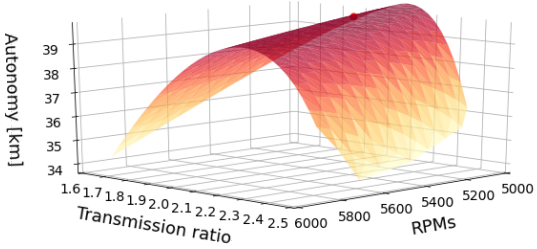

(d) **S1-W-Y-P1**: Maximum autonomy graph

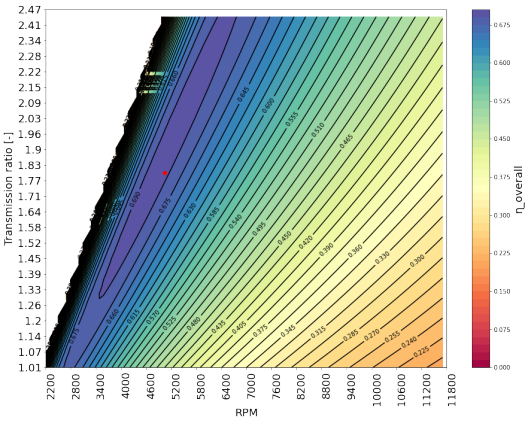

(e) **S1-W-Y-P1**: Transmission ratio efficiency map

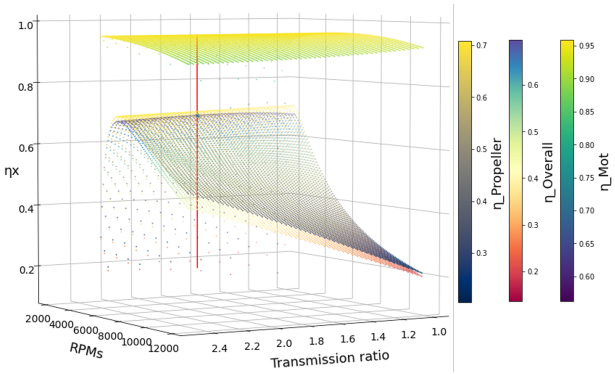

(f) **S1-W-Y-P1**: Motor-Transmission-Propeller matching

transmission_ratios	1.861429
transmission_ratios_i_values	1.155027
RPMs_mot	5000.100000
RPMs_propeller	2686.162701
diameter [in]	13.500000
pitch	1.166670
slip_ratio	0.179929
speed_of_advance	42.833200
hull_efficiency	1.050000
eta_r	0.980000
advance_coefficient	0.850446

P_D	1.030000
AE_A0	0.480000
Z	3.000000
eta_open_water	0.708370
QPC	0.728913
torque_motor	127.642013
eta_motor	0.955374
GLOBAL_EFFICIENCY	0.696384
POWER	66.834538
AUTONOMY	39.481086

Name: 2664, dtype: float64

(g) **S1-W-Y-P1**: Numerical results

Figure A.1: *Results for "Wolong EG80-Yamaha F100BETX-Propeller 1" Matching*

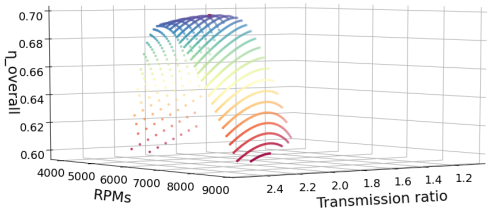

(a) **S1-W-S-P1**: Maximum overall efficiency graph

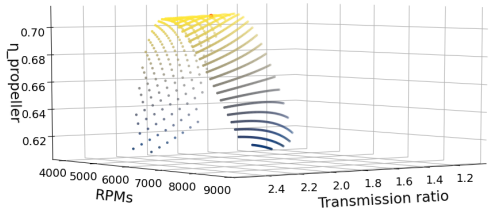

(b) **S1-W-S-P1**: Maximum propeller efficiency graph

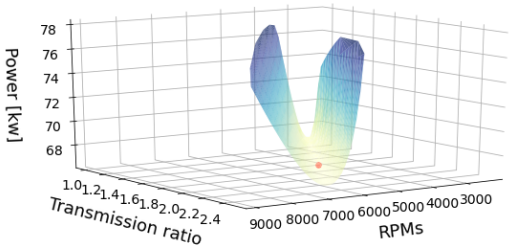

(c) **S1-W-S-P1**: Minimum power graph

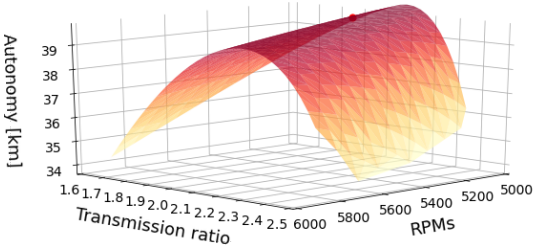

(d) **S1-W-S-P1**: Maximum autonomy graph

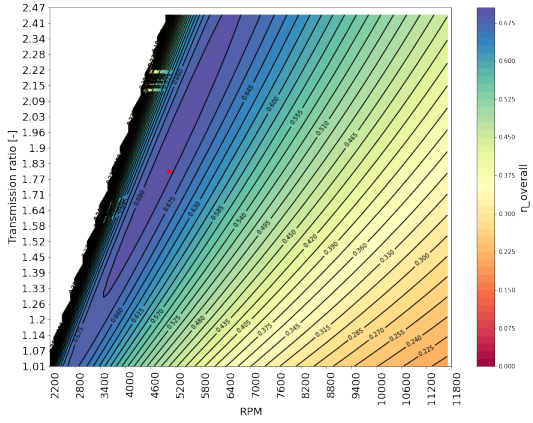

(e) **S1-W-S-P1**: Transmission ratio efficiency map

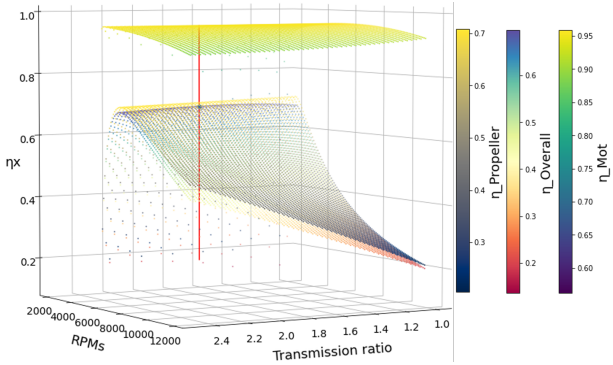

(f) **S1-W-S-P1**: Motor-Transmission-Propeller matching

transmission_ratios	1.861429
transmission_ratios_i_values	1.391404
RPMs_mot	5000.100000
RPMs_propeller	2686.162701
diameter [in]	13.500000
pitch	1.166670
slip_ratio	0.179929
speed_of_advance	42.833200
hull_efficiency	1.050000
eta_r	0.980000
advance_coefficient	0.850446

P_D	1.030000
AE_A0	0.480000
Z	3.000000
eta_open_water	0.708370
QPC	0.728913
torque_motor	127.642013
eta_motor	0.955374
GLOBAL_EFFICIENCY	0.696384
POWER	66.834538
AUTONOMY	39.481086
Name: 2664, dtype: float64	

(g) **S1-W-S-P1**: Numerical results

Figure A.2: *Results for "Wolong EG80-Suzuki DF90-Propeller 1" Matching*

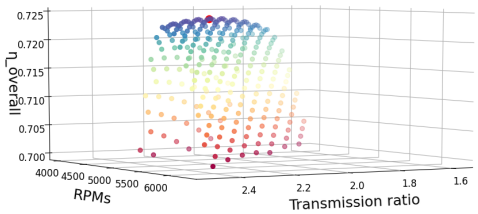

(a) **S1-W-Y-P2**: Maximum overall efficiency graph

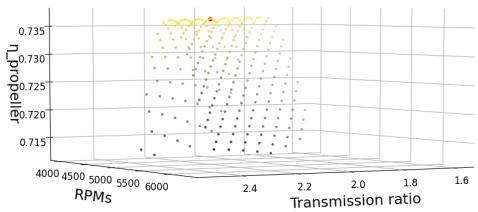

(b) **S1-W-Y-P2**: Maximum propeller efficiency graph

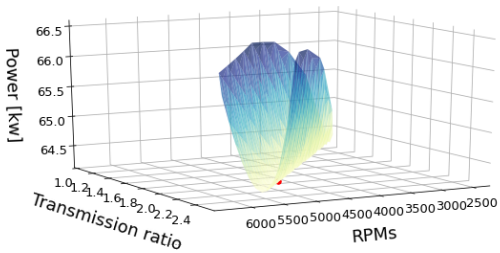

(c) **S1-W-Y-P2**: Minimum power graph

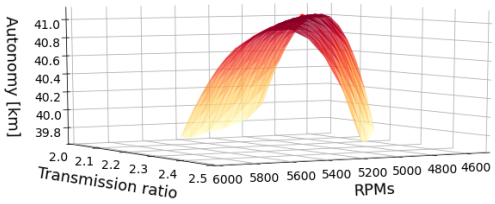

(d) **S1-W-Y-P2**: Maximum autonomy graph

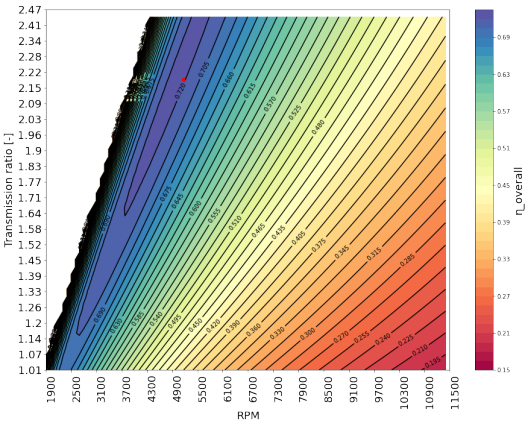

(e) **S1-W-Y-P2**: Transmission ratio efficiency map

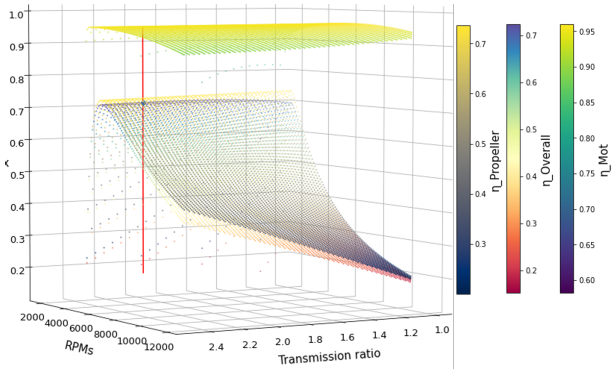

(f) **S1-W-Y-P2**: Motor-Transmission-Propeller matching

transmission_ratios	2.195918
transmission_ratios_i_values	0.979089
RPMs_mot	5000.100000
RPMs_propeller	2276.997212
diameter [in]	13.500000
pitch	1.333330
slip_ratio	0.153491
speed_of_advance	42.833200
hull_efficiency	1.050000
eta_r	0.980000
advance_coefficient	1.003268

P_D	1.200000
AE_A0	0.470000
Z	3.000000
eta_open_water	0.736484
QPC	0.757842
torque_motor	122.769458
eta_motor	0.955171
GLOBAL_EFFICIENCY	0.723869
POWER	64.283224
AUTONOMY	41.039321
Name: 3584, dtype: float64	

(g) **S1-W-Y-P2**: Numerical results

Figure A.3: *Results for "Wolong EG80-Yamaha F100BETX-Propeller 2" Matching*

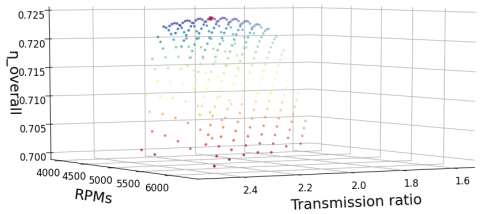

(a) **S1-W-S-P2**: Maximum overall efficiency graph

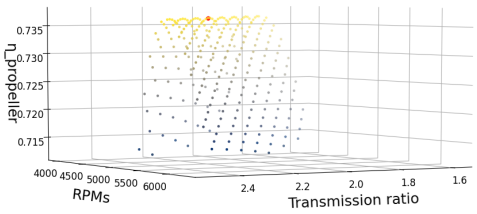

(b) **S1-W-S-P2**: Maximum propeller efficiency graph

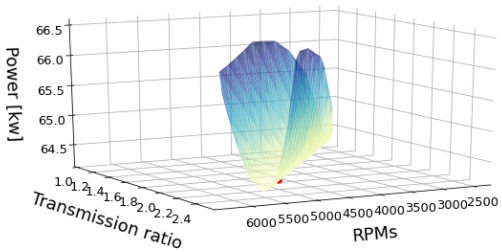

(c) **S1-W-S-P2**: Minimum power graph

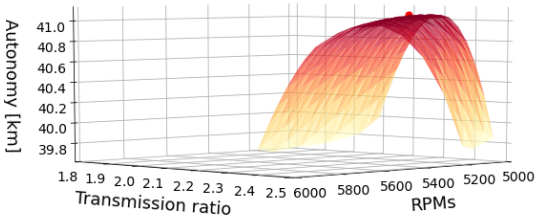

(d) **S1-W-S-P2**: Maximum autonomy graph

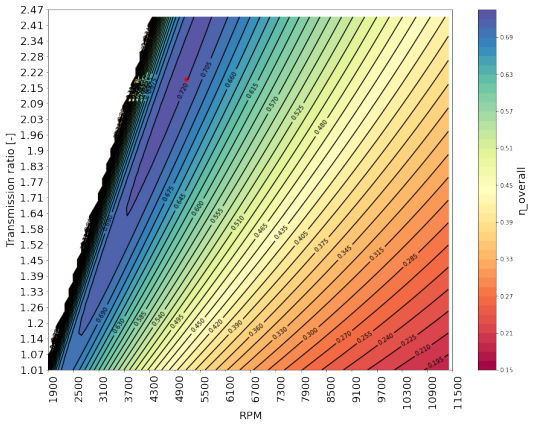

(e) **S1-W-S-P2**: Transmission ratio efficiency map

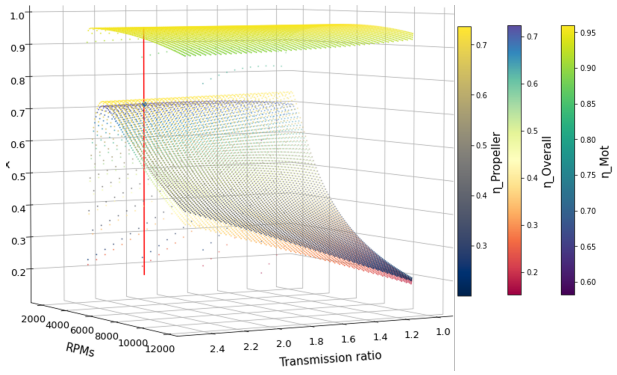

(f) **S1-W-S-P2**: Motor-Transmission-Propeller matching

transmission_ratios	2.195918	P_D	1.200000
transmission_ratios_i_values	1.179461	AE_A0	0.470000
RPMs_mot	5000.100000	Z	3.000000
RPMs_propeller	2276.997212	eta_open_water	0.736484
diameter [in]	13.500000	QPC	0.757842
pitch	1.333330	torque_motor	122.769458
slip_ratio	0.153491	eta_motor	0.955171
speed_of_advance	42.833200	GLOBAL_EFFICIENCY	0.723869
hull_efficiency	1.050000	POWER	64.283224
eta_r	0.980000	AUTONOMY	41.039321
advance_coefficient	1.003268	Name: 3584, dtype: float64	

(g) **S1-W-S-P2**: Numerical results

Figure A.4: *Results for "Wolong EG80-Suzuki DF90-Propeller 2" Matching*

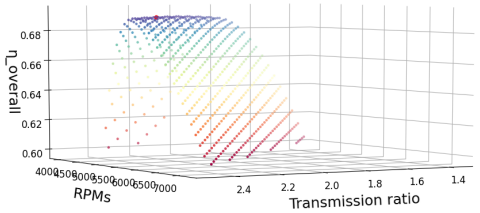

(a) **S1-W-Y-P3**: Maximum overall efficiency graph

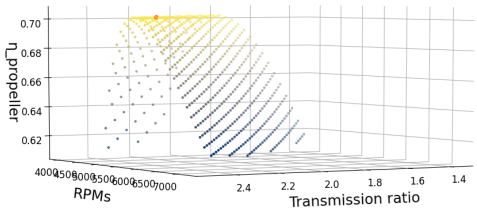

(b) **S1-W-Y-P3**: Maximum propeller efficiency graph

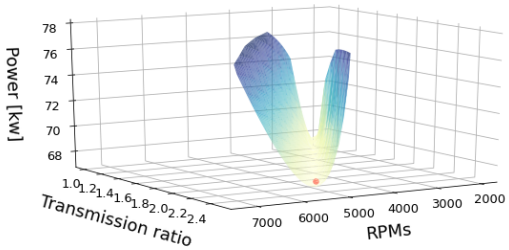

(c) **S1-W-Y-P3**: Minimum power graph

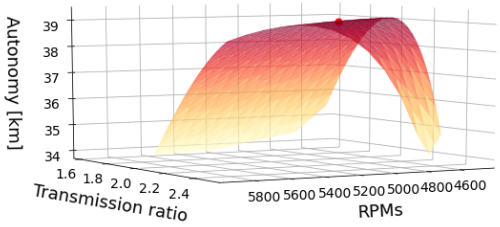

(d) **S1-W-Y-P3**: Maximum autonomy graph

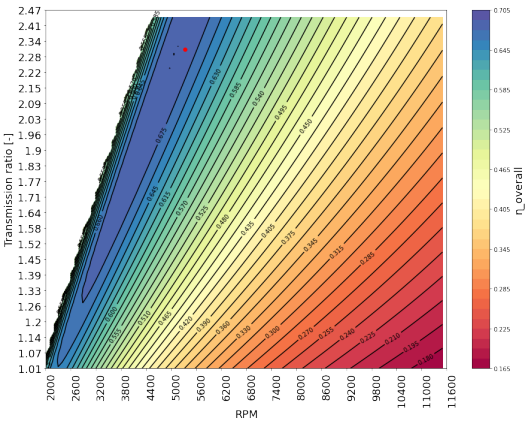

(e) **S1-W-Y-P3**: Transmission ratio efficiency map

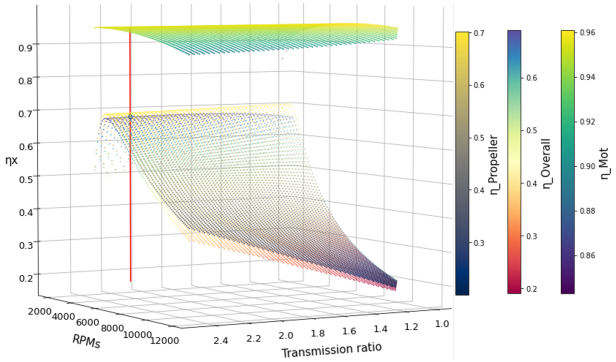

(f) **S1-W-Y-P3**: Motor-Transmission-Propeller matching

transmission_ratios	2.317551	P_D	1.300000
transmission_ratios_i_values	0.927703	AE_A0	0.610000
RPMs_mot	5100.100000	Z	3.000000
RPMs_propeller	2200.641951	eta_open_water	0.701870
diameter [in]	12.999960	QPC	0.722225
pitch	1.416670	torque_motor	126.298113
slip_ratio	0.175646	eta_motor	0.955435
speed_of_advance	42.833200	GLOBAL_EFFICIENCY	0.690039
hull_efficiency	1.050000	POWER	67.453451
eta_r	0.980000	AUTONOMY	39.121335
advance_coefficient	1.078007	Name: 3854, dtype: float64	

(g) **S1-W-Y-P3**: Numerical results

Figure A.5: *Results for "Wolong EG80-Yamaha F100BETX-Propeller 3" Matching*

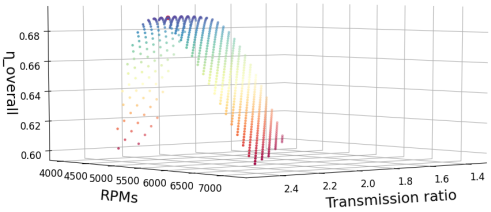

(a) **S1-W-S-P3**: Maximum overall efficiency graph

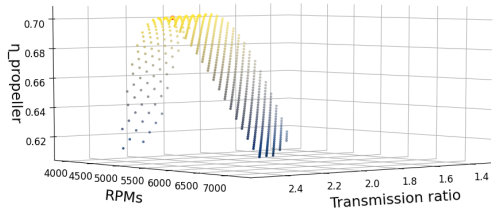

(b) **S1-W-S-P3**: Maximum propeller efficiency graph

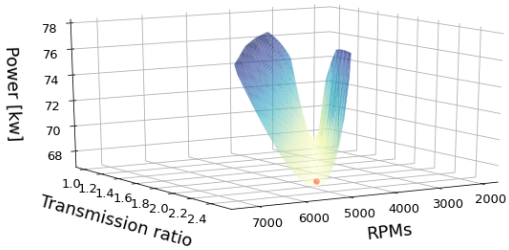

(c) **S1-W-S-P3**: Minimum power graph

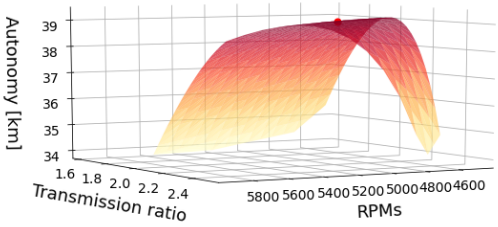

(d) **S1-W-S-P3**: Maximum autonomy graph

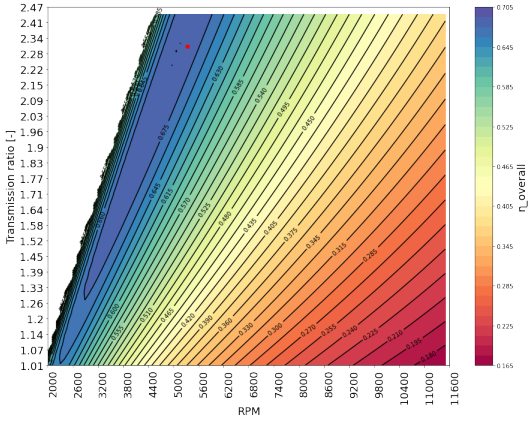

(e) **S1-W-S-P3**: Transmission ratio efficiency map

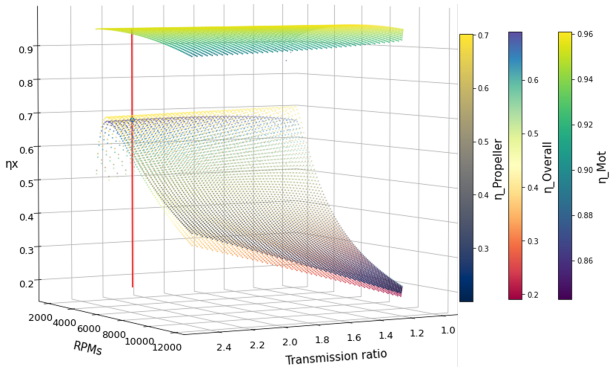

(f) **S1-W-S-P3**: Motor-Transmission-Propeller matching

transmission_ratios	2.317551
transmission_ratios_i_values	1.117559
RPMs_mot	5100.100000
RPMs_propeller	2200.641951
diameter [in]	12.999960
pitch	1.416670
slip_ratio	0.175646
speed_of_advance	42.833200
hull_efficiency	1.050000
eta_r	0.980000
advance_coefficient	1.078007

P_D	1.300000
AE_A0	0.610000
Z	3.000000
eta_open_water	0.701870
QPC	0.722225
torque_motor	126.298113
eta_motor	0.955435
GLOBAL_EFFICIENCY	0.690039
POWER	67.453451
AUTONOMY	39.121335
Name: 3854, dtype: float64	

(g) **S1-W-S-P3**: Numerical results

Figure A.6: *Results for "Wolong EG80-Suzuki DF90-Propeller 3" Matching*

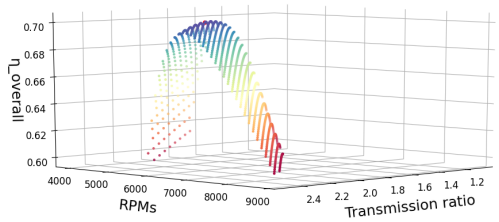

(a) **S1-A-Y-P1**: Maximum overall efficiency graph

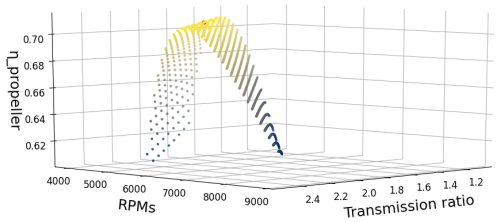

(b) **S1-A-Y-P1**: Maximum propeller efficiency graph

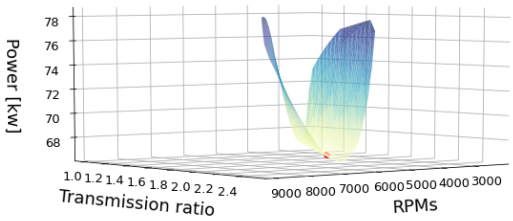

(c) **S1-A-Y-P1**: Minimum power graph

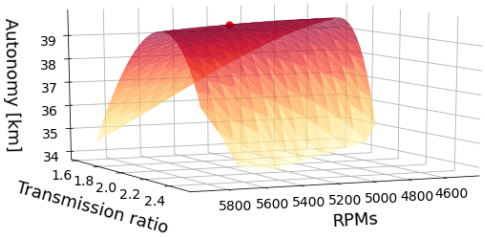

(d) **S1-A-Y-P1**: Maximum autonomy graph

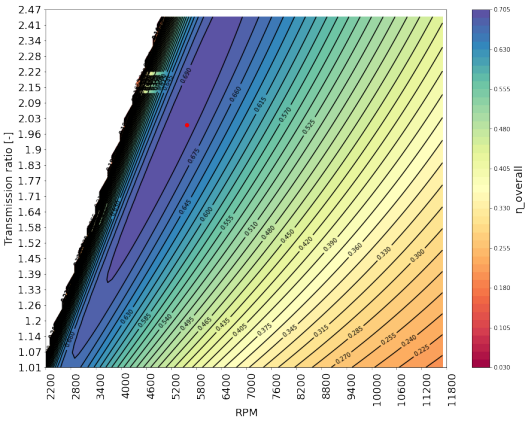

(e) **S1-A-Y-P1**: Transmission ratio efficiency map

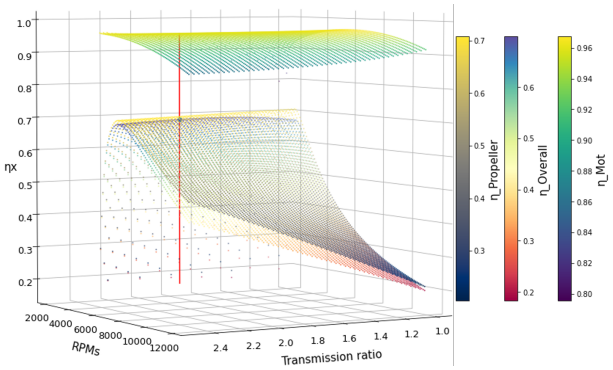

(f) **S1-A-Y-P1**: Motor-Transmission-Propeller matching

transmission_ratios	2.013469
transmission_ratios_i_values	1.067809
RPMs_mot	5400.100000
RPMs_propeller	2681.987634
diameter [in]	13.500000
pitch	1.166670
slip_ratio	0.178652
speed_of_advance	42.833200
hull_efficiency	1.050000
eta_r	0.980000
advance_coefficient	0.851770

P_D	1.030000
AE_A0	0.480000
Z	3.000000
eta_open_water	0.708379
QPC	0.728922
torque_motor	118.185695
eta_motor	0.960036
GLOBAL_EFFICIENCY	0.699792
POWER	66.833674
AUTONOMY	39.674281
Name: 3094, dtype: float64	

(g) **S1-A-Y-P1**: Numerical results

Figure A.7: *Results for "Alpha APEV528-Yamaha F100BETX-Propeller 1" Matching*

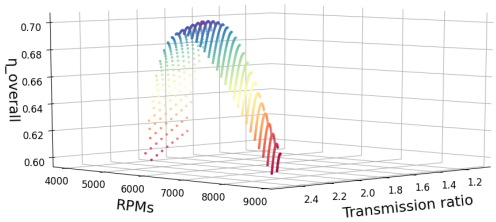

(a) **S1-A-S-P1**: Maximum overall efficiency graph

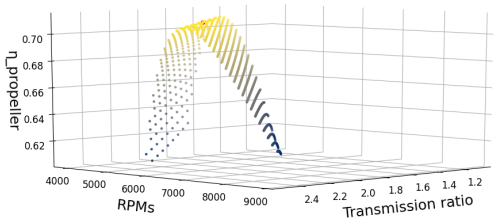

(b) **S1-A-S-P1**: Maximum propeller efficiency graph

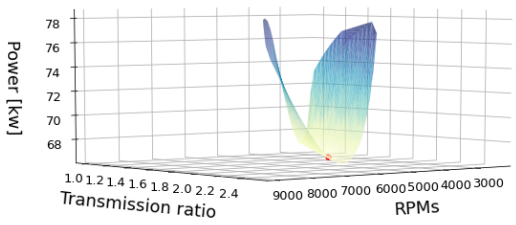

(c) **S1-A-S-P1**: Minimum power graph

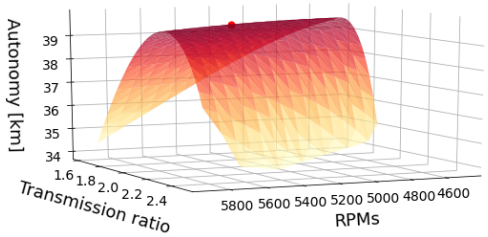

(d) **S1-A-S-P1**: Maximum autonomy graph

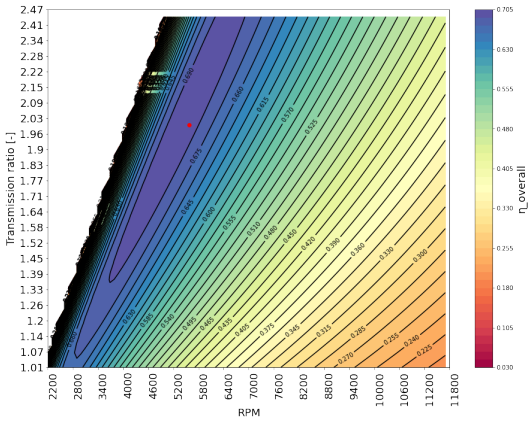

(e) **S1-A-S-P1**: Transmission ratio efficiency map

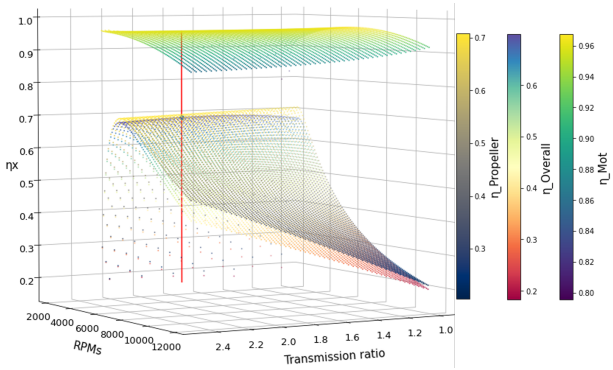

(f) **S1-A-S-P1**: Motor-Transmission-Propeller matching

transmission_ratios	2.013469	P_D	1.030000
transmission_ratios_i_values	1.286337	AE_A0	0.480000
RPMs_mot	5400.100000	Z	3.000000
RPMs_propeller	2681.987634	eta_open_water	0.708379
diameter [in]	13.500000	QPC	0.728922
pitch	1.166670	torque_motor	118.185695
slip_ratio	0.178652	eta_motor	0.960036
speed_of_advance	42.833200	GLOBAL_EFFICIENCY	0.699792
hull_efficiency	1.050000	POWER	66.833674
eta_r	0.980000	AUTONOMY	39.674281
advance_coefficient	0.851770	Name: 3094, dtype: float64	

(g) **S1-A-S-P1**: Numerical results

Figure A.8: *Results for "Alpha APEV528-Suzuki DF90-Propeller 1" Matching*

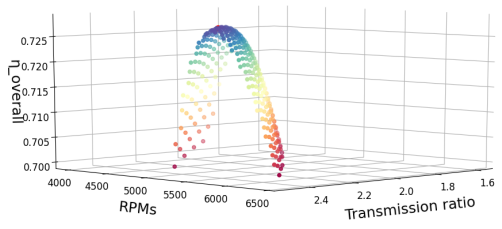

(a) **S1-A-Y-P2**: Maximum overall efficiency graph

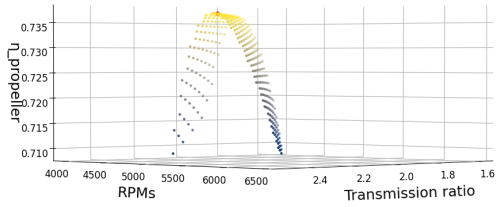

(b) **S1-A-Y-P2**: Maximum propeller efficiency graph

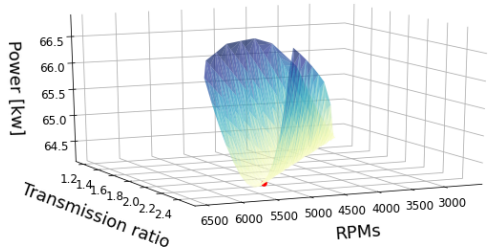

(c) **S1-A-Y-P2**: Minimum power graph

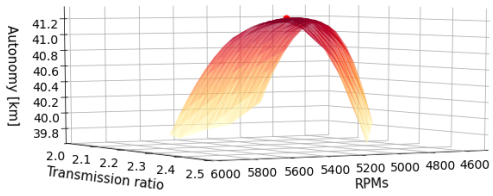

(d) **S1-A-Y-P2**: Maximum autonomy graph

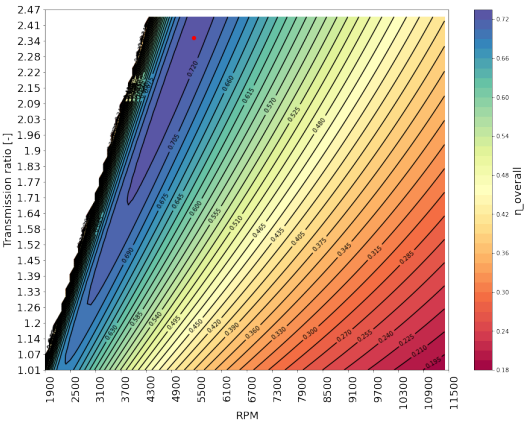

(e) **S1-A-Y-P2**: Transmission ratio efficiency map

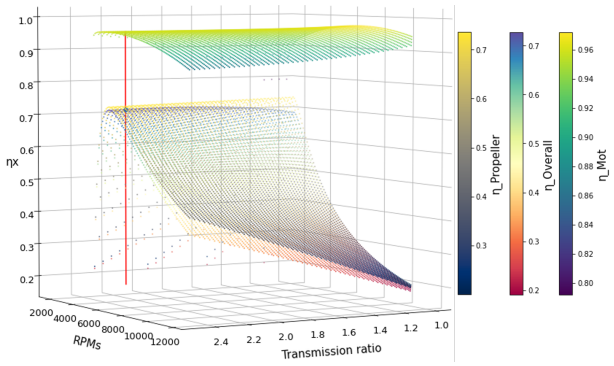

(f) **S1-A-Y-P2**: Motor-Transmission-Propeller matching

transmission_ratios	2.378367	P_D	1.200000
transmission_ratios_i_values	0.903981	AE_A0	0.470000
RPMs_mot	5400.100000	Z	3.000000
RPMs_propeller	2270.507122	eta_open_water	0.736499
diameter [in]	13.500000	QPC	0.757858
pitch	1.333330	torque_motor	113.673262
slip_ratio	0.151071	eta_motor	0.959862
speed_of_advance	42.833200	GLOBAL_EFFICIENCY	0.727439
hull_efficiency	1.050000	POWER	64.281906
eta_r	0.980000	AUTONOMY	41.241711
advance_coefficient	1.006135	Name: 4062, dtype: float64	

(g) **S1-A-Y-P2**: Numerical results

Figure A.9: *Results for "Alpha APEV528-Yamaha F100BETX-Propeller 2" Matching*

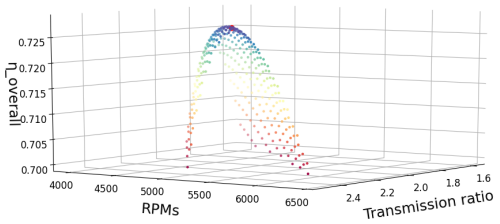

(a) **S1-A-S-P2**: Maximum overall efficiency graph

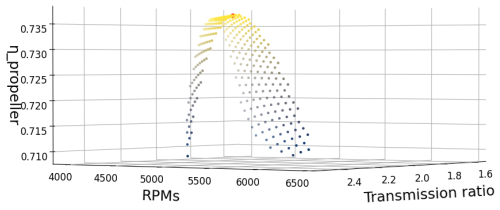

(b) **S1-A-S-P2**: Maximum propeller efficiency graph

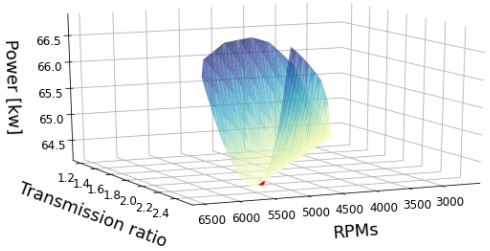

(c) **S1-A-S-P2**: Minimum power graph

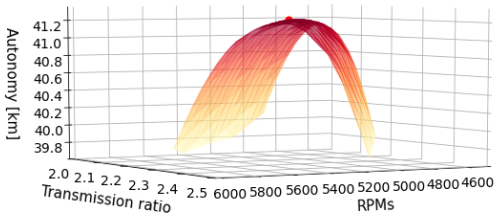

(d) **S1-A-S-P2**: Maximum autonomy graph

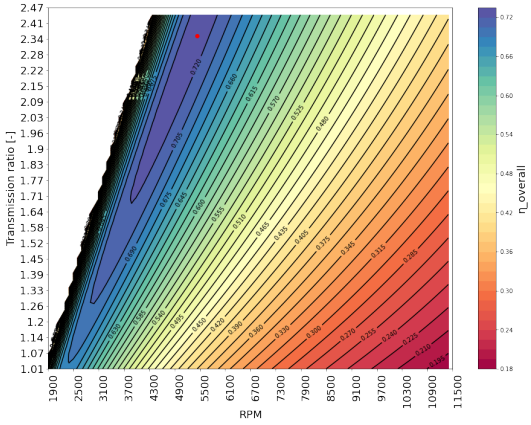

(e) **S1-A-S-P2**: Transmission ratio efficiency map

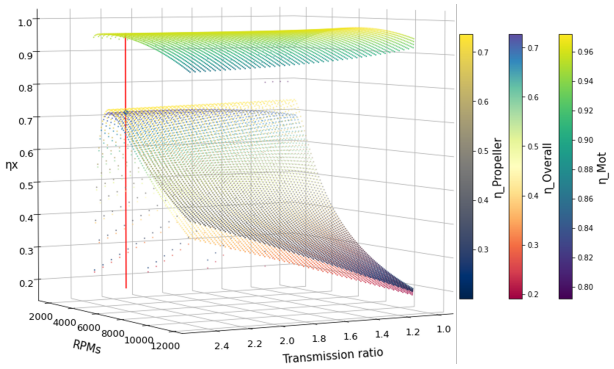

(f) **S1-A-S-P2**: Motor-Transmission-Propeller matching

transmission_ratios	2.378367
transmission_ratios_i_values	1.088982
RPMs_mot	5400.100000
RPMs_propeller	2270.507122
diameter [in]	13.500000
pitch	1.333330
slip_ratio	0.151071
speed_of_advance	42.833200
hull_efficiency	1.050000
eta_r	0.980000
advance_coefficient	1.006135

P_D	1.200000
AE_A0	0.470000
Z	3.000000
eta_open_water	0.736499
QPC	0.757858
torque_motor	113.673262
eta_motor	0.959862
GLOBAL_EFFICIENCY	0.727439
POWER	64.281906
AUTONOMY	41.241711
Name: 4062, dtype: float64	

(g) **S1-A-S-P2**: Numerical results

Figure A.10: *Results for "Alpha APEV528-Suzuki DF90-Propeller 2" Matching*

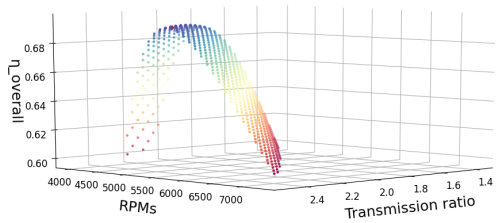

(a) **S1-A-Y-P3**: Maximum overall efficiency graph

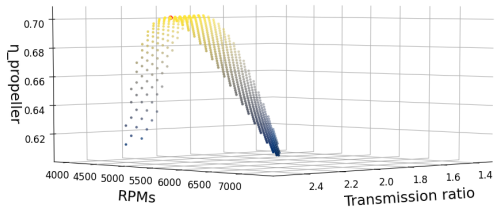

(b) **S1-A-Y-P3**: Maximum propeller efficiency graph

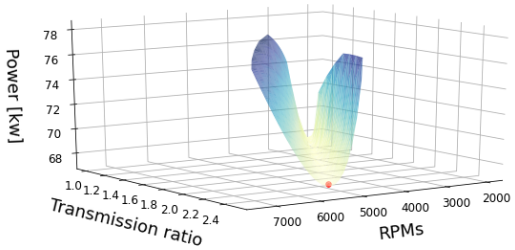

(c) **S1-A-Y-P3**: Minimum power graph

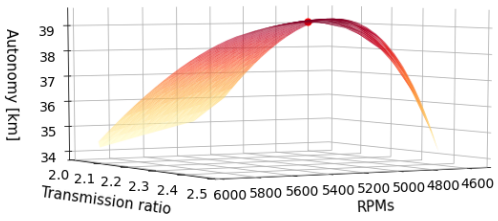

(d) **S1-A-Y-P3**: Maximum autonomy graph

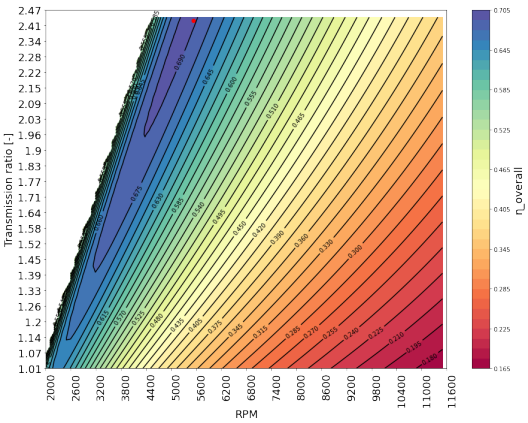

(e) **S1-A-Y-P3**: Transmission ratio efficiency map

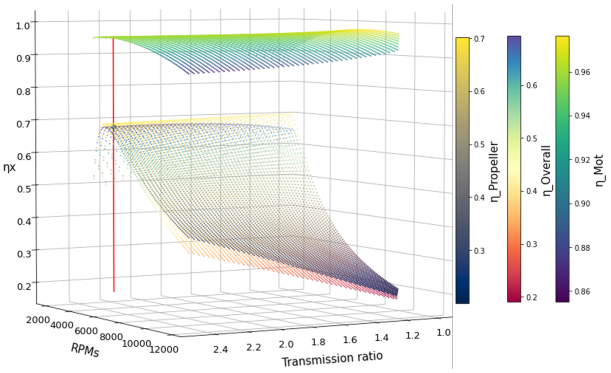

(f) **S1-A-Y-P3**: Motor-Transmission-Propeller matching

transmission_ratios	2.439184	P_D	1.300000
transmission_ratios_i_values	0.881442	AE_A0	0.610000
RPMs_mot	5400.100000	Z	3.000000
RPMs_propeller	2213.896419	eta_open_water	0.701868
diameter [in]	12.999960	QPC	0.722222
pitch	1.416670	torque_motor	119.282091
slip_ratio	0.180581	eta_motor	0.960079
speed_of_advance	42.833200	GLOBAL_EFFICIENCY	0.693390
hull_efficiency	1.050000	POWER	67.453683
eta_r	0.980000	AUTONOMY	39.311357
advance_coefficient	1.071553	Name: 4161, dtype: float64	

(g) **S1-A-Y-P3**: Numerical results

Figure A.11: *Results for "Alpha APEV528-Yamaha F100BETX-Propeller 3" Matching*

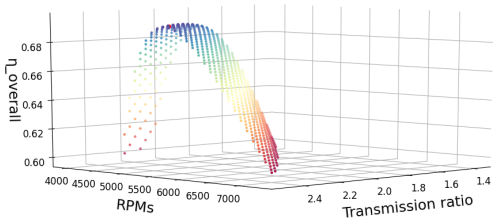

(a) **S1-A-S-P3**: Maximum overall efficiency graph

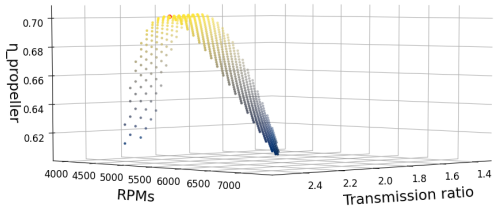

(b) **S1-A-S-P3**: Maximum propeller efficiency graph

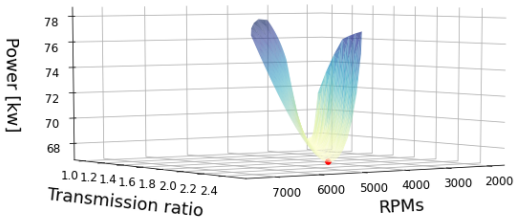

(c) **S1-A-S-P3**: Minimum power graph

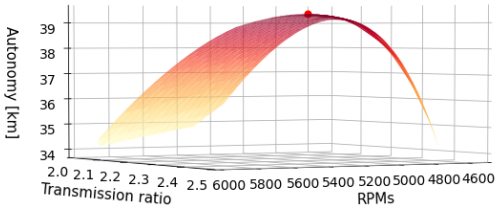

(d) **S1-A-S-P3**: Maximum autonomy graph

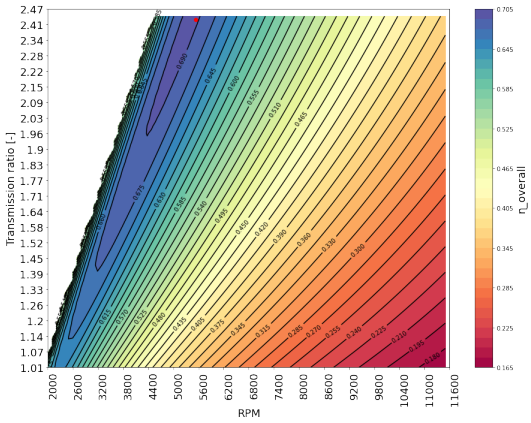

(e) **S1-A-S-P3**: Transmission ratio efficiency map

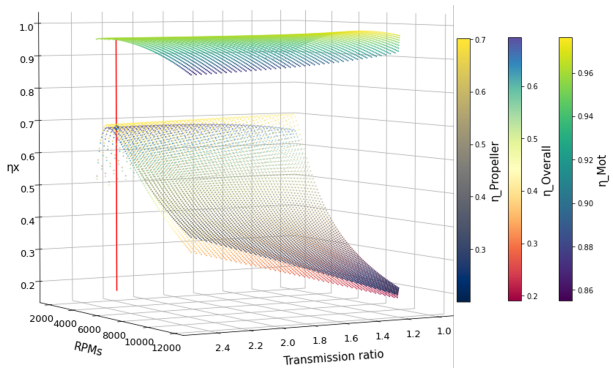

(f) **S1-A-S-P3**: Motor-Transmission-Propeller matching

transmission_ratios	2.439184
transmission_ratios_i_values	1.061831
RPMs_mot	5400.100000
RPMs_propeller	2213.896419
diameter [in]	12.999960
pitch	1.416670
slip_ratio	0.180581
speed_of_advance	42.833200
hull_efficiency	1.050000
eta_r	0.980000
advance_coefficient	1.071553

P_D	1.300000
AE_A0	0.610000
Z	3.000000
eta_open_water	0.701868
QPC	0.722222
torque_motor	119.282091
eta_motor	0.960079
GLOBAL_EFFICIENCY	0.693390
POWER	67.453683
AUTONOMY	39.311357
Name: 4161, dtype: float64	

(g) **S1-A-S-P3**: Numerical results

Figure A.12: *Results for "Alpha APEV528-Suzuki DF90-Propeller 3" Matching*

A.2 Results maps for speed 2 (55 km/h)

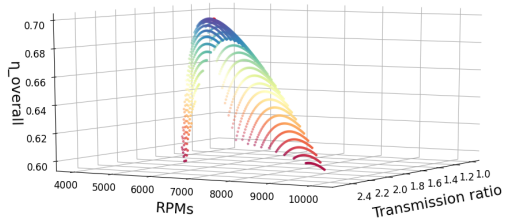

(a) **S2-W-Y-P1**: Maximum overall efficiency graph

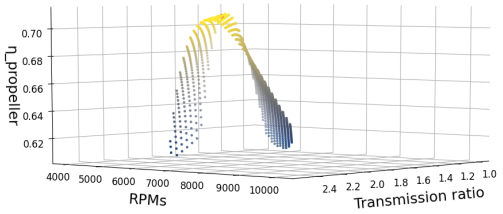

(b) **S2-W-Y-P1**: Maximum propeller efficiency graph

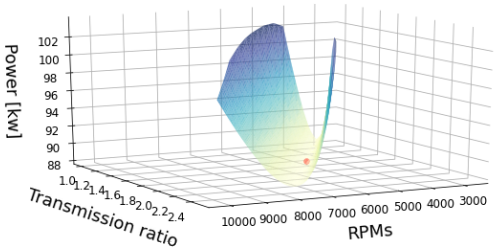

(c) **S2-W-Y-P1**: Minimum power graph

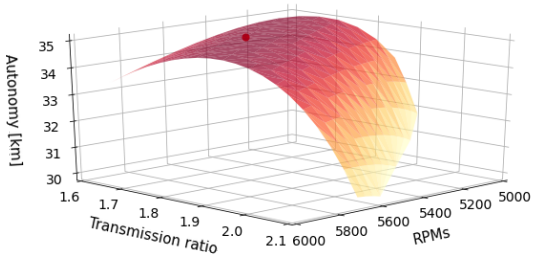

(d) **S2-W-Y-P1**: Maximum autonomy graph

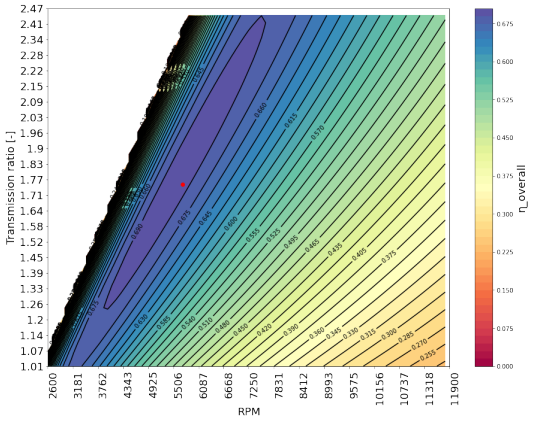

(e) **S2-W-Y-P1**: Transmission ratio efficiency map

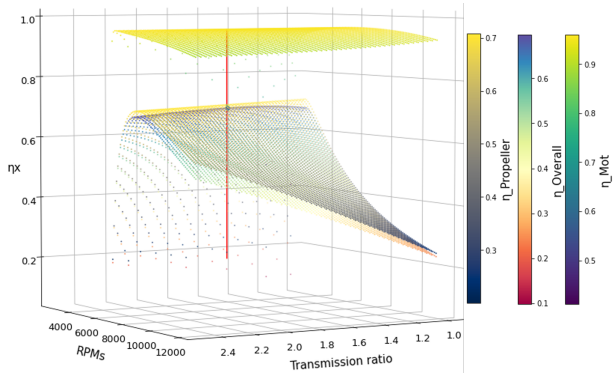

(f) **S2-W-Y-P1**: Motor-Transmission-Propeller matching

transmission_ratios	1.739796
transmission_ratios_i_values	1.235777
RPMs_mot	5500.100000
RPMs_propeller	3161.347801
diameter [in]	13.500000
pitch	1.166670
slip_ratio	0.184590
speed_of_advance	50.123900
hull_efficiency	1.050000
eta_r	0.980000
advance_coefficient	0.845612

P_D	1.030000
AE_A0	0.480000
Z	3.000000
eta_open_water	0.708256
QPC	0.728796
torque_motor	153.945752
eta_motor	0.956985
GLOBAL_EFFICIENCY	0.697447
POWER	88.668000
AUTONOMY	34.883443
Name: 2215, dtype: float64	

(g) **S2-W-Y-P1**: Numerical results

Figure A.13: *Results for "Wolong EG80-Yamaha F100BETX-Propeller 1" Matching*

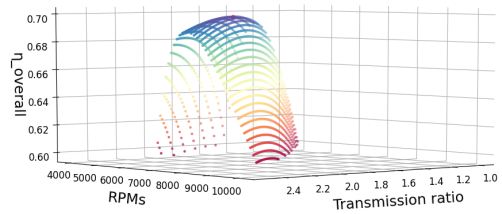

(a) **S2-W-S-P1**: Maximum overall efficiency graph

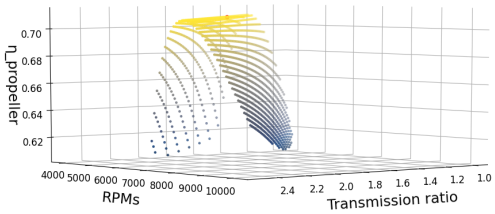

(b) **S2-W-S-P1**: Maximum propeller efficiency graph

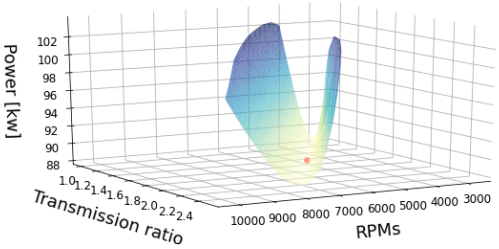

(c) **S2-W-S-P1**: Minimum power graph

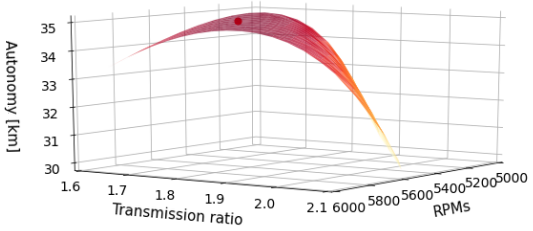

(d) **S2-W-S-P1**: Maximum autonomy graph

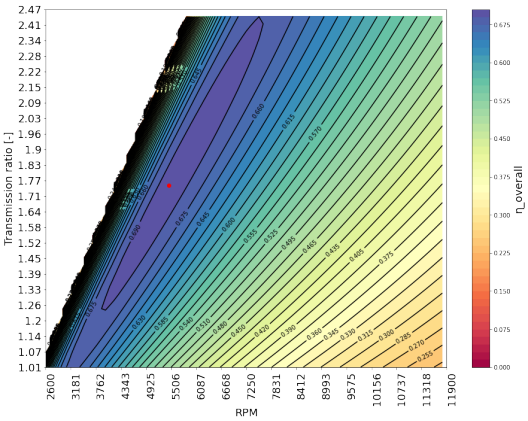

(e) **S2-W-S-P1**: Transmission ratio efficiency map

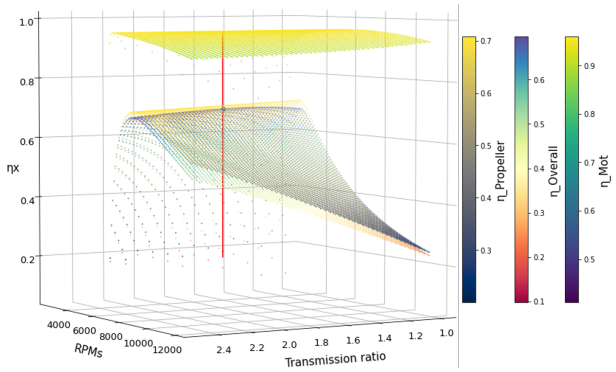

(f) **S2-W-S-P1**: Motor-Transmission-Propeller matching

transmission_ratios	1.739796
transmission_ratios_i_values	1.488680
RPMs_mot	5500.100000
RPMs_propeller	3161.347801
diameter [in]	13.500000
pitch	1.166670
slip_ratio	0.184590
speed_of_advance	50.123900
hull_efficiency	1.050000
eta_r	0.980000
advance_coefficient	0.845612
P_D	1.030000
AE_A0	0.480000
Z	3.000000
eta_open_water	0.708256
QPC	0.728796
torque_motor	153.945752
eta_motor	0.956985
GLOBAL_EFFICIENCY	0.697447
POWER	88.668000
AUTONOMY	34.883443
Name: 2215, dtype: float64	

(g) **S2-W-S-P1**: Numerical results

Figure A.14: *Results for "Wolong EG80-Suzuki DF90-Propeller 1" Matching*

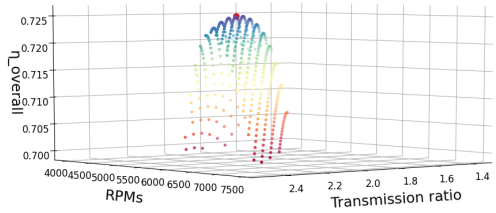

(a) **S2-W-Y-P2**: Maximum overall efficiency graph

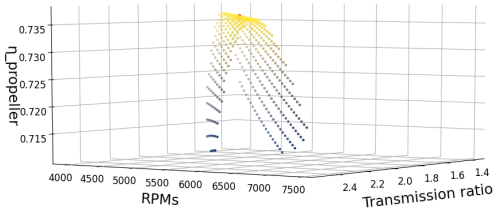

(b) **S2-W-Y-P2**: Maximum propeller efficiency graph

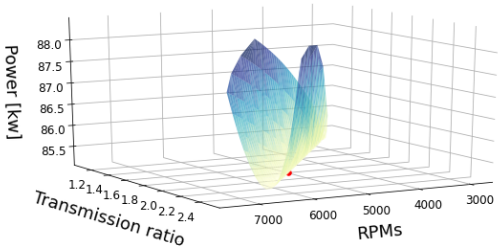

(c) **S2-W-Y-P2**: Minimum power graph

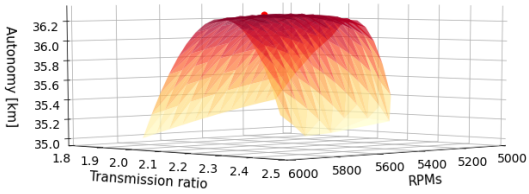

(d) **S2-W-Y-P2**: Maximum autonomy graph

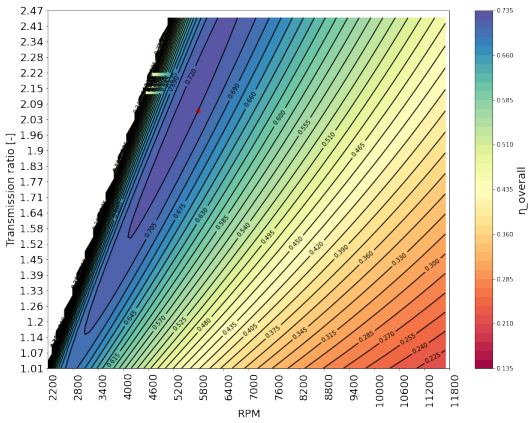

(e) **S2-W-Y-P2**: Transmission ratio efficiency map

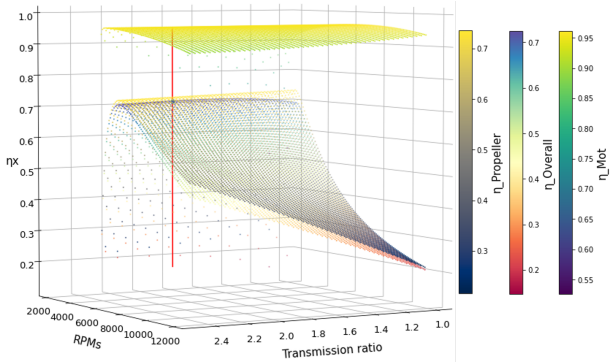

(f) **S2-W-Y-P2**: Motor-Transmission-Propeller matching

transmission_ratios	2.074286	P_D	1.200000
transmission_ratios_i_values	1.036501	AE_A0	0.470000
RPMs_mot	5500.100000	Z	3.000000
RPMs_propeller	2651.563361	eta_open_water	0.736489
diameter [in]	13.500000	QPC	0.757847
pitch	1.333330	torque_motor	148.044404
slip_ratio	0.149339	eta_motor	0.956771
speed_of_advance	50.123900	GLOBAL_EFFICIENCY	0.725085
hull_efficiency	1.050000	POWER	85.269006
eta_r	0.980000	AUTONOMY	36.265831
advance_coefficient	1.008188	Name: 3094, dtype: float64	

(g) **S2-W-Y-P2**: Numerical results

Figure A.15: *Results for "Wolong EG80-Yamaha F100BETX-Propeller 2" Matching (Mira et al., 2021)*

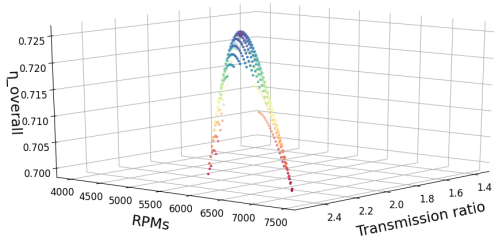

(a) **S2-W-S-P2**: Maximum overall efficiency graph

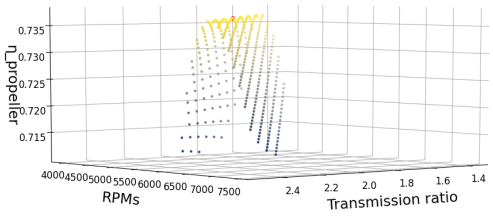

(b) **S2-W-S-P2**: Maximum propeller efficiency graph

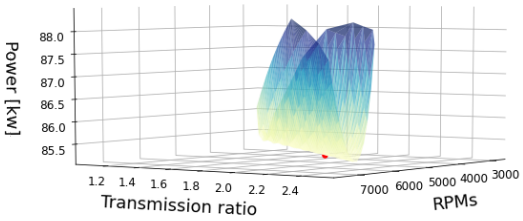

(c) **S2-W-S-P2**: Minimum power graph

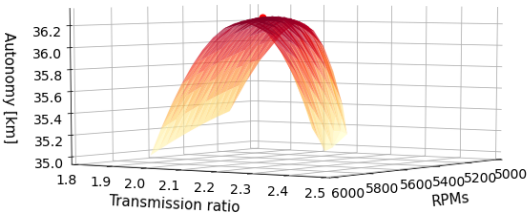

(d) **S2-W-S-P2**: Maximum autonomy graph

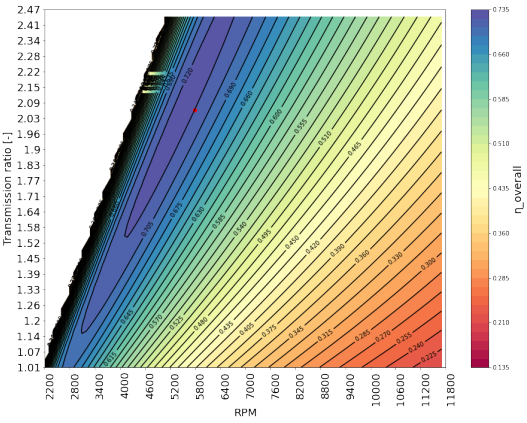

(e) **S2-W-S-P2**: Transmission ratio efficiency map

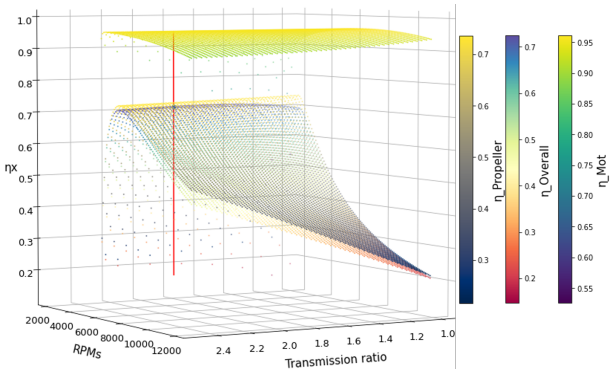

(f) **S2-W-S-P2**: Motor-Transmission-Propeller matching

transmission_ratios	2.074286
transmission_ratios_i_values	1.248623
RPMs_mot	5500.100000
RPMs_propeller	2651.563361
diameter [in]	13.500000
pitch	1.333330
slip_ratio	0.149339
speed_of_advance	50.123900
hull_efficiency	1.050000
eta_r	0.980000
advance_coefficient	1.008188

P_D	1.200000
AE_A0	0.470000
Z	3.000000
eta_open_water	0.736489
QPC	0.757847
torque_motor	148.044404
eta_motor	0.956771
GLOBAL_EFFICIENCY	0.725085
POWER	85.269006
AUTONOMY	36.265831

Name: 3094, dtype: float64

(g) **S2-W-S-P2**: Numerical results

Figure A.16: *Results for "Wolong EG80-Suzuki DF90-Propeller 2" Matching (Mira et al., 2021)*

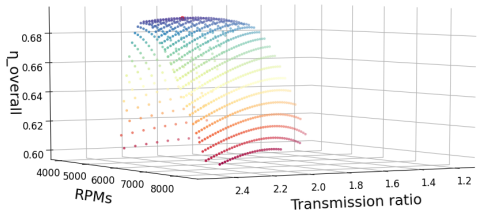

(a) **S2-W-Y-P3**: Maximum overall efficiency graph

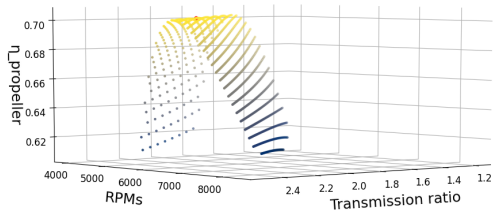

(b) **S2-W-Y-P3**: Maximum propeller efficiency graph

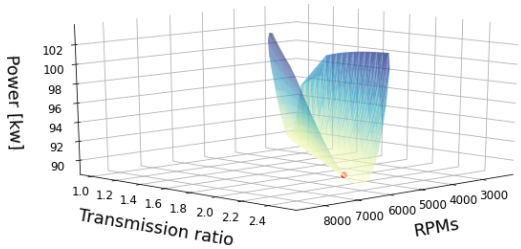

(c) **S2-W-Y-P3**: Minimum power graph

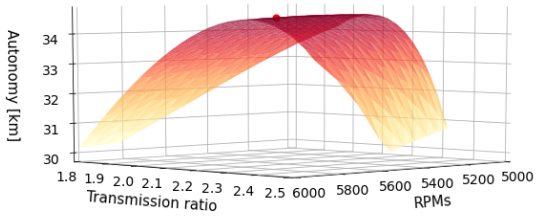

(d) **S2-W-Y-P3**: Maximum autonomy graph

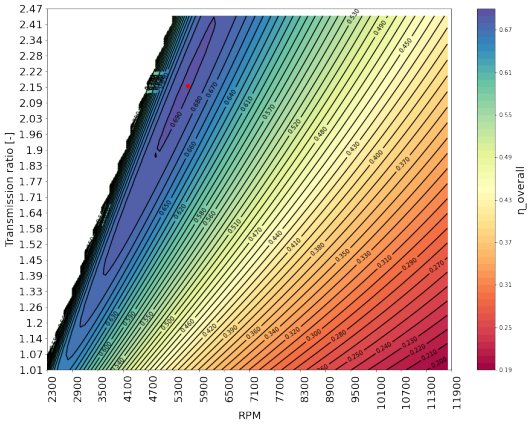

(e) **S2-W-Y-P3**: Transmission ratio efficiency map

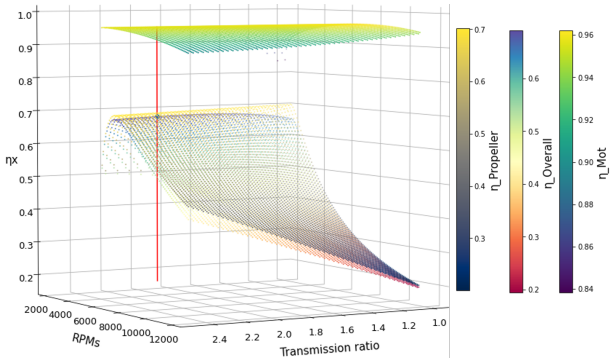

(f) **S2-W-Y-P3**: Motor-Transmission-Propeller matching

transmission_ratios	2.165510	P_D	1.300000
transmission_ratios_i_values	0.992838	AE_A0	0.610000
RPMs_mot	5600.100000	Z	3.000000
RPMs_propeller	2586.041843	eta_open_water	0.701886
diameter [in]	12.999960	QPC	0.722240
pitch	1.416670	torque_motor	152.569080
slip_ratio	0.179097	eta_motor	0.957052
speed_of_advance	50.123900	GLOBAL_EFFICIENCY	0.691222
hull_efficiency	1.050000	POWER	89.472779
eta_r	0.980000	AUTONOMY	34.572098
advance_coefficient	1.073494	Name: 3274, dtype: float64	

(g) **S2-W-Y-P3**: Numerical results

Figure A.17: *Results for "Wolong EG80-Yamaha F100BETX-Propeller 3" Matching*

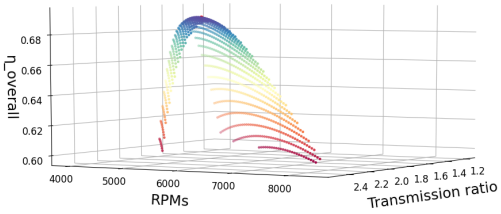

(a) **S2-W-S-P3**: Maximum overall efficiency graph

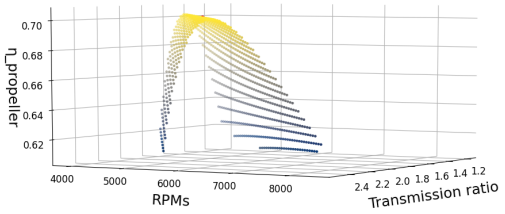

(b) **S2-W-S-P3**: Maximum propeller efficiency graph

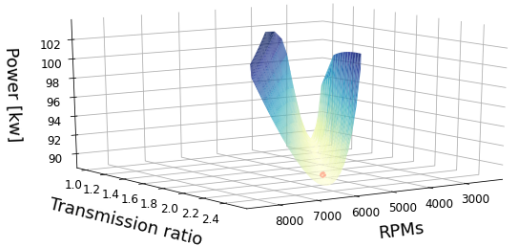

(c) **S2-W-S-P3**: Minimum power graph

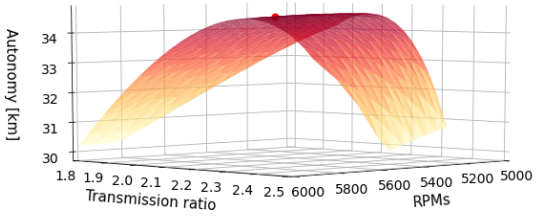

(d) **S2-W-S-P3**: Maximum autonomy graph

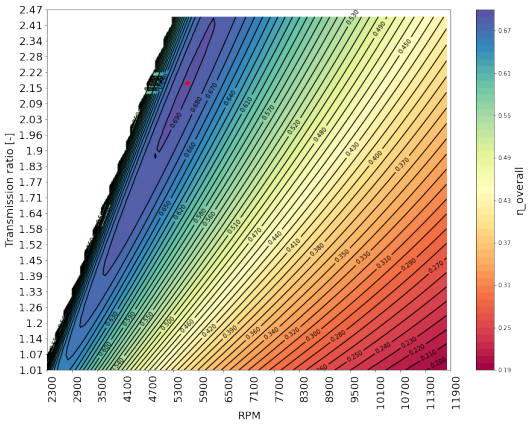

(e) **S2-W-S-P3**: Transmission ratio efficiency map

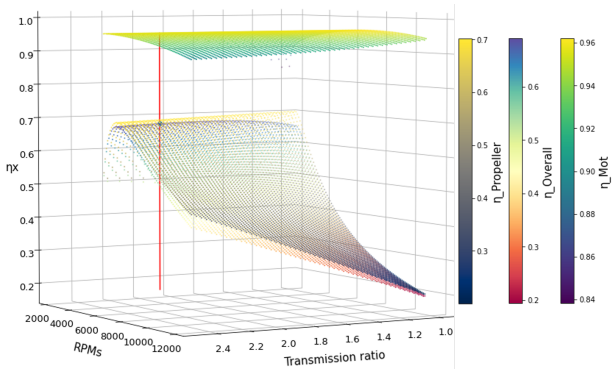

(f) **S2-W-S-P3**: Motor-Transmission-Propeller matching

transmission_ratios	2.165510
transmission_ratios_i_values	1.196023
RPMs_mot	5600.100000
RPMs_propeller	2586.041843
diameter [in]	12.999960
pitch	1.416670
slip_ratio	0.179097
speed_of_advance	50.123900
hull_efficiency	1.050000
eta_r	0.980000
advance_coefficient	1.073494

P_D	1.300000
AE_A0	0.610000
Z	3.000000
eta_open_water	0.701886
QPC	0.722240
torque_motor	152.569080
eta_motor	0.957052
GLOBAL_EFFICIENCY	0.691222
POWER	89.472779
AUTONOMY	34.572098
Name: 3274, dtype: float64	

(g) **S2-W-S-P3**: Numerical results

Figure A.18: *Results for "Wolong EG80-Suzuki DF90-Propeller 3" Matching*

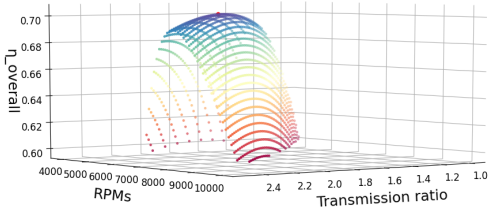

(a) **S2-A-Y-P1**: Maximum overall efficiency graph

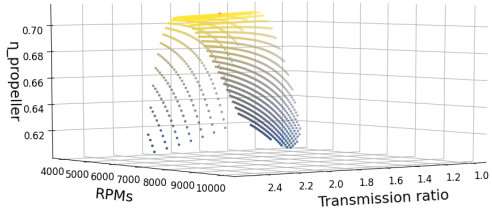

(b) **S2-A-Y-P1**: Maximum propeller efficiency graph

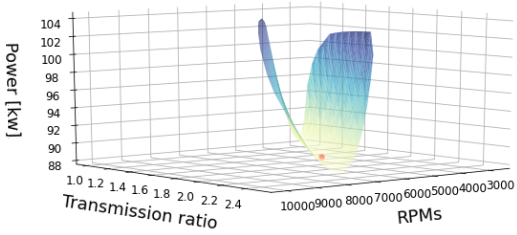

(c) **S2-A-Y-P1**: Minimum power graph

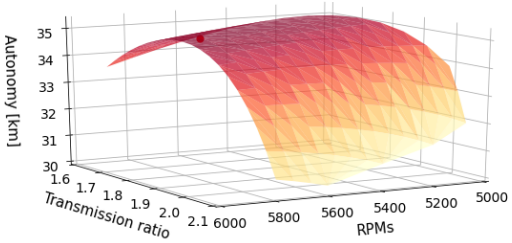

(d) **S2-A-Y-P1**: Maximum autonomy graph

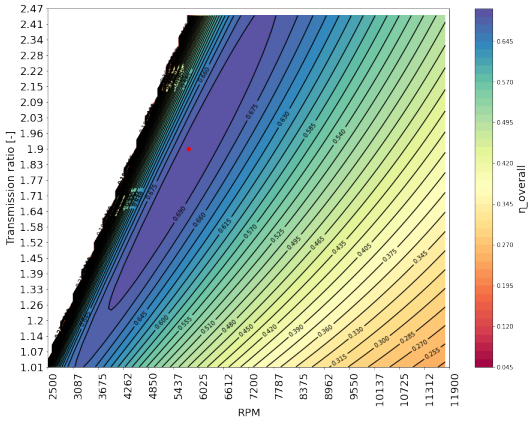

(e) **S2-A-Y-P1**: Transmission ratio efficiency map

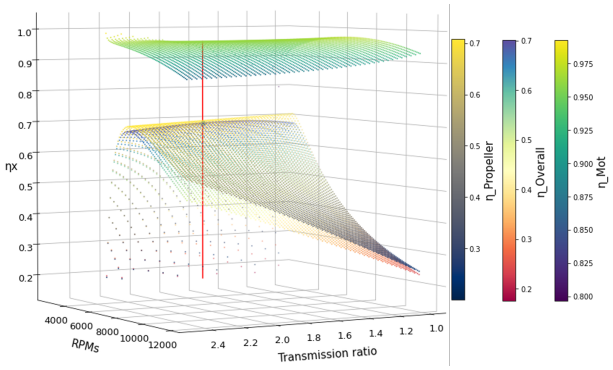

(f) **S2-A-Y-P1**: Motor-Transmission-Propeller matching

transmission_ratios	1.861429
transmission_ratios_i_values	1.155027
RPMs_mot	5800.100000
RPMs_propeller	3115.940138
diameter [in]	13.500000
pitch	1.166670
slip_ratio	0.172708
speed_of_advance	50.123900
hull_efficiency	1.050000
eta_r	0.980000
advance_coefficient	0.857935

P_D	1.030000
AE_A0	0.480000
Z	3.000000
eta_open_water	0.708294
QPC	0.728834
torque_motor	145.975452
eta_motor	0.962135
GLOBAL_EFFICIENCY	0.701237
POWER	88.663307
AUTONOMY	35.073008
Name: 2546, dtype: float64	

(g) **S2-A-Y-P1**: Numerical results

Figure A.19: *Results for "Alpha APEV528-Yamaha F100BETX-Propeller 1" Matching*

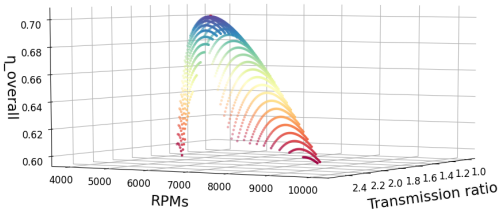

(a) **S2-A-S-P1**: Maximum overall efficiency graph

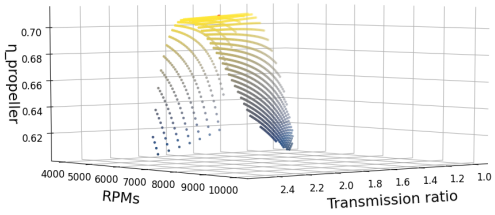

(b) **S2-A-S-P1**: Maximum propeller efficiency graph

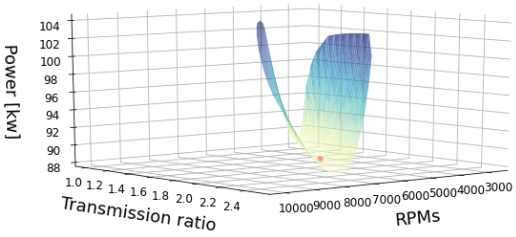

(c) **S2-A-S-P1**: Minimum power graph

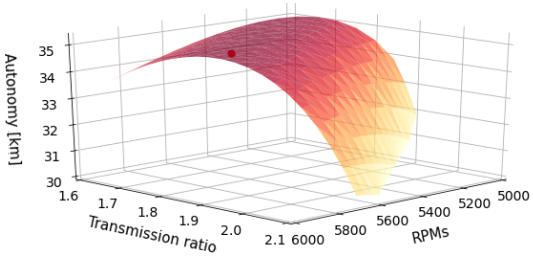

(d) **S2-A-S-P1**: Maximum autonomy graph

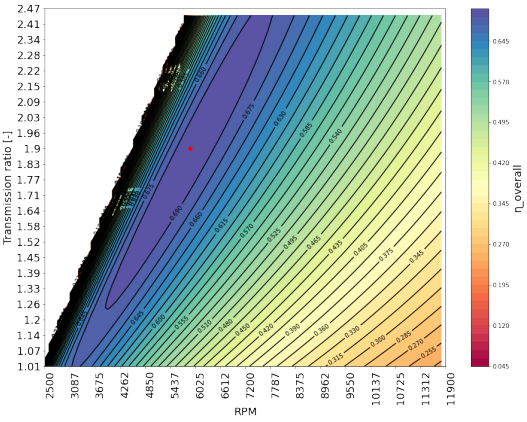

(e) **S2-A-S-P1**: Transmission ratio efficiency map

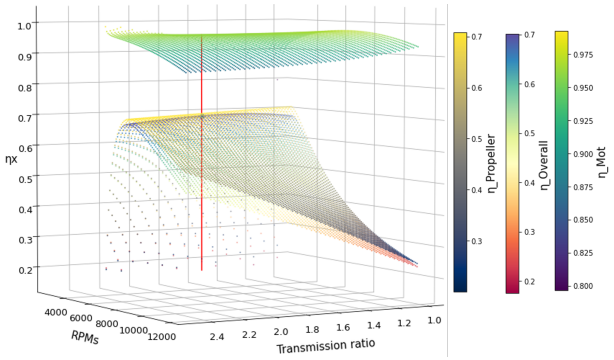

(f) **S2-A-S-P1**: Motor-Transmission-Propeller matching

transmission_ratios	1.861429
transmission_ratios_i_values	1.391404
RPMs_mot	5800.100000
RPMs_propeller	3115.940138
diameter [in]	13.500000
pitch	1.166670
slip_ratio	0.172708
speed_of_advance	50.123900
hull_efficiency	1.050000
eta_r	0.980000
advance_coefficient	0.857935

P_D	1.030000
AE_A0	0.480000
Z	3.000000
eta_open_water	0.708294
QPC	0.728834
torque_motor	145.975452
eta_motor	0.962135
GLOBAL_EFFICIENCY	0.701237
POWER	88.663307
AUTONOMY	35.073008
Name: 2546, dtype: float64	

(g) **S2-A-S-P1**: Numerical results

Figure A.20: *Results for "Alpha APEV528-Suzuki DF90-Propeller 1" Matching*

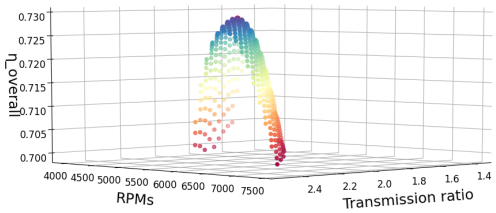

(a) **S2-A-Y-P2**: Maximum overall efficiency graph

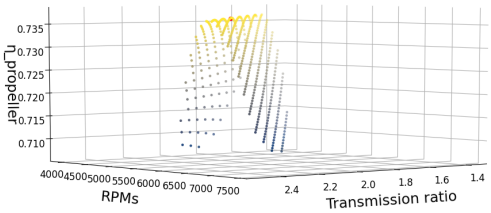

(b) **S2-A-Y-P2**: Maximum propeller efficiency graph

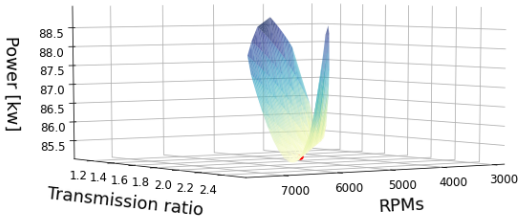

(c) **S2-A-Y-P2**: Minimum power graph

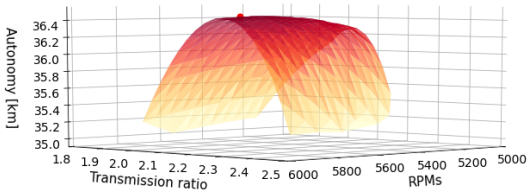

(d) **S2-A-Y-P2**: Maximum autonomy graph

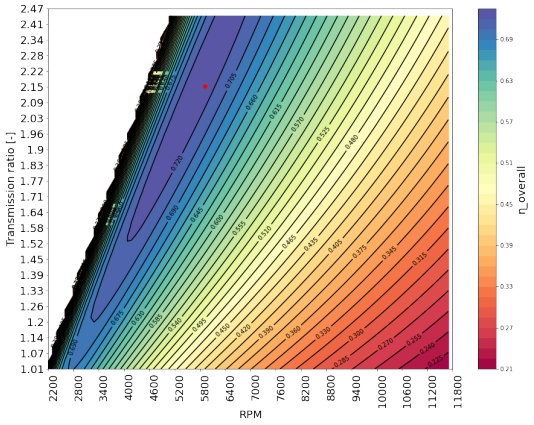

(e) **S2-A-Y-P2**: Transmission ratio efficiency map

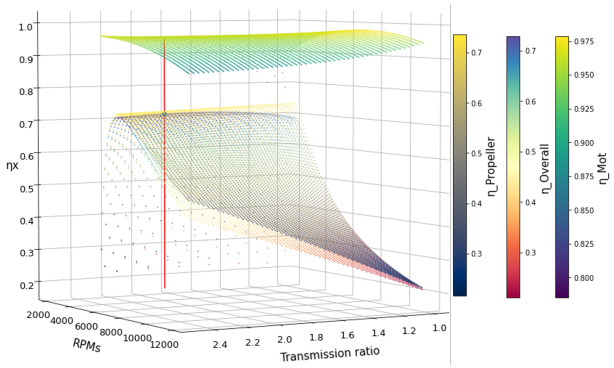

(f) **S2-A-Y-P2**: Motor-Transmission-Propeller matching

transmission_ratios	2.135102
transmission_ratios_i_values	1.006978
RPMs_mot	5700.100000
RPMs_propeller	2669.708469
diameter [in]	13.500000
pitch	1.333330
slip_ratio	0.155121
speed_of_advance	50.123900
hull_efficiency	1.050000
eta_r	0.980000
advance_coefficient	1.001336

P_D	1.200000
AE_A0	0.470000
Z	3.000000
eta_open_water	0.736455
QPC	0.757812
torque_motor	142.856558
eta_motor	0.961746
GLOBAL_EFFICIENCY	0.728822
POWER	85.272948
AUTONOMY	36.452728
Name: 3248, dtype: float64	

(g) **S2-A-Y-P2**: Numerical results

Figure A.21: *Results for "Alpha APEV528-Yamaha F100BETX-Propeller 2" Matching (Mira et al., 2021)*

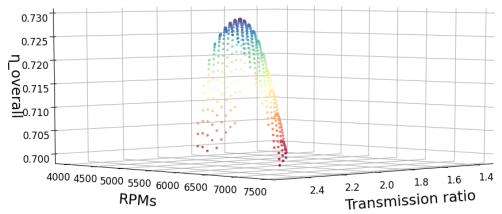

(a) **S2-A-S-P2**: Maximum overall efficiency graph

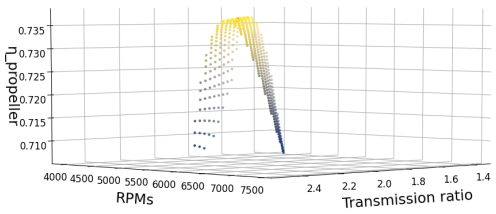

(b) **S2-A-S-P2**: Maximum propeller efficiency graph

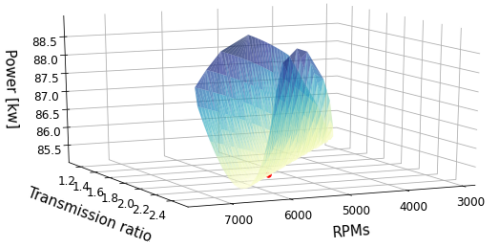

(c) **S2-A-S-P2**: Minimum power graph

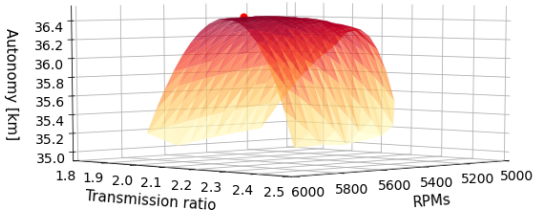

(d) **S2-A-S-P2**: Maximum autonomy graph

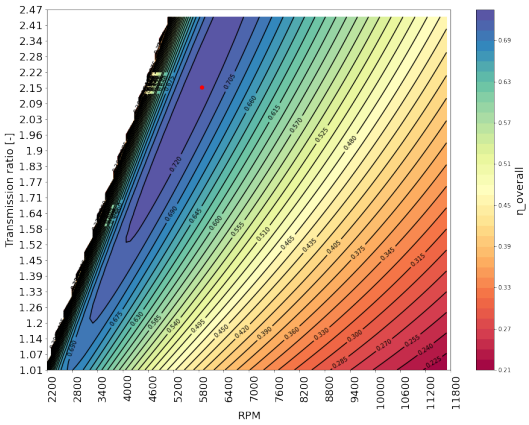

(e) **S2-A-S-P2**: Transmission ratio efficiency map

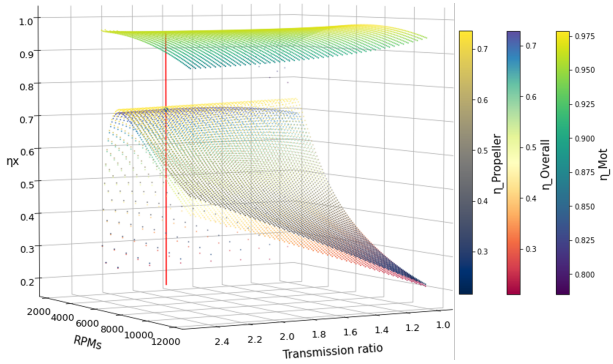

(f) **S2-A-S-P2**: Motor-Transmission-Propeller matching

transmission_ratios	2.135102
transmission_ratios_i_values	1.213057
RPMs_mot	5700.100000
RPMs_propeller	2669.708469
diameter [in]	13.500000
pitch	1.333330
slip_ratio	0.155121
speed_of_advance	50.123900
hull_efficiency	1.050000
eta_r	0.980000
advance_coefficient	1.001336

P_D	1.200000
AE_A0	0.470000
Z	3.000000
eta_open_water	0.736455
QPC	0.757812
torque_motor	142.856558
eta_motor	0.961746
GLOBAL_EFFICIENCY	0.728822
POWER	85.272948
AUTONOMY	36.452728
Name: 3248, dtype: float64	

(g) **S2-A-S-P2**: Numerical results

Figure A.22: *Results for "Alpha APEV528-Suzuki DF90-Propeller 2" Matching (Mira et al., 2021)*

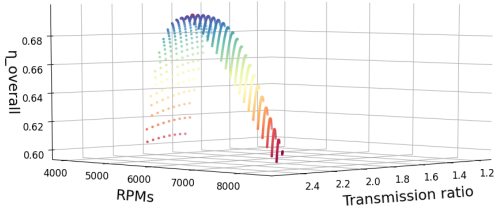

(a) **S2-A-Y-P3**: Maximum overall efficiency graph

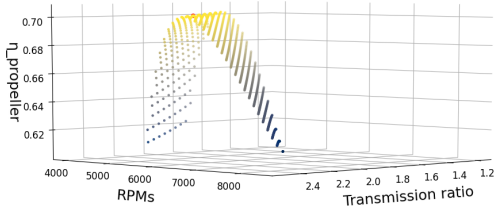

(b) **S2-A-Y-P3**: Maximum propeller efficiency graph

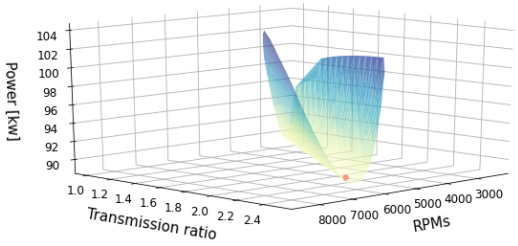

(c) **S2-A-Y-P3**: Minimum power graph

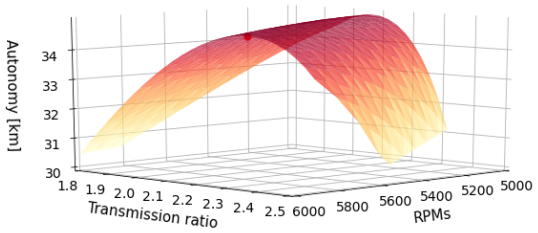

(d) **S2-A-Y-P3**: Maximum autonomy graph

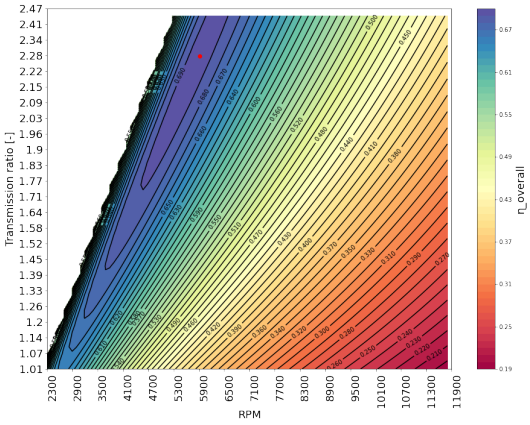

(e) **S2-A-Y-P3**: Transmission ratio efficiency map

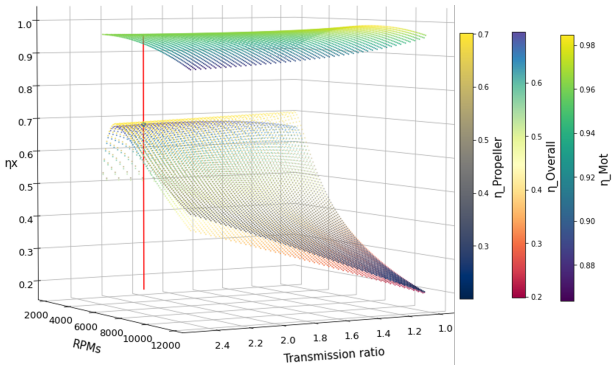

(f) **S2-A-Y-P3**: Motor-Transmission-Propeller matching

transmission_ratios	2.287143
transmission_ratios_i_values	0.940037
RPMs_mot	5900.100000
RPMs_propeller	2579.681449
diameter [in]	12.999960
pitch	1.416670
slip_ratio	0.177073
speed_of_advance	50.123900
hull_efficiency	1.050000
eta_r	0.980000
advance_coefficient	1.076141

P_D	1.300000
AE_A0	0.610000
Z	3.000000
eta_open_water	0.701886
QPC	0.722241
torque_motor	144.811319
eta_motor	0.962188
GLOBAL_EFFICIENCY	0.694931
POWER	89.472691
AUTONOMY	34.757645

Name: 3564, dtype: float64

(g) **S2-A-Y-P3**: Numerical results

Figure A.23: *Results for "Alpha APEV528-Yamaha F100BETX-Propeller 3" Matching*

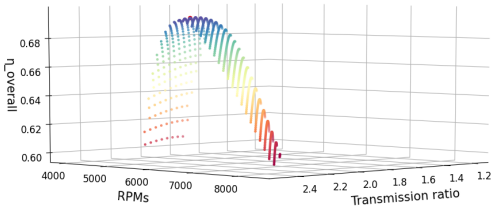

(a) **S2-A-S-P3**: Maximum overall efficiency graph

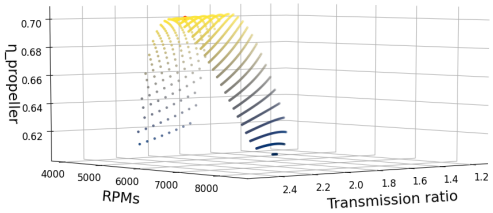

(b) **S2-A-S-P3**: Maximum propeller efficiency graph

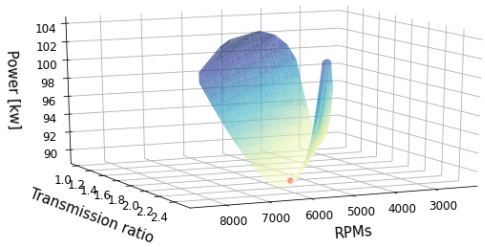

(c) **S2-A-S-P3**: Minimum power graph

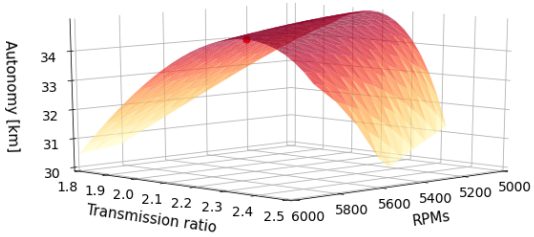

(d) **S2-A-S-P3**: Maximum autonomy graph

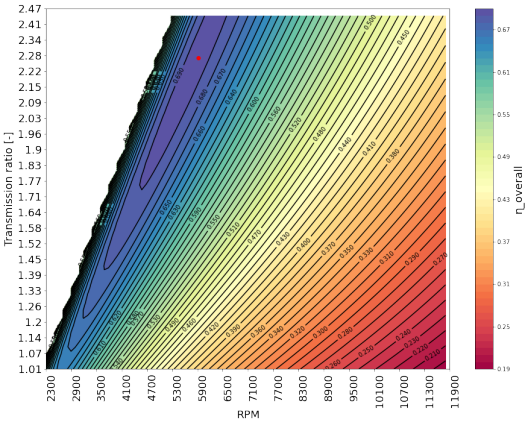

(e) **S2-A-S-P3**: Transmission ratio efficiency map

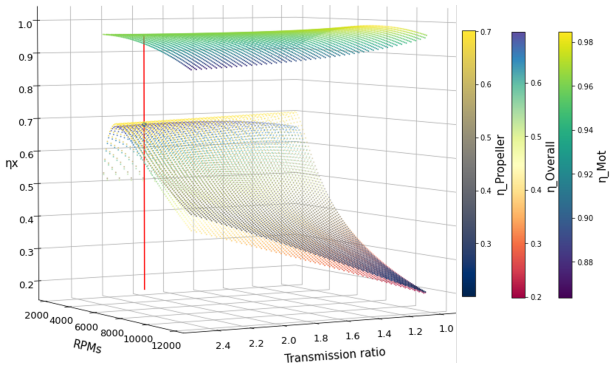

(f) **S2-A-S-P3**: Motor-Transmission-Propeller matching

transmission_ratios	2.287143
transmission_ratios_i_values	1.132417
RPMs_mot	5900.100000
RPMs_propeller	2579.681449
diameter [in]	12.999960
pitch	1.416670
slip_ratio	0.177073
speed_of_advance	50.123900
hull_efficiency	1.050000
eta_r	0.980000
advance_coefficient	1.076141

P_D	1.300000
AE_A0	0.610000
Z	3.000000
eta_open_water	0.701886
QPC	0.722241
torque_motor	144.811319
eta_motor	0.962188
GLOBAL_EFFICIENCY	0.694931
POWER	89.472691
AUTONOMY	34.757645
Name: 3564, dtype: float64	

(g) **S2-A-S-P3**: Numerical results

Figure A.24: *Results for "Alpha APEV528-Suzuki DF90-Propeller 3" Matching*